

## ABSTRACT

Poncelet Polygons Through the Lenses of Orthogonal Polynomials on the Unit Circle, Finite Blaschke Products, and Numerical Ranges

Taylor A. Poe, Ph.D.

Advisors: Co-Chairperson: Andrei Martínez-Finkelshtein, Ph.D.  
Co-Chairperson: Brian Z. Simanek, Ph.D.

The topics in this thesis fall in the intersection of projective geometry, complex analysis, and linear algebra. Each of these three fields gives a canonical construction of families of polygons inscribed in the unit circle with interlacing vertices. In projective geometry, we consider Poncelet curves which admit a family of circumscribed polygons. From the perspective of linear algebra, we consider the eigenvalues of a one parameter family of matrices called CMV matrices. Complex analysis gives two equivalent constructions of such polygons. One involves the preimages of points on  $\mathbb{T}$  under a Blaschke product. The other involves the zero sets of paraorthogonal polynomials on the unit circle.

In all three cases, the intersection of the polygons in this family forms part of an algebraic curve, which will be the primary focus of our study. A large part of this dissertation is dedicated to making each of these constructions precise in order to prove their equivalence. Particular attention is given to the notion of foci of an algebraic curve. In the latter chapters, we will focus on the specific case in which this inscribed curve (the intersection of the family of polygons) is an ellipse. We will give necessary and sufficient conditions in terms of the constructions of these families of

$n$ -gons for small  $n$  for which the inscribed curve is an ellipse. We will also provide algorithms for constructing such families of polygons with prescribed foci for the corresponding ellipse. We will conclude with possible directions for similar progress for larger  $n$ .

Poncelet Polygons Through the Lenses of Orthogonal Polynomials on the Unit Circle, Finite Blaschke Products, and Numerical Ranges

by

Taylor A. Poe, B.S., M.S.

A Dissertation

Approved by the Department of Mathematics

---

Dorina Mitrea, Ph.D., Chairperson

Submitted to the Graduate Faculty of  
Baylor University in Partial Fulfillment of the  
Requirements for the Degree  
of  
Doctor of Philosophy

Approved by the Dissertation Committee

---

Andrei Martínez-Finkelshtein, Ph.D., Co-Chairperson

---

Brian Z. Simanek, Ph.D., Co-Chairperson

---

Markus Hunziker, Ph.D.

---

Lance Littlejohn, Ph.D.

---

James D. Stamey, Ph.D.

Accepted by the Graduate School  
August 2021

---

J. Larry Lyon, Ph.D., Dean

Copyright © 2021 by Taylor A. Poe  
All rights reserved

## TABLE OF CONTENTS

LIST OF FIGURES	ix
ACKNOWLEDGMENTS	xiii
DEDICATION	xiv
CHAPTER ONE	1
Introduction . . . . .	1
CHAPTER TWO	7
History . . . . .	7
2.1 Historical Developments of Poncelet's Theorem . . . . .	7
2.2 Related Results and Recent Contributions . . . . .	14
CHAPTER THREE	18
Background . . . . .	18
3.1 Orthogonal Polynomials on the Unit Circle . . . . .	18
3.1.1 Defining OPUC . . . . .	18
3.1.2 Szegő Recursion . . . . .	20
3.1.3 Paraorthogonal Polynomials . . . . .	21
3.1.4 CMV Matrices . . . . .	22
3.2 Blaschke Products . . . . .	23
3.3 Numerical Range of a Matrix . . . . .	25
3.3.1 Definition and Basic Properties . . . . .	25
3.3.2 The Class $S_n$ . . . . .	26
3.3.3 Dilations . . . . .	28
3.3.4 Sketch of the Proof of Kippenhahn's Theorem . . . . .	30

3.4	Projective Geometry . . . . .	31
3.4.1	The Projective Plane . . . . .	32
3.4.2	Duality . . . . .	35
3.4.3	Reciprocation About $\mathbb{T}$ . . . . .	36
3.4.4	The Notion of an Envelope . . . . .	38
CHAPTER FOUR		40
	General Poncelet Curves . . . . .	40
4.1	The Poncelet Property . . . . .	40
4.1.1	Definitions . . . . .	40
4.1.2	Foci of a Curve . . . . .	42
4.2	Poncelet Curves . . . . .	43
4.3	Envelopes of Chords of Poncelet Polygons . . . . .	46
4.3.1	Complete Poncelet Curves . . . . .	53
4.4	Mirman's Parametrizations . . . . .	57
4.4.1	Mirman's parametrization . . . . .	57
4.4.2	Mirman's parametrization of a package of Poncelet curves . .	58
CHAPTER FIVE		67
	Constructing Complete Poncelet Curves with Given Foci . . . . .	67
5.1	Three Equivalent Realizations . . . . .	67
5.1.1	Composition of Blaschke Products and Factorization of OPUC	74
5.2	Mirman's Circular Iterations . . . . .	75
5.2.1	Nonelliptic packages with elliptic components . . . . .	78
5.2.2	Mirman's System . . . . .	81
5.3	Examples . . . . .	82
5.3.1	Poncelet Triangles . . . . .	82
5.3.2	Toy Version . . . . .	84

CHAPTER SIX	86
Quadrilateral and Hexagonal Cases . . . . .	86
6.1 Poncelet Quadrilaterals . . . . .	86
6.1.1 Packages of Poncelet-4 Ellipses . . . . .	86
6.1.2 Specified Combinations of Foci . . . . .	88
6.1.3 Mirman's Iterations for the Quadrilateral Case . . . . .	90
6.1.4 Examples of Poncelet Quadrilaterals . . . . .	92
6.2 Poncelet Hexagons . . . . .	95
6.2.1 Elliptic Components for Hexagons . . . . .	96
6.2.2 Package of Poncelet-6 Ellipses . . . . .	98
6.2.3 Mirman's Iterations for the Hexagon Case . . . . .	103
6.2.4 Specified Elliptic Components in the Package of Hexagons . .	105
6.2.5 Examples of Poncelet Hexagons . . . . .	111
CHAPTER SEVEN	116
Pentagonal Case . . . . .	116
7.1 Mirman's Iterations for the Pentagon Case . . . . .	116
7.2 Geometric Interpretations of the Solutions . . . . .	122
7.3 Examples of Poncelet Pentagons . . . . .	123
CHAPTER EIGHT	128
Future Work . . . . .	128
8.1 Poncelet Heptagons . . . . .	128
8.1.1 Mirman's Iterations in the Heptagon Case . . . . .	129
8.2 Poncelet Dodecagons . . . . .	131
8.2.1 Mirman's Iterations in the Dodecagon Case . . . . .	132
8.3 Remaining Question over Poncelet Pentagons . . . . .	133

APPENDIX	135
List of Symbols and Notation . . . . .	136
BIBLIOGRAPHY	138

## LIST OF FIGURES

1.1 A triangle inscribed in $\mathbb{D}$ and circumscribing an ellipse. . . . .	1
1.2 The existence of a single such triangle as in Figure 1.1 guarantees that every point on $\mathbb{T}$ is the vertex of another in-and-circumscribed triangle. . . . .	2
1.3 Hexagons circumscribing a nonelliptic curve. . . . .	2
1.4 Connecting all the vertices of the hexagons in Figure 1.3 reveals a Poncelet curve with three components. . . . .	3
1.5 In black are the foci of the curve consisting of three components, only one of which is elliptic. . . . .	5
2.1 For the unit circle, $R = 1$ . Then if $C$ has radius $r = \frac{1}{2}$ , there exists infinitely many triangles inscribed in $\partial\mathbb{D}$ circumscribing $C$ . . . . .	8
2.2 Nonconcentric circles with in-and-circumscribed triangles. . . . .	9
2.3 A Poncelet 4-ellipse. . . . .	11
2.4 Envelopes of convex hulls (left) and of all closed polygons with vertices at a family of points on the circle. . . . .	14
3.1 Tangent lines at a node (left) and at a cusp. . . . .	35
3.2 Geometric construction of the dual curve via reciprocation. . . . .	38
3.3 The circle of radius $\frac{1}{2}$ is the envelope of the sides of the triangles, and the unit circle is the envelope of the vertices of the triangles. . . . .	39
4.1 Rather than connecting adjacent vertices, we can connect alternate vertices to form a nonconvex pentagon. . . . .	41
4.2 A family of Poncelet hexagons. . . . .	44
4.3 Convexity images. . . . .	45
4.4 Examples of cusps and intersections. . . . .	48
4.5 The curves $C_1^*$ and $C_2^*$ associated to a convex Poncelet curve of rank 5. . . . .	50
4.6 On the left, $C_1$ and $C_7$ and on the right, $C_5$ and $C_{11}$ circumscribe 24-Poncelet curves. . . . .	55
4.7 On the left, $C_2$ and $C_{10}$ are 12-Poncelet curves. On the right, $C_3$ and	

$C_9$ circumscribe 8-Poncelet curves. . . . .	56
4.8 On the left, $C_4$ is a 6-Poncelet curve and $C_6$ is a 4-Poncelet curve. On the right, $C_8$ is a 3-Poncelet curve and $C_{12}$ is a 2-Poncelet curve. . .	56
4.9 A replica of Figure 3.2 for convenience here. . . . .	58
4.10 Illustration for Example 4.16 not satisfying Mirman's condition . . .	64
4.11 Illustration with dual for Example 4.16 . . . . .	65
4.12 Illustration for Example 4.17 . . . . .	66
5.1 Figure for Theorem 5.1. . . . .	72
5.2 Illustration for Example 5.5 . . . . .	79
5.3 Poncelet-3 ellipse with foci $0.25 - 0.25i$ and $0.7 + 0.3i$ as in Example 5.10	84
5.4 Line segments through $f_1 = 0.5$ . . . . .	85
6.1 A Poncelet-4 ellipse given by $\phi_3(z) = \Phi_0(z; 0.04 + 0.23i)\Phi_1(z; 0.04 + 0.23i, -0.25i)$ . . . . .	87
6.2 Two Poncelet 4-ellipses with the same Pentagram point, $0.4 + 0.3i$ . .	91
6.3 The numerical range of $A$ in Example 6.4. . . . .	93
6.4 The numerical range of $A$ in Example 6.5. . . . .	94
6.5 The numerical range of $A$ in Example 6.6. . . . .	95
6.6 A 6-Poncelet curve such that the Pentagram curve is an ellipse but the Brianchon curve is not a single point. . . . .	97
6.7 A 6-Poncelet curve such that the Brianchon curve is a degenerate ellipse but the Pentagram curve is not an ellipse. . . . .	98
6.8 Using the foci from Example 6.17, the figure on the left represents Corollary 6.9 (i) and the figure on the right represents Corollary 6.9 (ii). .	98
6.9 A Poncelet 6-ellipse along with the Pentagram ellipse and Brianchon point. . . . .	99
6.10 A family of Poncelet hexagons. The foci of the ellipse bounding $C_1$ are $f_1 = -0.3i$ and $f_2 = 0.4i$ . . . . .	102
6.11 An example of a family of Poncelet hexagons circumscribing an ellipse with specified pentagram ellipse foci. . . . .	106
6.12 As in Lemma 6.15, here the line segments joining $z_j^i$ and $z_j^{-i}$ all meet at a single point. . . . .	107

6.13	Two Poncelet 6-Ellipses with the same Brianchon point.	108
6.14	Figure for Theorem 6.16	109
6.15	Figure for Example 6.17.	112
6.16	Figure for Example 6.18.	113
6.17	Figure for Example 6.19.	114
6.18	The triangles circumscribing the ellipse with foci $0.5$ and $0.1i$ with the diagonals meeting at a single point.	114
6.19	Figure for Example 6.20.	115
7.1	A family of Poncelet pentagons.	117
7.2	Collinearity of the points $f_1$ , $f_2$ , $z_j$ 's and $w_j$ 's, as explained in Theorem 7.1.	118
7.3	Pairs $(z_1, w_1)$ and $(z_2, w_2)$ as foci of the Pentagram and the Poncelet ellipses, respectively.	122
7.4	The numerical range and pentagram curve of $\mathbf{A}$ in Example 7.2.	125
7.5	The numerical range and pentagram curve of $A$ in Example 7.3.	127
8.1	A family of Poncelet Heptagons where $C_1, C_2, C_3$ are almost elliptic.	129
8.2	The three nontrivial solutions inside $\mathbb{D}^4$ of Mirman's iterations. In red are the given $f_1, f_2$ that initiated Mirman's iterations.	130
8.3	Colinearity in the heptagon case.	131
8.4	Poncelet Dodecagons formed by a composition of degree three and two degree two Blaschke products.	132
8.5	Poncelet Dodecagons formed by a composition of degree two and degree six Blaschke products.	133

## ACKNOWLEDGMENTS

First and foremost, all the glory for this can only go to Jesus Christ. The salvation He gives alone is enough to praise Him forever, and yet He still has poured out blessing on top of blessing. He has guided me every step of my life's journey so far, showing me where to go to school, revealing His calling on my life to teach, and opening up a door I did not think would be possible—moving in ways that show that it is only by His grace that I am able to complete this dissertation at this time.

Mom and Dad, there are too many thank you's to list. You believed in me through this process when I did not have confidence in myself. Thank you for your prayers, support, and encouragement throughout my life. Thank you for the hours spent going over flashcards and notes, for teaching me how to study, and for always encouraging me to work “as to the Lord.” You showed me from a young age the opportunities that education could provide, and I hope you see how your work has paid off. The support and prayers of the entire family, including my in-laws, have carried me through.

Jonathan, my husband, again this thank you will not scratch the surface of your support the last few years. Thank you for patiently listening and encouraging me through moments of frustration. Thank you for always giving me perspective, for your confidence in me, and for all the work you do to help me. Thank you for building in breaks for me and listening to me talk through math problems when I'm stuck. Graduate school has been a much more pleasant journey with you beside me.

Thank you to my advisors and mentors, Dr. Andrei Martínez-Finkelshtein and Dr. Brian Simanek. Thank you for investing your time and energy, for answering my many questions, and for your patience and guidance. Thank you for sharing your expertise and teaching me how to be a better researcher. Thank you also to the Baylor

Mathematics Department for your support through core classes and comprehensive exams, for guidance on how to teach, and for introducing me to math research. Thank you to Dr. Mark Sepanski and Mrs. Margaret Salinas for overseeing the graduate program the last four years. A huge thanks also to my committee- Dr. Markus Hunziker, Dr. Lance Littlejohn, and Dr. James Stamey- for your time and the revisions you have made to this dissertation.

Thank you also to my fellow math graduate students. I cannot imagine my time at Baylor without the advice and guidance of those who graduated before me. The community of graduate students has been a unique blessing. Thank you to Dr. Erica Swindle Oldaker, Dr. Jennifer Loe, and Jorge Marchena-Menendez for your help with latex formatting and mathematica constructions. I could not have completed this dissertation without your technical expertise. Jorge, I am also so grateful for the stories and laughs through such busy and stressful seasons.

To the Mississippi College professors and mentors who encouraged me to go to graduate school and pursue a doctorate, and who then had the confidence in me to hire me back before I knew when I would complete my degree, thank you for investing in me far beyond the call of duty as professors. I am so thankful for the opportunity to work alongside you and continue learning from you.

I cannot forget the North Pike High School teachers who prepared me for future studies. A special thank you to Coach Campbell for giving me a solid mathematical foundation and for having the confidence in me to allow me to teach my peers. I would never have imagined as a high school junior substituting in precalculus that I would eventually complete a doctorate in order to fulfill a calling of teaching college mathematics.

Finally, thank you to the ladies of If:Baylor, the church family at First Baptist Robinson, and our adopted Waco families. Thank you for investing in us over the last four years and making us part of the Waco community.

To the teachers and mentors who guided me here

## CHAPTER ONE

### Introduction

Consider an ellipse,  $E$ , inside the unit disk. Pick one point  $\lambda_1$  on the unit circle and draw a tangent to the ellipse passing through  $\lambda_1$ . At the point where this tangent again meets the unit circle,  $\lambda_2$ , draw another tangent to the ellipse through  $\lambda_2$ . Repeating this process, could the third tangent end back at  $\lambda_1$ , forming a triangle inscribed in the circle and circumscribing the ellipse? The answer depends on  $E$  but not on  $\lambda_1$ , a result known as Poncelet's Theorem. The existence of one guarantees an infinite family (see Figures 1.1 and 1.2). If the three tangents form a triangle, we can even say that every point of the unit circle,  $\mathbb{T}$ , is the vertex of one of these triangles while every point of the ellipse is a point of tangency to one of these triangles. These

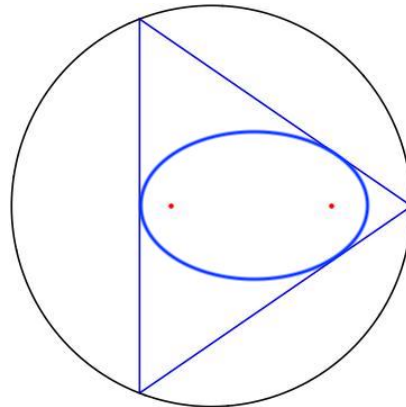


Figure 1.1. A triangle inscribed in  $\mathbb{D}$  and circumscribing an ellipse.

families of polygons inscribed in the unit circle and circumscribing a curve have been commonly called *Poncelet polygons* after a theorem by Jean Victor Poncelet, and similarly the curve is said to exhibit the *Poncelet property*. The above construction can be generalized to  $n$ -gons for any  $n$ , including nonconvex polygons. There are also

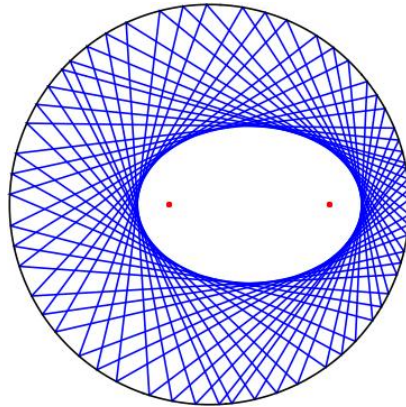


Figure 1.2. The existence of a single such triangle as in Figure 1.1 guarantees that every point on  $\mathbb{T}$  is the vertex of another in-and-circumscribed triangle.

examples of curves for which the Poncelet Property holds that are not ellipses, see for example Figure 1.3. The curve pictured there is inscribed in a collection of hexagons.

The curve in Figure 1.3 is clearly not an ellipse, so we are naturally led to look for a

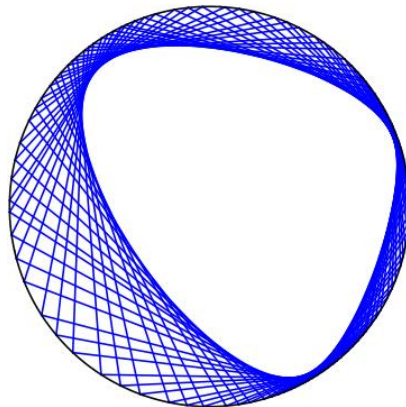


Figure 1.3. Hexagons circumscribing a nonelliptic curve.

description of this curve. It turns out to be just one component of a larger curve that we now describe. If we consider the hexagons in Figure 1.3 and connect the diagonals of each hexagon, we see not only one curve but three, each in a sense exhibiting this property of being circumscribed by polygons inscribed in the circle, see Figure 1.4.

By connecting alternate vertices, each hexagon is split into two interlacing triangles that circumscribe what here appears to be (and in fact is) an ellipse. Connecting every third vertex (the main diagonals of the hexagons) yields a third component of the curve. It appears that this curve has cusps that even appears to intersect the ellipse. These three curves are not separate but are all connected components of the

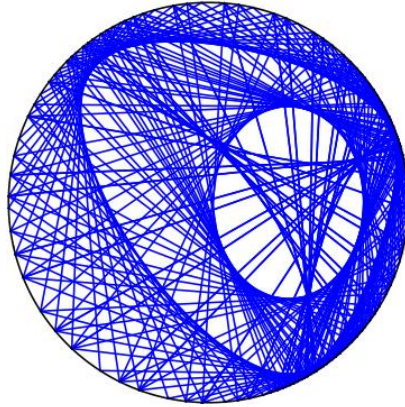


Figure 1.4. Connecting all the vertices of the hexagons in Figure 1.3 reveals a Poncelet curve with three components, some of which are nonconvex and intersecting.

same curve. This curve lends itself to a convenient description, and it is reasonable to inquire about its properties. As Figure 1.4 shows, we notice:

1. the components can intersect
2. the components can have cusps
3. the components can be elliptic even if the outermost component is not
4. the outermost curve is smooth and convex
5. the number of connected components is  $\left\lfloor \frac{n}{2} \right\rfloor$  where  $n$  is the number of sides of the circumscribing polygons.

One wonders what can be said about these curves in general. Naturally this yields the question of how to find and construct these curves. For the case of ellipses, the

key to the construction is their foci. The same is true more generally, but the use of the word “foci” requires some care. Foci, in this general sense, can be interpreted through multiple lenses. In understanding foci and Poncelet curves, we will see interactions between matrix theory, geometry, and complex analysis. Simultaneously, the circumscribing polygons can be realized from each perspective. We will outline these perspectives here, but the terminology and tools will be explained in much greater detail in the following chapters.

From the perspective of matrix theory, we can first consider the outermost curve, the intersection of the convex hull of the vertices of the polygons. This curve bounds the image the Euclidean unit sphere under the continuous map  $x \rightarrow x^*Ax$  where  $A$  is an almost unitary matrix. This set is also called the numerical range of the matrix  $A$ . The eigenvalues of the matrix are the foci and the eigenvalues of unitary dilations of these square matrices form the vertices of the circumscribing polygons. At the same time, these vertices are the set of preimages of points on the circle under canonical rational functions on  $\overline{\mathbb{D}}$  called Blaschke products, and the foci are the zeros of the Blaschke product. We will also see how to interpret these vertices and foci through the lens of orthogonal polynomials on the unit circle. As we will show in the following chapters, these perspectives are completely equivalent.

We will pay special attention case of a component of the curve being an ellipse. As noted above, it is possible that some components are ellipses while others are not, but the implications of an elliptic component are more subtle than one might guess. For example, results from projective geometry prove that if the outermost component of the curve is an ellipse, the other smaller components will also be ellipses. The case in which all components are ellipses will require specific conditions on the matrices, Blaschke products, and paraorthogonal polynomials. We will give details of these conditions for  $n = 2, 3, 4, 5$  and  $6$  in later chapters as well as a conjecture for generalizing to any  $n$ . In the elliptic case, one may also wonder if the foci of the

ellipse are connected in any way to the matrix, Blaschke product, or paraorthogonal polynomials defining it. In fact, they are very much related.

Again, there is more depth to these connections between foci and constructions of the curve. The main difficulty is that the relationship between the foci and the curve is not easily expressed using Euclidean distance. We will use more sophisticated geometric tools to make this relationship precise. With this interpretation of foci, we can construct Poncelet curves with given foci even if none of the components are elliptic using the same methods described above, see for example Figure 1.5.

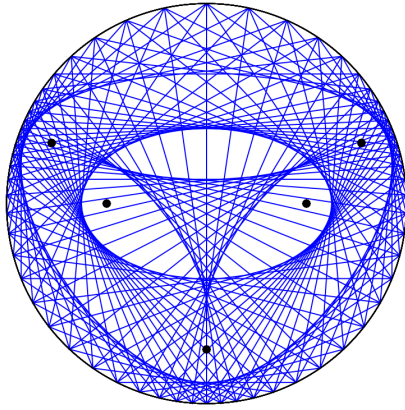


Figure 1.5. In black are the foci of the curve consisting of three components, only one of which is elliptic.

In the following chapters, we will rigorously define and prove the claims we have made and then provide specific constructions in the elliptic case for small  $n$ -gons. In Chapter Two, we will summarize the long and rich history of this study. Then, in Chapter Three, we will introduce formally the tools mentioned above: orthogonal polynomials, Blaschke products, numerical ranges, and unitary dilations. We will also define some basic projective geometry terms and ideas that will be useful in Chapter Four where we carefully define Poncelet polygons, seek to unify the terminology surrounding the topic, and clarify misconceptions about Poncelet curves and

polygons found in the literature. In this chapter, we will often use the projective dual to better understand these Poncelet curves. We will also discuss the work of Boris Mirman, which was apparently largely overlooked previously, including a necessary but insufficient condition on a set of points to be the foci of a union of Poncelet ellipse.

Once we have introduced all of these tools and clarified terminology, in Chapter Five, we will prove the statement above that each of the three perspectives mentioned there are equivalent. Then we will use all of the tools and knowledge accumulated so far to give specific algorithms for finding Poncelet ellipses circumscribed by certain smaller polygons. We will start with the “toy” examples of line segments and triangles at the end of Chapter Five. Then in Chapter Six, we will characterize Poncelet quadrilaterals and hexagons, largely through the lenses of numerical ranges, orthogonal polynomials, and Blaschke products. Pentagons are the focus of Chapter Seven, where Mirman’s formulas will be the most useful tool. Lastly, in Chapter Eight we will share some current progress towards understanding Poncelet heptagons and dodecagons in seeking to find generalizations to any  $n$ -gon.

## CHAPTER TWO

### History

The history of the questions discussed in this dissertation is both rich and involved. This story also includes many renowned mathematicians over the centuries, as we will see momentarily. Andrea Del Centina tells the story well in a 150 page, two-part publication [16, 17] showing both the history of the topic and details of many of the proofs and calculations involved. For brevity, we highlight here some of the major players and events. The longevity of the developments of Poncelet's theorem credits the beauty and depth of the result. In the words of H.S. White as quoted by Del Centina,

Most new ideas in geometry die early, or pass, by publication, into the condition of mummies or fossils; let our grateful recognition and praise follow then those fortunate worthies like Poncelet, whose genius has given us the fruitful ideas, problems and theories with a significance stretching far beyond their accidental first form, reappearing through the years in new embodiment, and so achieving a life if not perpetual, at least as long enduring as the present era of intellectual culture. [78]

Now, over a century after White's above comment praising the endurance of Poncelet's theorem, over two hundred years after Poncelet's imprisonment, new results and interest in the theorem are appearing again and renewing the interest of the international mathematical community.

#### *2.1 Historical Developments of Poncelet's Theorem*

Although Poncelet's porism provides the launching point for the discussions in this dissertation, the question of polygons inscribed in and circumscribed about two conics (called *in-and-circumscribed*) actually goes back to the Hellenistic period. It has been known since that time that given two concentric circles with radii  $r, R$  for

$r < R$ , an inscribed and circumscribing triangle only exists if  $r = \frac{R}{2}$ . The existence of infinitely many such triangles given one, a concept known as a *closure property*, was also known in this case, and similar results existed for other regular polygons. Del Centina aptly titled the article “a long story of renewed discoveries” as we will see shortly that many initial results went unnoticed. English surveyor William Chapple,

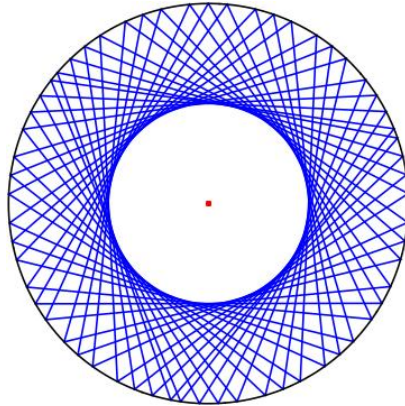


Figure 2.1. For the unit circle,  $R = 1$ . Then if  $C$  has radius  $r = \frac{1}{2}$ , there exists infinitely many triangles inscribed in  $\partial\mathbb{D}$  circumscribing  $C$ .

nearly a century before Poncelet, appears to be the first to consider the question with nonconcentric circles. Most of his work focused on triangles. He proved that if a triangle exists inscribed in a circle of radius  $R$  and circumscribed about another circle of radius  $r$ , then the distance between the centers of the circles,  $a$ , must satisfy

$$a^2 = R^2 - 2rR. \quad (2.1)$$

If the outer circle is  $\mathbb{D}$ , then

$$r = \frac{1 - a^2}{2}. \quad (2.2)$$

Chapple’s proofs were flawed, but his formulas are correct. He also had an understanding of the existence of the infinite family of such triangles. Much of Chapple’s

work on the subject remained unnoticed by the mathematical world of the time. In order to draw more attention to his results, he submitted the question of proving (2.1) in the 1746 *Ladies Diary*. John Landen submitted a solution and later considered the question of inscribed and circumscribed triangles in circles from a more projective viewpoint. Landen also considered the case of two ellipses rather than two circles. Similar to Chapple, though, Landen's work was not well-known outside of England, although it contained some core ideas that Poncelet would study 60 years later.

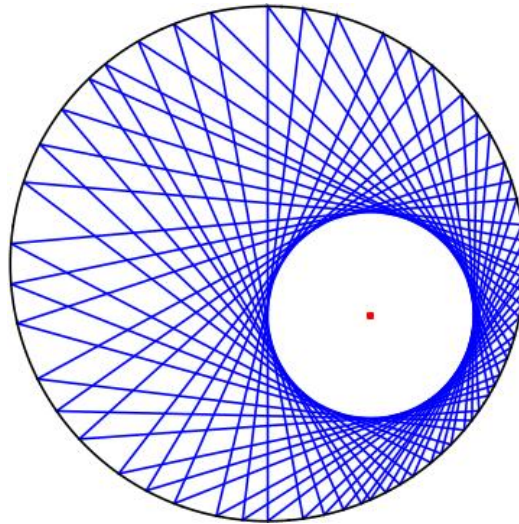


Figure 2.2. Nonconcentric circles with in-and-circumscribed triangles.

Chapple's result was often credited to Euler by nineteenth-century mathematicians. In his 1765 paper on triangle geometry, Euler studied the positions and placements of the barycenter, orthocenter, incenter, and circumcenter of triangles. Euler did develop an equation that the centers of the circles inscribing and circumscribing a triangle must satisfy, but his equation centers on the lengths of the sides of the triangles rather than the radii of the circles. Euler was likely familiar with Chapple's work, and one can recover Chapple's equation (2.1) from Euler's work. Euler's formulas did not imply a closure property.

In 1797, Nicholas Fuss became the first to study the problem of inscribed and circumscribed quadrilaterals. He generalized (2.1) to the case of quadrilaterals and brought (2.1) to the attention of the international mathematical community, though sadly again Fuss's work remained largely unnoticed. Some new proofs of the closure theorem were published in subsequent years, but the next major contributions came from Poncelet.

Jean Victor Poncelet served as Lieutenant of Engineers in Napoleon's 1812 campaign against Russia. In the Battle of Krasnoi in September of that year, Poncelet was shot off of his horse and left for dead as the defeated French army retreated. He was marched as a prisoner of war across the frozen tundra for five months before reaching Saratov prison. There he was placed on house arrest because of his officer status. During his two years at Saratov, Poncelet penned seven notebooks, the final of which he hoped to present to the Academy of Sciences of St. Petersburg with the hope of being called to Moscow until a peace agreement could be reached, but this never came to fruition due to the national events of 1814. Poncelet returned to France and published some of his results from his imprisonment, presenting the "principle of continuity" which he used to prove his porism to the Paris Academy in 1820. He published *Traité sur les propriétés projectives des figures* [62] in 1822, which included the theorem that has become known as *Poncelet's closure theorem* or Poncelet's porism.

Here we restate Poncelet's Theorem in its simplified form, adjusted to our context:

Theorem 2.1 (Poncelet, 1813). [62] *Let  $C$  be an ellipse in  $\mathbb{D}$ , and suppose there is an  $n$ -sided polygon  $\mathcal{P}_0$  inscribed in  $\mathbb{T}$  and circumscribed about  $C$ . Then for any point  $z \in \mathbb{T}$ , there exists an  $n$ -sided polygon  $\mathcal{P}(z)$  inscribed in  $\mathbb{T}$  and circumscribed about  $C$  such that  $z$  is a vertex of  $\mathcal{P}(z)$ .*

Many mathematicians viewed the theory of continuity used by Poncelet with skepticism. He had developed a concept he coined an “ideal cord” which allowed him to find many results that modern mathematicians derive by imbedding the real plane into the complex one. Poncelet used these tools in his “synthetic” proof of the porism after his release, although he proved the theorem analytically originally.

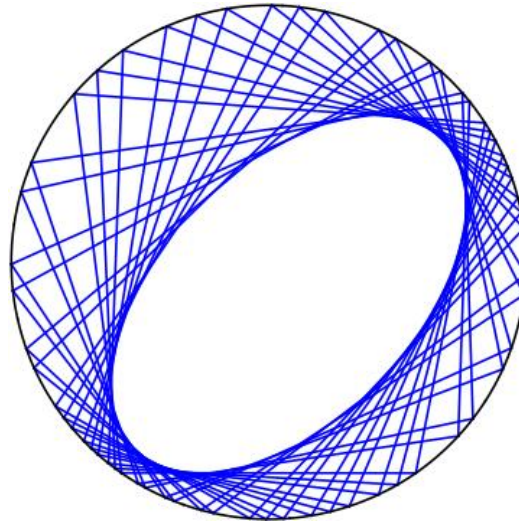


Figure 2.3. A Poncelet 4-ellipse.

Carl Gustav Jacob Jacobi came to Paris in 1829 and met with Poncelet several times, exchanging ideas on the subject of polygons interscribed to two conics. Jacobi represented the conics as elliptic differentials of the first kind and reproved Poncelet’s General Theorem, of which Poncelet’s porism is a corollary, using these elliptic integrals in the case when  $C$  is a circle. Jacobi also found a necessary and sufficient condition for the existence of such polygons in terms of the elliptic integrals.

Jacobi’s work was actually completed by Nicola Trudi in 1839. Jacobi restricted his results to circles in particular positions, possibly not fully believing Poncelet’s generalizations to conics. Trudi answered the question of general conics and any polygons using elliptic integrals. He also derived necessary and sufficient conditions

for two conics to admit an inscribed  $n$ -gon. Trudi provided another proof of Poncelet's porism, and he began connecting  $2 \times 2$  minors of matrices to the question. Again, his work remained practically unknown outside of the Neapolitan milieu.

Around the same time that Trudi's work was circulated, Arthur Cayley published on the same subject. Cayley used Abel's theorem and power series expansions of the square roots of certain determinants to prove Poncelet's closure theorem and found explicit criterion for ellipses to have the  $n$ -Poncelet property in terms of the same power series expansions. He also considered curves of degree higher than two and connected the  $(2, 2)$ -correspondences to the problem. Cayley also looked at the problem in terms of dual curves. Cayley did not explain the geometrical interpretations of his results, but a century later Griffiths and Harris gave a modern interpretation of Cayley's criterion [38]. Cayley's criterion makes it possible to determine, for example, for which semi-minor axes an ellipse with prescribed foci has the  $n$ -Poncelet property. George Salmon later rederived Cayley's results without the use of elliptic functions [64, 65].

In the following years, many of the contributions around the question of these in-and-circumscribed conics centered on new proofs of Poncelet's theorems, and debates over recognition for various results arose. For example, Trudi's work on this topic was largely forgotten until Dragović recalled his work in 2011 [18], which frustrated Trudi during his lifetime.

In the late 1860's, G. Darboux started to investigate the question of algebraic curves of higher degree exhibiting the Poncelet property, and he realized that this question is best approached by considering the dual problem of finding curves passing through the intersection points of  $n$  tangent lines to  $\mathbb{T}$ . By introducing a convenient system of plane coordinates, now called Darboux coordinates, he was able to give a new proof of Poncelet's closure theorem and generalizations (see e.g. [16, Ch. 9].) Adjusted to our context, Darboux's results can be summarized as follows:

Theorem 2.2 (Darboux [15], 1917). *Let  $C$  be a closed convex curve in  $\mathbb{D}$  and suppose that there is an  $n$ -sided polygon  $\mathcal{P}_0$  inscribed in  $\mathbb{T}$  and circumscribed about  $C$ . If the curve  $C$  is a connected component of a real algebraic curve  $\Gamma$  in  $\mathbb{D}$  of class<sup>1</sup>  $n - 1$  such that each diagonal of  $\mathcal{P}_0$  is tangent to  $\Gamma$ , then for every point  $z \in \mathbb{T}$ , there exists an  $n$ -sided polygon  $\mathcal{P}(z)$  inscribed in  $\mathbb{T}$  and circumscribed about  $C$  such that  $z$  is a vertex of  $\mathcal{P}(z)$  and each diagonal of  $\mathcal{P}(z)$  is tangent to  $\Gamma$ . In the special case when  $C$  is an ellipse, there always exists such an algebraic curve  $\Gamma$  and this curve decomposes into  $(n - 1)/2$  ellipses if  $n$  is odd, and  $(n - 2)/2$  ellipses and an isolated point if  $n$  is even.*

From these results, curves with components tangent to the diagonals of polygons are commonly called *Poncelet-Darboux curves*. Darboux was likely unaware of Trudi's results, whose proof of Poncelet's Theorem was very similar to Darboux's.

If  $C$  and  $\Gamma$  are as in the theorem, then  $\Gamma$  can be recovered from  $C$  as the envelope of all the diagonals of the family of  $n$ -sided polygons inscribed in  $\mathbb{T}$  and circumscribed about  $C$  (see Figure 2.4). This will be made precise in Chapter Four in terms of Darboux's curve of degree  $n - 1$  that is dual to  $\Gamma$ . We note that even though the curve  $\Gamma$  is singular in general, it has exactly  $n - 1$  tangent lines in each arbitrarily given direction (just as in the special case when  $\Gamma$  decomposes into ellipses).

In the late 1870's, Georges Henri Halphen began studying Poncelet polygons. Halphen wanted to find the number of conics in a particular family which are  $n$ -inscribed in a given conic from the same family, which he found to be Euler's totient function. He proved Poncelet's theorems by means of the symmetric  $(2, 2)$ -correspondences, found the closure conditions, and rederived Cayley's formulas algebraically without elliptic integrals. He was also the first to consider the problem using continued fractions.

---

<sup>1</sup>The class of a plane algebraic curve is the degree of its dual curve, see Section 3.4 for details.

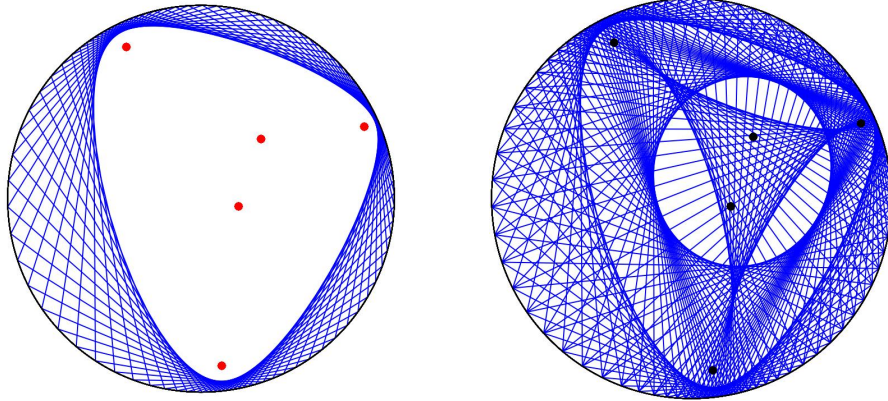


Figure 2.4. Envelopes of convex hulls (left) and of all closed polygons with vertices at a family of points on the circle.

In the 1920’s, Henri Lebesgue, with the aid of more developed tools in complex projective geometry, provided geometric proofs of Poncelet’s theorems and Cayley’s results. Lebesgue also formulated a geometric condition on the conics  $\Gamma$  and  $\Gamma_1$  for the existence of an in-and-circumscribed polygon. Lebesgue’s proofs inspired John Arthur Todd to find a new “elementary” geometric proof of the Cayley conditions. After this point, Poncelet’s theorem fell out of the spotlight. As Del Centina says,

In the following years, mathematicians’ interest in Poncelet polygons decreased, and within a decade, all related questions seemed to sink into the midst of history. . . [until] 1976 [when] Phillip A Griffiths attracted again the attention of the mathematical world on Poncelet’s porism.

As we mentioned before, Griffiths and Harris rediscovered and geometrically interpreted the Cayley conditions. They also extended Poncelet’s closure theorem to three-dimensional projective space.

## 2.2 Related Results and Recent Contributions

The contributions in the previous section all directly related to Poncelet’s theorem, either by offering new proofs of the theorem or conditions for a curve or polygon to have this “Poncelet” property (this concept is loosely defined in the literature but

made rigorous in Chapter Four). In this section, we will discuss some results that may not have immediately been connected to Poncelet's theorem but which will shape much of our discussion in future chapters. Several of the concepts mentioned here will be defined in greater detail in Chapter Three. We will also note some recent developments on Poncelet's theorem due to a renewed interest in the subject over the last two decades.

In the study of conic sections, the idea of foci plays a central role. In 1832, J. Plücker defined foci of higher degree algebraic curves (see the definition in Section 4.1.2). Cayley actually used Plücker's formula in his work on Poncelet's theorem. It turns out that a curve  $\Gamma$  as in Theorem 2.2 has exactly  $n - 1$  real foci (counted with multiplicity) and  $(n - 1)(n - 2)$  nonreal foci. Furthermore, all the real foci are in  $\mathbb{D}$ . We will later see that the  $n - 1$  real foci determine  $\Gamma$  completely. A priori, this fact is by no means obvious and was not discovered until twenty years ago.

One way to find an algebraic curve with given foci is using the notion of the numerical range of a matrix (see the definition in Section 3.3).

**Theorem 2.3** (Kippenhahn [46, 47]). *For an  $n \times n$  complex matrix  $\mathbf{A}$  there exists a real algebraic curve  $\Gamma$  of class  $n$  whose real foci are the eigenvalues of  $\mathbf{A}$  and such that the numerical range of  $\mathbf{A}$  is the convex hull of the real points of  $\Gamma$ .*

Kippenhahn's proof is constructive and elegant, and we will explain his arguments briefly in Section 3.3.4.

Starting in 1998, H.-L. Gau and P. Y. Wu and, independently, B. Mirman studied when the boundary of the numerical range of an  $n \times n$  matrix  $\mathbf{A}$  exhibits the  $(n + 1)$ -Poncelet property with respect to the unit circle  $\mathbb{T}$ . In a series of papers, Gau and Wu [27, 28, 30, 79] showed that a necessary and sufficient condition is that  $\mathbf{A}$  belongs to the class  $S_n$  of completely non-unitary contractions with defect index 1 (see Section 3.3.2). This class can also be identified with the compressed multiplication operators on  $\mathbb{T}$ . The corresponding Poncelet polygons will join the eigenvalues of all

rank 1 unitary extensions of  $\mathbf{A} \in S_n$ . Mirman, using slightly different terminology and more geometric techniques, gave beautiful new proofs of many of Darboux's results, apparently without being aware of Darboux's work until 2005 (see the comments in the introduction to [57]). Mirman and Shukla proved the following existence result specifically connecting the existence of Poncelet  $n$ -ellipses and numerical ranges.

**Theorem 2.4.** [57] *Suppose  $f_1, f_2 \in \mathbb{D}$ . There exists a Poncelet  $n$ -ellipse with foci at  $f_1$  and  $f_2$ . Furthermore, this ellipse forms the boundary of the numerical range of a matrix  $A \in S_{n-1}$  and  $f_1, f_2$  are eigenvalues of  $A$ .*

A seemingly alternative approach to the problem above, using rational functions, can be traced back to the following result of J. Siebeck, popularized in Marden's 1948 book [53, Ch. 1, §4], *Geometry of Polynomials*:

**Theorem 2.5** (Siebeck [69]). *Let  $\{w_1, \dots, w_n\}$  be the vertices of a convex polygon in  $\mathbb{C}$  ordered counter-clockwise. Let*

$$M(z) = \sum_{j=1}^n \frac{m_j}{z - w_j}, \quad (2.3)$$

where  $m_1, \dots, m_n$  are real numbers. Then the zeros of  $M(z)$  are the foci of a real algebraic curve of class  $n - 1$  which intersects each of the line segments  $[w_j, w_k]$ ,  $j \neq k$ , at the point dividing the line in ratio  $m_j/m_k$ .

Daepp, Gorkin and collaborators [10, 13, 14, 37] published a series of papers concerning finite Blaschke products  $B(z)$ . These are the Schur functions (analytic maps of  $\mathbb{D}$  to itself) which are analytic in a neighborhood of  $\overline{\mathbb{D}}$ , of magnitude 1 on  $\partial\mathbb{D}$ , with  $n$  zeros in  $\mathbb{D}$  (see Section 3.2 for details). A connection with Siebeck's theorem is through the formula (see [13])

$$\sum_{j=1}^n \frac{m_j(\lambda)}{z - w_j} = \frac{b(z)}{zb(z) - \bar{\lambda}},$$

which shows that solutions of equations of the form

$$zb(z) = \bar{\lambda} \in \mathbb{T} \quad (2.4)$$

generate configurations of points on  $\mathbb{T}$  such that the envelope of the convex hull of these points is a (component) of an algebraic curve whose foci coincide with the zeros of  $b$ . Furthermore, Fujimura [22, 23, 24] extended their analysis to the whole interior curve and its dual, see details in Chapter Four and Chapter Five.

As we will see, both approaches (via the numerical range or using Blaschke products) are equivalent, and in this sense, provide the only possible construction of algebraic curves in  $\mathbb{D}$  with prescribed foci having a Poncelet property. In a recent work [54], Martínez-Finkelshtein, Simanek and Simon showed that both points of view are naturally connected via orthogonal polynomials on the unit circle (OPUC), initially studied in a systematic way by Szegő [76] and Geronimus [33]; for a modern account on the theory, see the treatise by Simon [70]. In particular, it was shown that the class  $S_n$  is exactly the class of the truncated CMV matrices that are the natural family of matrices to be studied in the theory of OPUC and that equations (2.4) define the zeros of the so-called *paraorthogonal* polynomials on the unit circle. We will discuss these OPUC and CMV matrices in Sections 3.1 and 3.1.4 and the equivalence of these tools in Chapter Five.

Poncelet's construction can be approached also from a point of view of the theory of elliptic billiards [19, 20, 48, 61] and discrete dynamical systems such as the pentagram map [60, 66, 67, 77].

## CHAPTER THREE

### Background

In the following sections, we will introduce the tools we will use throughout this dissertation to characterize Poncelet ellipses. First, we will introduce three main tools used in Chapter Five, Chapter Six, Chapter Seven: orthogonal polynomials on the unit circle, finite Blaschke products, and numerical ranges of matrices in the class  $S_n$ . Then, we will give a brief introduction to concepts of projective geometry that will be useful in clarifying terminology in Chapter Four as well as in some proofs later on. Projective geometry will be especially useful in that it will allow us to prove statements using the dual curve. Tools from projective geometry will also help us carefully define and therefore better understand many of the objects we study.

#### *3.1 Orthogonal Polynomials on the Unit Circle*

Barry Simon, author of a two-volume modern reference [70] on orthogonal polynomials on the unit circle, describes orthogonal polynomials as “the Rodney Dangerfield of analysis [71].” In this dissertation, we will focus on orthogonal polynomials on the unit circle (OPUC). In beginning *OPUC on one foot* [71], Simon summarizes, “OPUC is the study of probability measures on  $\partial\mathbb{D}$ , that is, positive measures,  $\mu$  with  $\mu(\partial\mathbb{D}) = 1$ .” In this section, we will provide a brief introduction to OPUC emphasizing properties that will be used in our later analysis. Simon’s volumes fill over 1100 pages, so this introduction will be far from comprehensive. For further details on orthogonal polynomials on the unit circle see, e.g. Simon’s volumes [70], or the more classical texts [33] and [76]. For a more brief introduction, see e.g. [71] or [54, Section 2]. The following definitions and theorems can be found in [42, 43, 54, 71] and in greater detail in [70].

### 3.1.1 Defining OPUC

Throughout the rest of the dissertation we reserve the notation  $\Phi_n(z)$  for monic polynomials of degree exactly  $n$ ; when we need to make the dependence on the zeros explicit, we will write

$$\Phi_n(z; f_1, \dots, f_n) := \prod_{j=1}^n (z - f_j), \quad f_j \in \mathbb{D}. \quad (3.1)$$

Moreover, if

$$\Phi_n(z) = \sum_{j=0}^n c_j z^j, \quad c_n = 1,$$

then its reversed polynomial is

$$\Phi_n^*(z) = \sum_{j=0}^n \overline{c_j} z^{n-j} = z^n \overline{\Phi_n(1/\bar{z})}. \quad (3.2)$$

In general,  $\Phi_n^*(z)$  conjugates the coefficients of  $\Phi_n(z)$  and reverses their order. For example, if  $\Phi_1(z) = z - f_1$ , then  $\Phi_1^*(z) = 1 - \overline{f_1}z$ . Observe that  $\Phi_n^*(z)$  can be of degree strictly less than  $n$ . If  $\Phi_1(z) = z = 0z^0 + z$ , then  $\Phi_1^*(z) = 1z^0 + 0z^1 = 1$ . Also note that  $\Phi_n^*(0) = 1$ .

If  $\Phi_n(z) = \Phi_n(z; f_1, \dots, f_n)$  is a monic polynomial of degree  $n$  with all its zeros  $f_j \in \mathbb{D}$ , then there exists a measure  $\mu$  on the unit circle  $\mathbb{T}$  such that  $\Phi_n(z)$  is orthogonal to  $\{z^j\}_{j=0}^{n-1}$  in  $L^2(\mathbb{T}, \mu)$ . There are actually many such measures  $\mu$  and one example is

$$c \cdot |\Phi_n(e^{i\theta}; f_1, \dots, f_n)|^{-2} d\theta,$$

where  $c$  is a normalization constant. Here we identify measures on  $\mathbb{T}$  and measures on  $[0, 2\pi]$  in the usual way. This means that the polynomial  $\Phi_n(z)$  has all the properties of an orthogonal polynomial on the unit circle: zeros inside  $\mathbb{D}$  and orthogonal to  $\{z^j\}_{j=0}^{n-1}$  in  $L^2(\mathbb{T}, \mu)$ . These polynomials are orthogonal in the sense that

$\int \Phi_j(z) \overline{\Phi_k(z)} d\mu = 0$ ,  $0 \leq j < k$ . If  $\{z^j\}_{j=0}^\infty$  are linearly independent as functions in  $L^2(\partial\mathbb{D}, d\mu)$ , then we can use Gram-Schmidt to define monic orthogonal polynomials  $\Phi_n(z; d\mu)$ .

### 3.1.2 Szegő Recursion

The most important property of OPUC for our investigation is the *Szegő recursion*, which states that if  $\Phi_n(z)$  and  $\Phi_{n+1}(z)$  are consecutive orthogonal polynomials for a measure  $\mu$  on  $\mathbb{T}$ , then there exists some  $\alpha_n \in \mathbb{D}$  so that

$$\begin{aligned}\Phi_{n+1}(z) &= z\Phi_n(z) - \overline{\alpha_n}\Phi_n^*(z) \\ \Phi_{n+1}^*(z) &= \Phi_n^*(z) - \alpha_n z\Phi_n(z)\end{aligned}\tag{3.3}$$

or in matrix form

$$\begin{pmatrix} \Phi_{n+1}(z) \\ \Phi_{n+1}^*(z) \end{pmatrix} = \begin{pmatrix} z & -\overline{\alpha_n} \\ -\alpha_n z & 1 \end{pmatrix} \begin{pmatrix} \Phi_n(z) \\ \Phi_n^*(z) \end{pmatrix}.\tag{3.4}$$

We define the notation

$$\Phi_n(z) = \mathcal{S}_{\alpha_{n-1}}(\Phi_{n-1}(z)), \quad \Phi_n^*(z) = \mathcal{T}_{\alpha_{n-1}}(\Phi_{n-1}^*(z))\tag{3.5}$$

to say that  $\Phi_n(z)$  is related to  $\Phi_{n-1}(z)$  by the Szegő recursion and the parameter  $\alpha_{n-1}$ . Clearly,  $\alpha_n = -\overline{\Phi_{n+1}(0)}$ . These  $\alpha_k$  are known as *Verblunsky coefficients*.

Notice that the Szegő recursion can be inverted,

$$\begin{pmatrix} \Phi_{n-1}(z) \\ \Phi_{n-1}^*(z) \end{pmatrix} = \frac{1}{1 - |\alpha_n|^2} \begin{pmatrix} 1 & \overline{\alpha_n} \\ \alpha_n z & z \end{pmatrix} \begin{pmatrix} \Phi_n(z) \\ \Phi_n^*(z) \end{pmatrix}.\tag{3.6}$$

This allows one to recover the orthogonal polynomials of degree smaller than  $n$  from the degree  $n$  orthogonal polynomial. This tells us that even though there are many

choices of orthogonality measure for the polynomial  $\Phi_n(z)$ , they all have the same first  $n$  orthogonal polynomials  $\{\Phi_j(z)\}_{j=0}^{n-1}$  and hence they all have the same first  $n$  Verblunsky coefficients (see [70, Theorem 1.7.5]).

Thus we can parametrize a family of OPUC by its Verblunsky coefficients. When we need to make this dependence explicit, we will use the notation

$$\Phi_n(z) = \Phi_n^{(\alpha_0, \dots, \alpha_{n-1})}(z) \quad (3.7)$$

in contrast to (3.1). The following theorems, restated in our terms, summarize this result.

**Theorem 3.1.** (*Verblunsky*)[80] *Let  $\{\alpha_i\}_{i=0}^{\infty}$  be a sequence of numbers in  $\mathbb{D}$ . Then there exists a unique probability measure  $\nu$  on  $\mathbb{T}$  such that  $\alpha_i(\nu) = \alpha_i$  for all  $i$ .*

**Theorem 3.2.** (*Wendroff's Theorem for OPUC*)[32] *All the zeros of  $\Phi_n(z)$  lie in  $\mathbb{D}$ . Conversely, given any labelled set of  $n$ , not necessarily distinct, points in  $\mathbb{D}$ , there exists a measure so that those points are exactly the zeros (counting multiplicity) of the associated  $\Phi_n(z)$ . Any two such measures have the same  $\{\alpha_j\}_{j=0}^{n-1}$  and so also the same  $\{\Phi_j\}_{j=0}^n$ .*

### 3.1.3 Paraorthogonal Polynomials

A *paraorthogonal polynomial* on the unit circle (POPUC) can be generated by the Szegő recursion (3.4) if we replace the last Verblunsky coefficient  $\alpha_{n-1}$  by a value  $\lambda \in \mathbb{T}$ :

$$\Phi_n^{(\alpha_0, \dots, \alpha_{n-2}, \lambda)}(z) = z \Phi_{n-1}(z) - \bar{\lambda} \Phi_{n-1}^*(z), \quad \Phi_{n-1}(z) = \Phi_{n-1}^{(\alpha_0, \dots, \alpha_{n-2})}(z). \quad (3.8)$$

The  $n$  zeros  $z_j = z_{n,j}^\lambda$ ,  $j = 1, \dots, n$ , of  $\Phi_n^{(\alpha_0, \dots, \alpha_{n-2}, \lambda)}(z)$  are distinct and belong to  $\mathbb{T}$ .

The following theorem allows us to move between interlacing sets on  $\mathbb{T}$  and families of OPUC.

**Theorem 3.3. (Wendroff's theorem for POPUC) [35]** *The zeros of POPUC's for two values of  $\lambda$  interlace. Conversely, given two sets of  $n + 1$  interlacing points on  $\partial\mathbb{D}$ , there exist unique  $\{\alpha_j\}_{j=0}^{n-1}$  in  $\mathbb{D}$  and  $\lambda, \tau \in \partial\mathbb{D}$  so these points are zeros of the associated POPUCs.*

The following definition will also be useful in the upcoming chapters.

**Definition 3.4.** If in (3.8),  $\Phi_{n-1}(z) = \Phi_{n-1}(z; f_1, \dots, f_{n-1})$ , that is, if  $f_1, \dots, f_{n-1}$  are the zeros of  $\Phi_{n-1}(z)$ , then the 1-parametric family of points  $\mathcal{Z}_n^\lambda = \{z_{n,1}^\lambda, \dots, z_{n,n}^\lambda\}$  on  $\mathbb{T}$ , where  $\mathcal{Z}_n^\lambda$  is the zero set of  $\Phi_n^\lambda(z)$ , is called the *paraorthogonal extension* of the zeros  $f_1, \dots, f_{n-1}$  of  $\Phi_{n-1}(z)$ .

Theorem 3.3 tells us that two sets  $\mathcal{Z}_n^{\lambda_1}$  and  $\mathcal{Z}_n^{\lambda_2}$  from this extension, with  $\lambda_1, \lambda_2 \in \mathbb{T}$ ,  $\lambda_1 \neq \lambda_2$ , determine the original points  $f_1, \dots, f_{n-1}$ , and hence  $\Phi_{n-1}(z)$ , completely.

### 3.1.4 CMV Matrices

If the orthogonality measure  $\mu$  on  $\mathbb{T}$  has infinitely many points in its support, then the sequence of its Verblunsky coefficients is also infinite. In this case, one can define a sequence of  $2 \times 2$  matrices  $\{\Theta_j\}_{j=0}^\infty$  by

$$\Theta_j = \begin{pmatrix} \bar{\alpha}_j & \sqrt{1 - |\alpha_j|^2} \\ \sqrt{1 - |\alpha_j|^2} & -\alpha_j \end{pmatrix}$$

and the operators  $\mathcal{L}$  and  $\mathcal{M}$  by

$$\mathcal{L} = \Theta_0 \oplus \Theta_2 \oplus \Theta_4 \oplus \dots, \quad \mathcal{M} = \mathbf{1} \oplus \Theta_1 \oplus \Theta_3 \oplus \dots$$

where the initial  $\mathbf{1}$  in the definition of  $\mathbf{M}$  is a  $1 \times 1$  identity matrix. The *CMV matrix* corresponding to  $\mu$  is then given by  $\mathbf{G} = \mathbf{G}(\{\alpha_j\}) := \mathcal{L}\mathbf{M}$ , or explicitly,

$$\mathbf{G} := \begin{pmatrix} \overline{\alpha_0} & \overline{\alpha_1}\rho_0 & \rho_1\rho_0 & 0 & 0 & \dots \\ \rho_0 & -\overline{\alpha_1}\alpha_0 & -\rho_1\alpha_0 & 0 & 0 & \dots \\ 0 & \overline{\alpha_2}\rho_1 & -\overline{\alpha_2}\alpha_1 & \overline{\alpha_3}\rho_2 & \rho_3\rho_2 & \dots \\ 0 & \rho_2\rho_1 & -\rho_2\alpha_1 & -\overline{\alpha_3}\alpha_2 & -\rho_3\alpha_2 & \dots \\ 0 & 0 & 0 & \overline{\alpha_4}\rho_3 & -\overline{\alpha_4}\alpha_3 & \dots \\ \dots & \dots & \dots & \dots & \dots & \dots \end{pmatrix}, \quad \rho_n = \sqrt{1 - |\alpha_n|^2} \quad (3.9)$$

(see [70, Section 4.2]). Since each of  $\mathcal{L}$  and  $\mathbf{M}$  is a direct sum of unitary matrices, each of  $\mathcal{L}$  and  $\mathbf{M}$  is unitary and hence  $\mathbf{G}$  is unitary as an operator on  $\ell^2(\mathbb{N})$ . The principal  $n \times n$  submatrix of  $\mathbf{G}$ , which depends only on the Verblunsky coefficients  $\alpha_0, \dots, \alpha_{n-1}$ , will also be called the  $n \times n$  *cut-off CMV matrix*, which we will denote by  $\mathbf{G}^{(n)} = \mathbf{G}^{(n)}(\alpha_0, \dots, \alpha_{n-1})$ . The cut-off CMV matrices are the canonical representation of the compressed multiplication operator (see [54]) and satisfy

$$\Phi_n^{(\alpha_0, \dots, \alpha_{n-1})}(z) = \det(z\mathbf{I}_n - \mathbf{G}^{(n)}). \quad (3.10)$$

Thus the eigenvalues of  $\mathbf{G}^{(n)}$  are the zeros of  $\Phi_n(z)$  up to algebraic multiplicity and are in the unit disk  $\mathbb{D}$ . Furthermore, we see from the construction that the operator norm  $\|\mathbf{G}^{(n)}\| = 1$  and

$$\text{rank}(\mathbf{I}_n - \mathbf{G}^{(n)}\mathbf{G}^{(n)*}) = \text{rank}(\mathbf{I}_n - \mathbf{G}^{(n)*}\mathbf{G}^{(n)}) = 1.$$

### 3.2 Blaschke Products

In recent history, finite Blaschke products have been commonly used in seeking to define and characterize Poncelet ellipses. Masayo Fujimura, Boris Mirman, and

Pamela Gorkin et. al. each used Blaschke products to prove many results that we build upon in this thesis, see for example [11, 13, 14, 22, 24, 55, 56], with [11, 13] as the main references for this section. A finite Blaschke product is a complex function analytic in an open neighborhood of  $\mathbb{D}$  of the form

$$B_n(z) = e^{i\theta} \prod_{j=1}^n \frac{z - f_j}{1 - \overline{f_j}z}. \quad (3.11)$$

Each  $f_j$  is inside the disc, so all of the zeros of  $B_n(z)$  are inside  $\mathbb{D}$  and all the poles are outside. These zeros also need not be distinct. We call  $n$  the *degree* of the Blaschke product. For the purposes of this dissertation, we consider only *normalized Blaschke products* where  $\theta = 0$  thus  $e^{i\theta} = 1$ . Then

$$B_n(z) = \prod_{j=1}^N \frac{z - f_j}{1 - \overline{f_j}z} = \frac{\Phi_n(z)}{\Phi_n^*(z)}, \quad (3.12)$$

the quotient of a monic orthogonal polynomial and it's reversed polynomial.

Blaschke products are Schur functions, meaning they map  $\mathbb{D}$  to itself. If  $|z| = 1$ ,  $|B_n(z)| = 1$  also. In fact, any nonconstant function analytic on an open set containing the disk that maps  $\mathbb{D}$  to itself and  $\mathbb{T}$  to itself is a finite Blaschke product (see [13] for a proof). Blaschke products are also  $n$ -to-1 mappings, so the preimage of  $B_n(z) = w$  is a set of  $n$  points. If  $\lambda \in \mathbb{T}$ , then  $B_n(z) = \lambda$  has  $n$  distinct solutions, all on  $\mathbb{T}$ .

**Definition 3.5.** If  $z_1^\lambda, \dots, z_n^\lambda$  are the solutions of  $B_n(z) = \lambda$ , then we say that the Blaschke product  $B_n$  *identifies* the set of points  $\mathcal{Z}^\lambda = \{z_1^\lambda, \dots, z_n^\lambda\}$ .

Note that this notation is purposely similar to Definition 3.4. For  $\Phi_n(z)$ , the paraorthogonal extension is the same as the set of points identified by the Blaschke product  $B_{n+1}(z) = \frac{z\Phi_n(z)}{\Phi_n^*(z)}$ . Blaschke products of this form that map zero to itself are called *regular* Blaschke products, i.e.

$$B_n(z) = \frac{z\Phi_{n-1}(z)}{\Phi_{n-1}^*(z)}. \quad (3.13)$$

Most of our results will depend on regular Blaschke products. Another interesting and useful quality of Blaschke products, as proved by Chandler, Gorkin, and Partington in [7], is that  $\arg(B(e^{i\theta}))$  is a strictly increasing function of  $\theta \in \mathbb{R}$ . These facts along with the following theorem [11, Theorem 2.3] will be helpful in our later analysis. Note the similarities between Theorem 3.6 and Theorem 3.3.

**Theorem 3.6.** *Given two sets of points  $\{z_j\}_{j=1}^n$  and  $\{z'_j\}_{j=1}^n$  interlaced on the unit circle, there is a unique (up to rotation) regular Blaschke product  $B_n$  such that  $B_n(z_j) = B_n(z_k)$  and  $B_n(z'_j) = B_n(z'_k)$  for all  $j$  and  $k$ .*

### 3.3 Numerical Range of a Matrix

Our final tool, the numerical range of matrices of a particular class,  $S_n$  (defined in Section 3.3.2) will be the lense through which we formulate the questions in Chapter Five, Chapter Six, Chapter Seven, and Chapter Eight:

Given  $f_1, f_2 \in \mathbb{D}$ , find a matrix  $\mathbf{A} \in S_n$  whose numerical range is bounded by a Poncelet- $(n+1)$  ellipse with foci  $f_1, f_2$ .

Note that Poncelet- $(n+1)$  ellipses are explicitly defined in Section 4.2. At this time, the reader should consider them to be ellipses in  $\mathbb{D}$  circumscribed by an infinite family of  $(n+1)$ -gons. As we will see in this section and later in Chapter Five, OPUC and Blaschke products are intricately connected to this question. The notation and properties below can be found in [43, 54].

#### 3.3.1 Definition and Basic Properties

The *numerical range* or *field of values* of a matrix  $\mathbf{A} \in \mathbb{C}^{n \times n}$  is the subset of the complex plane  $\mathbb{C}$  given by

$$W(\mathbf{A}) = \{x^* \mathbf{A} x : x \in \mathbb{C}^n, x^* x = 1\}.$$

In other words, the numerical range is the image of the Euclidean unit sphere under the continuous map  $x \mapsto x^* \mathbf{A} x$ .

For a matrix  $\mathbf{A}$ , the numerical range  $W(\mathbf{A})$  is a compact and convex subset of  $\mathbb{C}$  (Toeplitz–Hausdorff Theorem) that contains the spectrum  $\sigma(\mathbf{A})$  of  $\mathbf{A}$ , and it is invariant by unitary conjugation of  $\mathbf{A}$ . This shows that for normal matrices we can reduce the analysis of  $W(\mathbf{A})$  to the case of diagonal  $\mathbf{A}$ ; a straightforward consequence is that for a normal  $\mathbf{A}$ ,  $W(\mathbf{A})$  is the convex hull of  $\sigma(\mathbf{A})$ . In particular, for a unitary matrix  $\mathbf{A}$ , its numerical range is a convex polygon with vertices at its eigenvalues, which lie on  $\mathbb{T}$ . Thus  $W(\mathbf{A})$  is an  $n$ -gon inscribed in  $\mathbb{T}$  if  $\mathbf{A}$  is unitary. The numerical range is also monotone; that is, if  $\mathbf{A}$  is a contraction of  $\mathbf{B}$ , then  $W(\mathbf{A}) \subset W(\mathbf{B})$ . We will discuss this further in Section 3.3.3.

The numerical range of the Jordan block, see (3.14) defined below, is the circular disk with center at 0 and radius  $r = \cos(\pi/(n+1))$  [39, Proposition 1] (notice that for  $n = 2$  it satisfies Chapple’s formula (2.1)).

### 3.3.2 The Class $S_n$

A square complex matrix  $\mathbf{A} \in \mathbb{C}^{n \times n}$  is a *completely non-unitary contraction* if  $\|\mathbf{A}\| \leq 1$  and all eigenvalues of  $\mathbf{A}$  are strictly inside the unit disk  $\mathbb{D}$ . The space  $S_n$  is the set of completely non-unitary contractions in  $\mathbb{C}^{n \times n}$  with defect index

$$\text{rank}(\mathbf{I}_n - \mathbf{A}\mathbf{A}^*) = \text{rank}(\mathbf{I}_n - \mathbf{A}^*\mathbf{A}) = 1.$$

The spaces  $S_n$  and their infinite-dimensional analogues have been studied extensively, initially in the work of Livshitz [52], and in the 1960s by Sz.-Nagy and collaborators [75]. A canonical example of a matrix in  $S_n$  is a shift operator or  $n \times n$  nilpotent Jordan block

$$\mathbf{J}_n = \begin{pmatrix} 0 & & & \\ 1 & 0 & & \\ & 1 & 0 & \\ & & \ddots & \ddots \\ & & & 1 & 0 \end{pmatrix}_{n \times n}. \quad (3.14)$$

A remarkable property of the class  $S_n$  is that the spectrum  $\sigma(\mathbf{A})$  of a matrix  $\mathbf{A} \in S_n$  determines the unitary equivalence class of  $\mathbf{A}$ . It turns out that the equivalence class of  $\mathbf{A} \in S_n$  is determined even by its numerical range  $W(\mathbf{A})$ .

There are several “canonical” representations for matrices (or rather, of their unitary equivalence classes) in  $S_n$ , each having its own merit. For instance, we can think of elements of  $S_n$  as the “compressions of the shift” [75] or “compressed multiplication operators” [54] in a Hardy space setting. We can characterize  $\mathbf{A} \in S_n$  via their singular value decomposition (SVD),  $\mathbf{A} = \mathbf{U}\mathbf{D}\mathbf{V}^*$ , where  $\mathbf{U}$  and  $\mathbf{V}$  are unitary and  $\mathbf{D}$  is the diagonal matrix  $\text{diag}(1, \dots, 1, a)$  with  $0 \leq a < 1$  (see [79]). Another representation, also in [79], says that each such matrix  $\mathbf{A} = (a_{ij})_{i,j=1}^n \in S_n$  if and only if it is unitarily similar to an upper triangular matrix with elements satisfying  $|a_{ii}| < 1$  for all  $i$ , while for  $i < j$ ,

$$a_{ij} = b_{ij} (1 - |a_{ii}|^2)^{\frac{1}{2}} (1 - |a_{jj}|^2)^{\frac{1}{2}}, \quad b_{ij} = \begin{cases} \prod_{k=i+1}^{j-1} (-\bar{a}_{kk}) & \text{if } i < j-1 \\ 1 & \text{if } i = j-1. \end{cases}$$

From our observations above it follows that the cut-off CMV matrix  $\mathbf{G}^{(n)}$  is in the class  $S_n$ . In fact, from [54, Theorem 2] we know that every matrix from the class  $S_n$  is unitarily equivalent to a cutoff CMV matrix. In short, CMV matrices are another canonical representation of elements in  $S_n$ , which have several advantages. For instance, CMV matrices give us an effective construction of the equivalence class of  $\mathbf{A} \in S_n$  from its eigenvalues  $f_1, \dots, f_n$ : from the monic polynomial  $\Phi_n(z; f_1, \dots, f_n)$ ,

use inverse Szegő recursion to obtain the Verblunsky coefficients  $\alpha_0, \dots, \alpha_{n-1}$  and take  $\mathbf{A} = \mathcal{G}^{(n)}(\alpha_0, \dots, \alpha_{n-1})$ .

From these results and properties of OPUC, we can summarize the above by rephrasing [54, Theorem 3] in our context as follows.

**Theorem 3.7.** *For any set of  $n$  elements (with multiplicity) in  $\mathbb{D}$ , there is a CMV matrix with those eigenvalues. Any other matrix in  $S_n$  with the same eigenvalues is unitarily equivalent to this CMV matrix.*

### 3.3.3 Dilations

We say that an  $m \times m$  matrix  $\mathbf{A}$  *dilates* to the  $n \times n$  matrix  $\mathbf{B}$  ( $m < n$ ) if there is an isometry  $\mathbf{V}$  from  $\mathbb{C}^m$  to  $\mathbb{C}^n$  such that  $\mathbf{A} = \mathbf{V}^* \mathbf{B} \mathbf{V}$ . This is equivalent to saying that  $\mathbf{B}$  is unitarily similar to an  $n \times n$  matrix of the form

$$\begin{pmatrix} \mathbf{A} & * \\ * & * \end{pmatrix},$$

in which  $\mathbf{A}$  appears in the upper left corner. Equivalently, we can view  $\mathbf{A}$  as a contraction of  $\mathbf{B}$ . As stated before, the numerical range is monotone by dilation: if  $\mathbf{A}$  dilates to  $\mathbf{B}$ , then  $W(\mathbf{A}) \subset W(\mathbf{B})$ .

An important dilation, which is also closely related to the results we discuss, is the *unitary dilation of completely non-unitary contractions*. A classical result of Halmos [40, Problem 222(a)] says that every completely non-unitary contraction  $\mathbf{A}$  has unitary dilations.

As we have seen in Section 3.3.2, OPUC provides an effective construction of a matrix  $\mathbf{A}$  from any equivalence class of  $S_{n-1}$ . In the next section, we will see how OPUC does the same for a 1-parametric family of rank 1 unitary dilations of  $\mathbf{A} \in S_n$  (meaning  $(n+1) \times (n+1)$  unitary dilations of  $\mathbf{A}$ ).

*3.3.3.1 Dilations of CMV Matrices.* Recall that the OPUC  $\Phi_{n-1}(z)$  is the characteristic polynomial of a cutoff CMV matrix  $\mathcal{G}^{(n-1)}(\alpha_0, \dots, \alpha_{n-2}) \in S_{n-1}$  and that the parameter  $\lambda \in \mathbb{T}$  defines the paraorthogonal extension of  $\Phi_{n-1}(z)$ , see Definition 3.4. Using this same parameter  $\lambda$ , we can characterize a family of rank one unitary dilations of  $\mathcal{G}^{(n-1)}$ . By adding one row and one column to  $\mathcal{G}^{(n-1)}$ , we define a unitary  $n \times n$  matrix whose characteristic polynomial is  $\Phi_n^{(\lambda)}(z)$ .

Theorem 3.8. [54, Theorem 2.11] Fix  $\{\alpha_j\}_{j=0}^{n-2}$  all in  $\mathbb{D}$  and let  $\mathbf{A}$  be the corresponding CMV matrix. The POPUC of degree  $n$  are in one to one correspondence with the rank one unitary dilations of  $\mathbf{A}$ . The eigenvalues of the unitary,  $\mathbf{U}_\lambda$ , associated to  $\Phi_n^{(\lambda)}(z)$  are the zeros of that polynomial so that

$$\det(z - \mathbf{U}_\lambda) = \Phi_n^{(\lambda)}(z) \quad (3.15)$$

Indeed, for  $\mathbf{A} = \mathcal{G}^{(n-1)}(\alpha_0, \dots, \alpha_{n-2}) \in S_{n-1}$ , its unitary dilations are given by  $\mathcal{G}^{(n)}(\alpha_0, \dots, \alpha_{n-2}, \lambda)$ , with  $\lambda \in \mathbb{T}$ . As unitary matrices, the numerical range of these unitary dilations  $\mathbf{U}_\lambda$  are  $n$ -gons inscribed in  $\mathbb{T}$  with the vertices of the  $n$ -gons corresponding to the eigenvalues of the dilations (or equivalently the zeros of the POPUC). The next theorem uses the fact that  $W(\mathbf{A}) \subset W(\mathbf{U}_\lambda)$ ,  $\forall \lambda \in \mathbb{T}$  and describes the geometric connections between  $W(\mathbf{A})$  and  $W(\mathbf{U}_\lambda)$ .

Theorem 3.9. [54, Theorem 5] For each  $\lambda \in \mathbb{T}$ ,  $W(\mathbf{U}_\lambda)$  is a solid  $n$ -gon whose sides are tangent to  $W(\mathbf{A})$ .  $\partial W(\mathbf{A})$  is a strictly analytic convex curve, and

$$W(\mathbf{A}) = \bigcap_{\lambda \in \mathbb{T}} W(\mathbf{U}_\lambda). \quad (3.16)$$

Thus  $W(\mathcal{G}^{(n-1)})$  has the Poncelet property.

Example 3.10. Given

$$\Phi_3(z) = (z - 0.4 - 0.2i)(z + 0.7i)(z + 0.226164 - 0.507761i),$$

we can use  $\Phi_3(0) = -\overline{\alpha_2} = 0.14 - 0.28i$ , we can recover  $\alpha_1, \alpha_0$  by the inverse Szegő recursion and find

$$\mathbf{A} = \begin{pmatrix} -0.460317 - 0.595761i & -0.148852 - 0.334188i & 0.547118 \\ 0.658162 & -0.40661 - 0.0989909i & 0.382653 - 0.495246i \\ 0 & 0.831282 & 0.226164 - 0.507761i \end{pmatrix}.$$

Then for  $\lambda = 1$ , the rank one unitary dilation of  $\mathbf{A}$  is

$$\mathbf{U}_1 = \begin{pmatrix} -0.460317 - 0.595761i & -0.148852 - 0.334188i & 0.547118 & 0 \\ 0.658162 & -0.40661 - 0.0989909i & 0.382653 - 0.495246i & 0 \\ 0 & 0.831282 & 0.226164 - 0.507761i & 0 \\ 0 & 0 & 0 & 1 \end{pmatrix}.$$

We will explain in Chapter Six, Example 6.4 the motivation for matrix  $\mathbf{A}$ .

Note that one could also view these matrices through the lense of finite Blaschke products by associating to a Blaschke product a compression of the shift matrix. See, for example, [13].

### 3.3.4 Sketch of the Proof of Kippenhahn's Theorem

In this section, we provide a sketch of Kippenhahn's proof for Theorem 2.3 in the Introduction, which states that *for  $\mathbf{A} \in \mathbb{C}^{n \times n}$  there exists a real algebraic curve  $\Gamma$  of class  $n$  whose foci are the eigenvalues of  $\mathbf{A}$ , such that  $W(\mathbf{A})$  is the convex hull of  $\Gamma(\mathbb{R})$* . Note that some of the projective geometry terminology used in this sketch will be defined in the following section. As numerical ranges are the focus of the theorem, we include the proof here for completion.

In fact, the proof of Kippenhahn's Theorem is constructive and contains the derivation of an equation for the dual  $\Gamma^*$  of the algebraic curve  $\Gamma$ . Indeed, for the given matrix  $\mathbf{A} \in \mathbb{C}^{n \times n}$ , consider the homogeneous polynomial

$$G_{\mathbf{A}}(u_1, u_2, u_3) := \det(u_1 \operatorname{Re} \mathbf{A} + u_2 \operatorname{Im} \mathbf{A} - u_3 \mathbf{I}), \quad (3.17)$$

where  $\operatorname{Re} \mathbf{A} := (\mathbf{A} + \mathbf{A}^*)/2$  and  $\operatorname{Im} \mathbf{A} := (\mathbf{A} - \mathbf{A}^*)/(2i)$  are the real and imaginary parts of  $\mathbf{A}$ , respectively, and  $\mathbf{I}$  in this case denotes the  $n \times n$  identity matrix. It is easy to see that  $G_{\mathbf{A}}(u_1, u_2, u_3)$  is a homogenous polynomial of degree  $n$  with real coefficients. Thus  $G_{\mathbf{A}}(u_1, u_2, u_3) = 0$  defines a real algebraic curve  $\Gamma_{\mathbf{A}}^* \subset \mathbb{P}^2(\mathbb{C})$  of degree  $n$  that is the dual of an algebraic curve  $\Gamma_{\mathbf{A}} \subset \mathbb{P}^2(\mathbb{C})$  of class  $n$ . We will call  $\Gamma_{\mathbf{A}}$  the *Kippenhahn curve* of  $\mathbf{A}$ . As it follows from [46, 47] (see also [49, Theorem 6.1]), if we denote by  $\lambda_{\varphi} \in \mathbb{R}$ ,  $\varphi \in [0, 2\pi]$ , the maximal eigenvalue of the matrix  $\operatorname{Re}(e^{-i\varphi} \mathbf{A})$  then  $(\cos \varphi : \sin \varphi : \lambda_{\varphi}) \in \mathbb{P}^2(\mathbb{R})$  belongs to  $\Gamma_{\mathbf{A}}^*(\mathbb{R})$  and the equation

$$u_1 \cos \varphi + u_2 \sin \varphi - u_3 \lambda_{\varphi} = 0$$

defines a supporting line to  $W(\mathbf{A})$ . In consequence, the numerical range  $W(\mathbf{A})$  is the convex hull of  $\Gamma_{\mathbf{A}}(\mathbb{R})$ . Finally, as seen in (4.2), the real foci of  $\Gamma_{\mathbf{A}}$  are the solutions of

$$G_{\mathbf{A}}(1, i, z) = \det(\mathbf{A} - z \mathbf{I}) = 0,$$

that is, the eigenvalues of  $\mathbf{A}$ .

### 3.4 Projective Geometry

Finally, we will define a few elementary notions from projective algebraic geometry, which we will need throughout this thesis. All these results are standard and can be found in practically any text on classical algebraic geometry, see e.g.

[3, 4, 34, 45, 63, 68]. For the reader unfamiliar with projective geometry, we also recommend [58] as a helpful introduction.

As we seek to understand and classify Poncelet ellipses with given foci, projective geometry allows us in Chapter Four to rigorously define the Poncelet property, to understand Poncelet curves through the lense of the dual curves, and to understand the connections between the curve bounding the numerical range and other components of the curve  $C$ . The following brief background will set up the notation and basic concepts we use to build upon in the next chapter.

### 3.4.1 The Projective Plane

For any field  $\mathbb{K}$  such as  $\mathbb{R}$  or  $\mathbb{C}$ , the *projective plane*  $\mathbb{P}^2(\mathbb{K})$  over  $\mathbb{K}$  is the set of all equivalence classes of triples  $(x_1, x_2, x_3) \in \mathbb{K}^3 \setminus \{(0, 0, 0)\}$ , where  $(x_1, x_2, x_3)$  and  $(x'_1, x'_2, x'_3)$  are equivalent if and only if  $(x'_1, x'_2, x'_3) = (\lambda x_1, \lambda x_2, \lambda x_3)$  for some  $\lambda \in \mathbb{K} \setminus \{0\}$ . The equivalence class of a triple  $(x_1, x_2, x_3) \in \mathbb{K}^3 \setminus \{(0, 0, 0)\}$  is denoted  $(x_1 : x_2 : x_3)$  and is called the point of  $\mathbb{P}^2(\mathbb{K})$  with *homogenous coordinates*  $(x_1, x_2, x_3)$ . As usual, we embed the affine plane  $\mathbb{K}^2$  in  $\mathbb{P}^2(\mathbb{K})$  by identifying the point  $(x_1, x_2) \in \mathbb{K}^2$  with the point  $(x_1 : x_2 : 1) \in \mathbb{P}^2(\mathbb{K})$  and conversely, any point  $(x_1 : x_2 : x_3) \in \mathbb{P}^2(\mathbb{K})$  such that  $x_3 \neq 0$  with the point  $(x_1/x_3, x_2/x_3) \in \mathbb{K}^2$ . The complement of  $\mathbb{K}^2$  in  $\mathbb{P}^2(\mathbb{K})$ , that is, the set  $\{(x_1 : x_2 : x_3) \in \mathbb{P}^2(\mathbb{K}) : x_3 = 0\}$ , is called the *line at infinity*.

The *real projective plane*  $\mathbb{P}^2(\mathbb{R})$  is canonically embedded in *complex projective plane*  $\mathbb{P}^2(\mathbb{C})$ . Furthermore, for much of this paper, we will identify  $\mathbb{R}^2$  with  $\mathbb{C}$  and hence  $\mathbb{C}$  is embedded in  $\mathbb{P}^2(\mathbb{R})$  as above:

$$\mathbb{C} = \mathbb{R}^2 \subset \mathbb{P}^2(\mathbb{R}), \quad x + iy = (x, y) \mapsto (x : y : 1). \quad (3.18)$$

We view  $\mathbb{P}^2(\mathbb{R})$  as a real two-dimensional compact manifold in the usual way so that (3.18) is an open embedding. The image of this embedding is dense in  $\mathbb{P}^2(\mathbb{R})$ , and

hence  $\mathbb{P}^2(\mathbb{R})$  is a compactification of  $\mathbb{C}$ . This compactification is not to be confused with the one-point compactification of  $\mathbb{C}$  which is the Riemann sphere.

*3.4.1.1 Real algebraic curves.* A curve defined by a homogeneous polynomial  $f(x, y, z) = 0$  in the projective plane is an *algebraic curve* [58]. A *plane real algebraic curve* of degree  $d$  is an algebraic curve  $\Gamma \subset \mathbb{P}^2(\mathbb{C})$  defined by an equation  $F(x_1, x_2, x_3) = 0$ , where  $F(x_1, x_2, x_3)$  is a nonzero homogeneous polynomial whose terms are all of degree  $d$  with *real* coefficients. Notice that  $F(x_1, x_2, x_3)$  being zero only depends on the equivalence class of the triplet  $(x_1, x_2, x_3)$  since  $F(kx, ky, kz) = k^d F(x, y, z)$ , and that although we speak about a real curve  $\Gamma$ , we have  $\Gamma \subset \mathbb{P}^2(\mathbb{C})$ . We say that the curve  $\Gamma$  is *irreducible* if the polynomial  $F(x_1, x_2, x_3)$  is irreducible over  $\mathbb{C}$ .

The *set of real points* of a real algebraic curve  $\Gamma \subset \mathbb{P}^2(\mathbb{C})$  is defined as the set

$$\Gamma(\mathbb{R}) := \Gamma \cap \mathbb{P}^2(\mathbb{R}).$$

In this dissertation, we will be very careful to always distinguish between  $\Gamma$  and  $\Gamma(\mathbb{R})$ .

If  $f(x, y)$  is any (not necessarily homogenous) polynomial of degree  $d$  with real coefficients, then  $F(x_1, x_2, x_3) := x_3^d f(x_1/x_3, x_2/x_3)$  is a homogenous polynomial of degree  $d$  with real coefficients. Thus, a nonzero polynomial  $f(x, y)$  with real coefficients defines a real algebraic curve  $\Gamma$  via this homogenization. Geometrically,  $\Gamma$  is the projective closure of the curve given by the equation  $f(x, y) = 0$ , that is,  $\Gamma = \text{clo}\{(x, y) \in \mathbb{C}^2 : f(x, y) = 0\}$ . Conversely,  $F(x_1, x_2, x_3)$  can be dehomogenized by setting  $f(x, y) := F(x, y, 1)$  and we have  $\Gamma \cap \mathbb{C}^2 = \{(x, y) \in \mathbb{C}^2 : f(x, y) = 0\}$ .

Remark 3.11. We should emphasize that a real plane algebraic curve  $\Gamma$  is more than its set of real points  $\Gamma(\mathbb{R})$  and even the set of complex points of  $\Gamma$  does not determine its defining polynomial  $F(x_1, x_2, x_3)$ . However, if we assume that  $F(x_1, x_2, x_3)$  is square-free, that is, without any repeated irreducible factors, then  $\Gamma$  determines

$F(x_1, x_2, x_3)$  uniquely up to a nonzero multiplicative constant. We will always make this assumption.

The following algebraic geometry theorem, known as Bezout's Theorem, will be useful for proofs in later sections.

**Theorem 3.12.** [21, Chapter 4] *Let  $F = 0, G = 0$  be two curves in the projective plane, where  $F$  and  $G$  are homogeneous polynomials without a common factor. Then the number of intersections of the two curves equals the product of the degrees of  $F$  and  $G$ , provided one counts multiplicities.*

*3.4.1.2 Nonsingular and singular points.* Suppose  $\Gamma$  is defined by the equation  $F(x_1, x_2, x_3) = 0$ . Then  $(a_1 : a_2 : a_3) \in \Gamma$  is called a *nonsingular point* of  $\Gamma$  if

$$\left( \frac{\partial F}{\partial x_1}(a_1, a_2, a_3), \frac{\partial F}{\partial x_2}(a_1, a_2, a_3), \frac{\partial F}{\partial x_3}(a_1, a_2, a_3) \right) \neq (0, 0, 0);$$

otherwise  $(a_1 : a_2 : a_3)$  is a *singular point*. We say that  $\Gamma$  (resp.,  $\Gamma(\mathbb{R})$ ) is *nonsingular*, if all points of  $\Gamma$  (resp.,  $\Gamma(\mathbb{R})$ ) are nonsingular. Note that if  $(a_1 : a_2 : a_3)$  is a nonsingular point, then the equation

$$\frac{\partial F}{\partial x_1}(a_1 : a_2 : a_3) x_1 + \frac{\partial F}{\partial x_2}(a_1 : a_2 : a_3) x_2 + \frac{\partial F}{\partial x_3}(a_1 : a_2 : a_3) x_3 = 0 \quad (3.19)$$

defines a line in  $\mathbb{P}^2(\mathbb{R})$  (resp.,  $\mathbb{P}^2(\mathbb{C})$ ) which is called the *tangent line* of  $\Gamma(\mathbb{R})$  (resp.,  $\Gamma$ ) at the point  $(a_1 : a_2 : a_3)$ . If  $(a_1 : a_2 : a_3)$  is a singular point, then the equation (3.19) is meaningless. However, since an algebraic curve has only finitely many singular points (and hence every singular point is an isolated point), tangent lines at a singular point

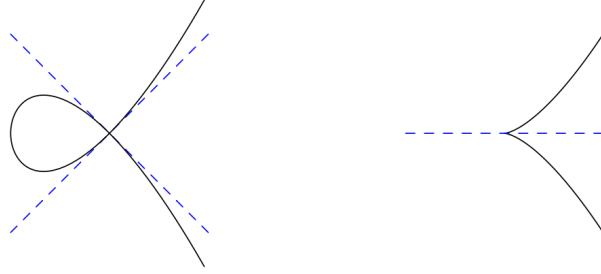


Figure 3.1. Tangent lines at a node (left) and at a cusp.

$(a_1 : a_2 : a_3)$  can be defined by continuity. For example, Figure 3.1 shows the tangent lines at a *node* (or *ordinary double point*) and at a *cusp* (or *return point*).

### 3.4.2 Duality

Points and lines are duals of one another. Thus as  $\mathbb{P}^2(\mathbb{K})$  is defined by equivalence classes of points, the *dual projective plane*  $\mathbb{P}^2(\mathbb{K})^*$  is the set of lines in  $\mathbb{P}^2(\mathbb{K})$ . We will identify  $\mathbb{P}^2(\mathbb{K})$  with  $\mathbb{P}^2(\mathbb{K})^*$  by letting the point  $(u_1 : u_2 : u_3) \in \mathbb{P}^2(\mathbb{K})$  correspond to the line in  $\mathbb{P}^2(\mathbb{K})$  given by the equation

$$u_1x_1 + u_2x_2 - u_3x_3 = 0. \quad (3.20)$$

Note that via this identification, we can view  $\mathbb{P}^2(\mathbb{R})^*$  as a subset of  $\mathbb{P}^2(\mathbb{C})^*$ . The motivation for the negative sign in (3.20) will be explained in the next subsection.

The *dual* of a real algebraic curve  $\Gamma \subset \mathbb{P}^2(\mathbb{C})$  is the real algebraic curve  $\Gamma^* \subset \mathbb{P}^2(\mathbb{C})$  whose points correspond to the tangent lines of  $\Gamma$ , that is,

$$\Gamma^* := \{(u_1 : u_2 : u_3) \in \mathbb{P}^2(\mathbb{C}) : u_1x_1 + u_2x_2 - u_3x_3 = 0 \text{ is a tangent line of } \Gamma\}. \quad (3.21)$$

In this context, triples  $(u_1 : u_2 : u_3)$  are known as the *tangent coordinates* of the dual  $\Gamma^*$ .

Given an equation  $F(x_1, x_2, x_3) = 0$  that defines  $\Gamma$ , we can find an equation  $G(u_1, u_2, u_3) = 0$  that defines  $\Gamma^*$  by eliminating the variables  $x_1, x_2, x_3$  from the system of equations

$$F(x_1, x_2, x_3) = 0, \quad \frac{\partial F}{\partial x_1}(x_1, x_2, x_3) = u_1, \quad \frac{\partial F}{\partial x_2}(x_1, x_2, x_3) = u_2, \quad \frac{\partial F}{\partial x_3}(x_1, x_2, x_3) = -u_3.$$

The terminology “dual” is justified by the fact that  $(\Gamma^*)^* = \Gamma$ . The degree of  $\Gamma^*$  is called the *class* of  $\Gamma$ . The relationship between the degree  $d$  and the class of  $\Gamma$ ,  $d'$ , is rather subtle and is described by Plücker’s formula

$$d' = d(d - 1) - 2r - 3s \tag{3.22}$$

where  $d$  is the degree of  $\Gamma^*$ ,  $r$  is the number of double points, and  $s$  is the number of singularities. In the special case when  $\Gamma$  is nonsingular, Plücker’s formula says that the class of  $\Gamma$  is equal to  $d(d - 1)$ . Since  $(\Gamma^*)^* = \Gamma$ , this means that if  $\Gamma$  is nonsingular and  $d > 2$ , then  $\Gamma^*$  must have singular points. The dual of nonsingular conic ( $d = 2$ ) is again a nonsingular conic; the dual of a line ( $d = 1$ ) is a point.

We will be mostly interested in the set of real points of the duals of real algebraic curves. Suppose  $C \subseteq \Gamma(\mathbb{R})$  is a union of path-components of the set of real points of a real algebraic curve  $\Gamma$ . Then we define the dual of  $C$  as the set

$$C^* := \{(u_1 : u_2 : u_3) \in \mathbb{P}^2(\mathbb{R}) : u_1 x_1 + u_2 x_2 - u_3 x_3 = 0 \text{ is a tangent line of } C\}. \tag{3.23}$$

In particular,  $C^* \subseteq \Gamma^*(\mathbb{R})$ . Furthermore, if  $C$  is a path-component of  $\Gamma(\mathbb{R})$ , then  $C^*$  is a path-component of  $\Gamma^*(\mathbb{R})$  and  $(C^*)^* = C$ .

### 3.4.3 Reciprocation About $\mathbb{T}$

A nice geometric interpretation of duality in the real projective plane  $\mathbb{P}^2(\mathbb{R})$  can be given in terms of so-called reciprocation about the unit circle  $\mathbb{T}$ . In the following, we will view  $\mathbb{C} \subset \mathbb{P}^2(\mathbb{R})$  as in (3.18). Then  $\mathbb{T}$  is the set of real points of the algebraic curve given by  $x_1^2 + x_2^2 - x_3^2 = 0$ .

The *reciprocal* or *polar* of a point  $\zeta = u + iv \neq 0$  in  $\mathbb{C}$  about  $\mathbb{T}$  is the line  $\ell$  that contains the point  $\zeta/|\zeta|^2$  and is perpendicular to the ray from 0 through  $\zeta$  (see Figure 3.2). We also say that  $\zeta$  is the *reciprocal* or the *pole* of  $\ell$ . The reciprocal of the origin 0 is the line at infinity  $\ell_\infty$ . We can extend reciprocation about  $\mathbb{T}$  to give a bijection between points and lines in  $\mathbb{P}^2(\mathbb{R})$ . It is an easy exercise to verify that the reciprocal of the point  $(u_1 : u_1 : u_3) \in \mathbb{P}^2(\mathbb{R})$  about  $\mathbb{T}$  is precisely the line given by the equation  $u_1x_1 + u_2x_2 - u_3x_3 = 0$  (which motivates the definition (3.20)–(3.21)).

Suppose  $l$  is a line in  $\mathbb{C}$  that intersects the unit circle  $\mathbb{T}$  in two distinct points  $z_1$  and  $z_2$ . Then  $l$  is given by the equation

$$z + z_1z_2\bar{z} - (z_1 + z_2) = 0 \quad (3.24)$$

in the complex variable  $z$ . If we write  $z = x+iy$  and compare (3.24) to  $ux+vy-1 = 0$ , we obtain

$$u = \frac{1 + z_1z_2}{z_1 + z_2}, \quad v = i\frac{1 - z_1z_2}{z_1 + z_2}, \quad \zeta = u + iv = \frac{2z_1z_2}{z_1 + z_2}. \quad (3.25)$$

Using (3.25), it is now straightforward to express the elementary symmetric functions  $z_1 + z_2$  and  $z_1z_2$  in terms of  $\zeta = u + iv$  as follows:

$$z_1 + z_2 = \frac{2}{\bar{\zeta}}, \quad z_1z_2 = \frac{\zeta}{\bar{\zeta}}. \quad (3.26)$$

This in turn allows us to write

$$z_1 = \frac{1 + i\sqrt{\zeta\bar{\zeta} - 1}}{\zeta}, \quad z_2 = \frac{1 - i\sqrt{\zeta\bar{\zeta} - 1}}{\zeta}. \quad (3.27)$$

Geometrically, the points  $z_1, z_2 \in \mathbb{T}$  are the points where the two tangent lines to  $\mathbb{T}$  containing the point  $\zeta$  touch  $\mathbb{T}$  (see Figure 3.2).

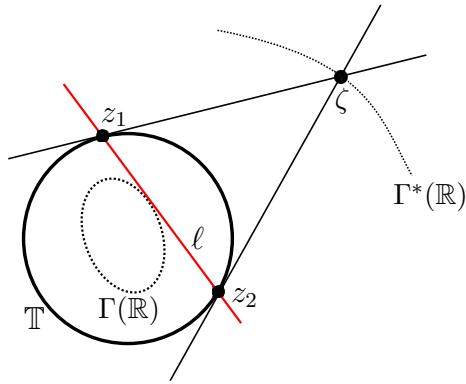


Figure 3.2. Geometric construction of the dual curve via reciprocation.

#### 3.4.4 The Notion of an Envelope

In the next chapter, we will use these concepts to carefully define and prove some theorems about curves exhibiting this Poncelet property. To do this, we must first understand one more projective geometry concept mentioned briefly in Chapter Two.

In discussing Darboux's work, we mentioned a connection between curves and the *envelope* of all the diagonals of the family of  $n$ -sided polygons. To define an envelope, begin with a one-parameter family of curves defined by a homogenous equation  $f(x, y, \lambda) = 0$  where  $\lambda$  is a parameter. A curve that is tangent to every curve in the family (i.e. every point of this second curve is tangent to one of the curves in the one-parameter family of curves) is called the *envelope* of this family. The envelope can be defined parametrically using the equation of the family of curves and its derivative with respect to  $\lambda$  then eliminating  $\lambda$  from this system. Note that not every family

of curves has an envelope. A necessary condition for the existence of an envelope is the computability of this system of equations. For example, the family of concentric circles  $x^2 + y^2 = C^2$  does not have an envelope. Several examples and pictures can be found at [74].

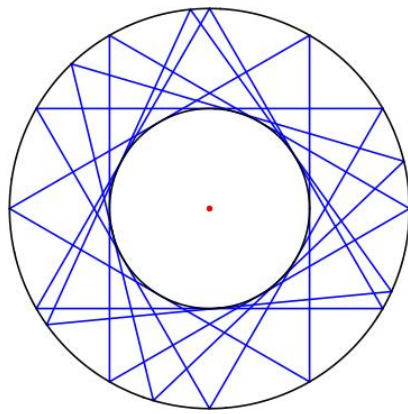


Figure 3.3. The circle of radius  $\frac{1}{2}$  is the envelope of the sides of the triangles, and the unit circle is the envelope of the vertices of the triangles.

In this dissertation, when we discuss the envelope, we do not formally compute it in this way. Instead, since we are working in the specific case of the circle, we can view the envelope geometrically through the dual of the dual curve. This will be explained more in Chapter Four.

## CHAPTER FOUR

### General Poncelet Curves

A majority of this chapter is submitted for publication as Markus Hunziker, Andrei Martíez-Finkelshtein, Taylor Poe, and Brian Simanek, *Poncelet-Darbous, Kippenhahn, and Szegő: interactions between projective geometry, matrices and orthogonal polynomials*, Preprint, 2021.

As discussed in Chapter Three, Poncelet's porism has inspired a significant amount of research both historically and presently. Many of the different results use similar terminology and notation, but these terms are not always well defined. In what follows, we seek to make these notions rigorous. Much of the terminology in the literature was left undefined because their meaning was fairly obvious, especially pictorially. For example, defining a polygon seems unnecessary. However, having the following formal definition of a general  $n$ -gon helps when we want to discuss atypical polygons.

#### *4.1 The Poncelet Property*

##### *4.1.1 Definitions*

We denote by  $[a, b]$  the straight segment joining points  $a, b \in \mathbb{C}$ . For  $n \geq 3$ , a *polygon* with  $n$  vertices in  $\mathbb{C}$  is a union of  $n$  distinct segments

$$\mathcal{P} = [z_1, z_2] \cup [z_2, z_3] \cup \cdots \cup [z_{n-1}, z_n] \cup [z_n, z_1], \quad (4.1)$$

where  $z_1, \dots, z_n \in \mathbb{C}$  are  $n$  distinct points, such that any two segments intersect in at most one point and any two segments sharing a common endpoint are noncollinear. The  $n$  segments are called the *sides* or the *edges* of the polygon. If the sides of  $\mathcal{P}$

only intersect when they share a common endpoint, then  $\mathcal{P}$  is called *simple*, and if all its vertices belong to  $\mathbb{T}$  we say that  $\mathcal{P}$  is *inscribed* in  $\mathbb{T}$ . It is well-known that any simple polygon inscribed in  $\mathbb{T}$  is convex.

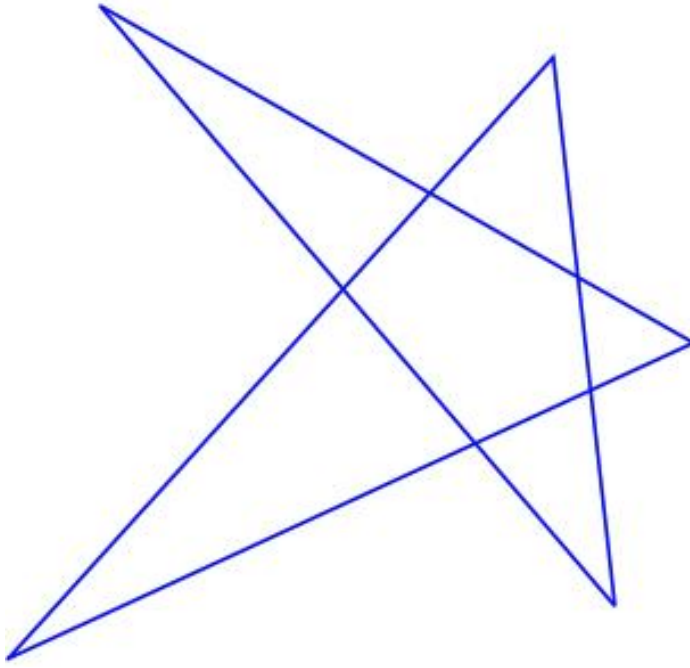


Figure 4.1. Rather than connecting adjacent vertices, we can connect alternate vertices to form a nonconvex pentagon.

We will often view the segments in (4.1) as directed line segments and hence  $\mathcal{P}$  as an oriented piecewise linear closed curve; in consequence, the notation  $-\mathcal{P}$  stands for the polygon  $\mathcal{P}$  traversed in the opposite direction. Note that every simple polygon is a Jordan curve and hence divides the complex plane  $\mathbb{C}$  into an interior region and an exterior region. As usual, we say that a simple polygon  $\mathcal{P}$  is *positively oriented* if the interior is to the left. Equivalently, a simple polygon is positively oriented if its winding number with respect to any point in its interior (integer number of times the curve travels counterclockwise around the given point) is equal to 1. For a general (not necessarily simple) oriented polygon  $\mathcal{P}$ , if we traverse  $\mathcal{P}$  in the direction of the

orientation, then at each vertex we turn by a nonzero angle between  $-\pi$  and  $\pi$ . The sum of these turning angles divided by  $2\pi$  is called the *turning number* of  $\mathcal{P}$ . If  $\mathcal{P}$  is simple, then the turning number is equal to the winding number with respect to a point in the interior. We say that  $\mathcal{P}$  is positively oriented if its turning number is positive.

**Definition 4.1.** By a *closed curve* we mean a subset  $C \subset \mathbb{P}^2(\mathbb{R})$  such that there exist a continuous map  $\gamma : \mathbb{T} \rightarrow \mathbb{P}^2(\mathbb{R})$  with  $C = \gamma(\mathbb{T})$  and a real algebraic curve  $\Gamma$  such that  $C \subset \Gamma(\mathbb{R})$  with the additional condition that either all points of  $C$  are nonsingular or the parametrization  $\gamma$  can be chosen such that if  $\gamma(t_0)$  is a singular point of  $\Gamma$ , then for some sufficiently small interval  $I \subset \mathbb{T}$  containing  $t_0$ , the curve  $\gamma(I)$  lies in a single local branch of  $\Gamma$ . If  $C$  is nonsingular, then  $C$  is a simple closed curve in  $\mathbb{C}$ . We also allow for the degenerate case when  $C$  consists of just a single point.

Notice that algebraicity is built into our definition of a closed curve; in the following, all closed curves that we consider will be duals of smooth closed curves in  $\mathbb{P}^2(\mathbb{R})$ .

#### 4.1.2 Foci of a Curve

In the study of real conics (real algebraic curves of degree 2), the points called foci have played a central role since antiquity. The term “foci” is especially well understood in the context of an ellipse, but for a general higher degree curve, this concept is not as clear. Plücker generalized the concept of foci to curves of higher degree as follows. A point  $(a_1 : a_2 : a_3) \in \mathbb{P}^2(\mathbb{C})$  is called a *focus* of a real algebraic curve  $\Gamma \subset \mathbb{P}^2(\mathbb{C})$  if the two lines through  $(a_1 : a_2 : a_3)$  and the so-called circular points at infinity  $(1 : \pm i : 0)$  are tangent to  $\Gamma$ . A focus  $(a_1 : a_2 : a_3)$  of  $\Gamma$  is called a *real focus* if  $(a_1 : a_2 : a_3) \in \mathbb{P}^2(\mathbb{R})$ .

It is easy to verify that the lines in  $\mathbb{P}^2(\mathbb{C})$  through  $(a_1 : a_2 : a_3)$  and  $(1 : \pm i : 0)$  are given by the equations  $a_3x_1 \pm a_3x_2 - (a_1 \pm ia_2)x_3 = 0$ , respectively. Thus, if

$G(u_1, u_2, u_3) = 0$  is the equation defining the dual curve  $\Gamma^*$ , then  $(a_1 : a_2 : a_3) \in \mathbb{P}^2(\mathbb{C})$  is a focus of  $\Gamma$  if and only if  $G(a_3, \pm ia_3, a_1 \pm ia_2) = 0$ . If  $(a_1 : a_2 : a_3) \in \mathbb{P}^2(\mathbb{R})$ , then  $G(a_3, -ia_3, a_1 - ia_2) = \overline{G(a_3, ia_3, a_1 + ia_2)}$  since the coefficients of  $G(u_1, u_2, u_3)$  are real. So,  $(a_1 : a_2 : a_3) \in \mathbb{P}^2(\mathbb{R})$  is a real focus of  $\Gamma$  if and only if  $G(a_3, ia_3, a_1 + ia_2) = 0$ . Viewing  $\mathbb{C} \subset \mathbb{P}^2(\mathbb{R})$  as in (3.18), we see that  $z \in \mathbb{C}$  is a real focus of  $\Gamma$  if and only if

$$G(1, i, z) = 0. \quad (4.2)$$

If  $C$  is an ellipse, then this definition aligns with our usual understanding of foci.

#### 4.2 Poncelet Curves

Definition 4.2. For  $n \geq 2$ , we say that a set of (not necessarily simple)  $n$ -sided polygons  $\{\mathcal{P}(z) : z \in \mathbb{T}\}$  inscribed in  $\mathbb{T}$  is a *family of n-Poncelet polygons* if for each  $z \in \mathbb{T}$ ,  $z$  is one of the vertices of  $\mathcal{P}(z)$ , and the following condition holds:

$$w \in \mathbb{T} \text{ is a vertex of } \mathcal{P}(z) \Rightarrow \mathcal{P}(z) = \mathcal{P}(w).$$

A closed curve  $C \subset \mathbb{D}$  is a *Poncelet curve of rank n* or an *n-Poncelet curve* with respect to  $\mathbb{T}$  if there is a family of  $n$ -Poncelet polygons  $\{\mathcal{P}(z) : z \in \mathbb{T}\}$  such that

- (i) for every  $z \in \mathbb{T}$ , each of the  $n$  sides of  $\mathcal{P}(z)$  is tangent to  $C$ , and each tangent line of  $C$  passing through  $z$  contains a side of  $\mathcal{P}(z)$ ;
- (ii) for every  $z \in \mathbb{T}$ , the two sides of  $\mathcal{P}(z)$  with the common vertex at  $z$  are the only tangents to  $C$  emanating from  $z$ ;
- (iii) for every  $\zeta \in C$  there exists  $z \in \mathbb{T}$  such that one of the sides of  $\mathcal{P}(z)$  is tangent to  $C$  at the point  $\zeta$ .

Note that we say a curve  $C$  has the  $n$ -Poncelet property if it is circumscribed by  $n$ -gons. For Poncelet polygons, the  $n$  describes the number of sides of the polygon.

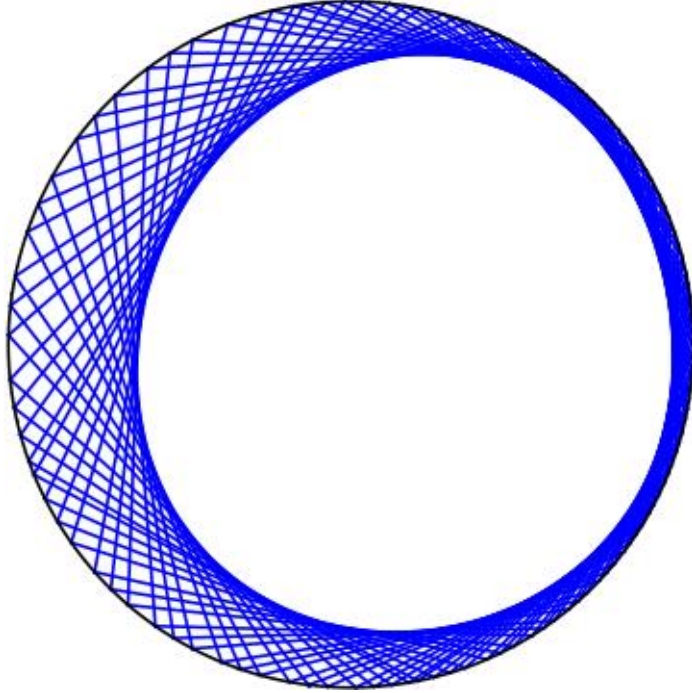


Figure 4.2. A family of Poncelet hexagons.

Notice that an  $n$ -Poncelet curve  $C$  determines the family  $\{\mathcal{P}(z) : z \in \mathbb{T}\}$  uniquely. Observe also that we set a convention that  $C \subset \mathbb{D}$  is a necessary condition for  $C$  being called a Poncelet curve.

If  $\mathcal{Z}^\lambda = \{z_1^\lambda, \dots, z_n^\lambda\}$  is a one-parametric family of pairwise distinct points on  $\mathbb{T}$  such that for every  $z \in \mathbb{T}$  there exists a unique value of the parameter  $\lambda$  for which  $z \in \mathcal{Z}^\lambda$ , then convex hulls of  $\mathcal{Z}^\lambda$  constitute a family of convex  $n$ -Poncelet polygons. An example of such a construction is the sets of points identified by a Blaschke product, see Definition 3.5, or the paraorthogonal extension, see Definition 3.4.

Recall that these polygons need not be convex for Poncelet's Theorem to hold. Convexity of a Poncelet curve does not imply convexity of its Poncelet polygons, see for example curve  $C_2$  in Figure 4.3, left. Surprisingly, the converse does not hold either (despite an assertion in [55, Remark 1]): there are non-convex Poncelet curves

with the corresponding family of convex Poncelet polygons; see Figure 4.3, right, for a non-convex 3-Poncelet curve.

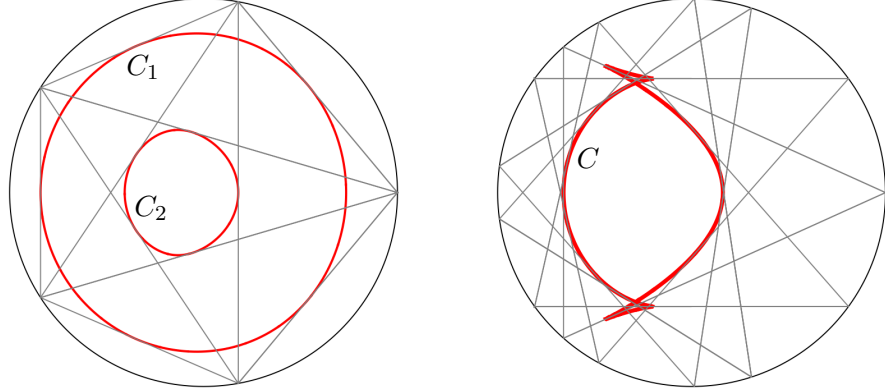


Figure 4.3. Left: two convex 5-Poncelet curves: for  $C_1$  all its Poncelet polygons  $\mathcal{P}(z)$  are convex, while for  $C_2$  they are not. Right: a non-convex 3-Poncelet curve.

Given a family of positively oriented  $n$ -Poncelet polygons  $\{\mathcal{P}(z) : z \in \mathbb{T}\}$  in the sense of Definition 4.2, we define the map  $\tau : \mathbb{T} \rightarrow \mathbb{T}$  as follows: if  $[z, w]$  is the edge of the polygon  $\mathcal{P}(z)$  emanating from  $z \in \mathbb{T}$  when traversed in the positive direction, then  $\tau(z) = w \in \mathbb{T}$ . The sequence  $\{\tau^j(z)\}_{j=1}^\infty$  is periodic with period  $n$  (that is,  $n$  is the smallest positive integer such that  $\tau^n = \text{Id}$ , where  $\text{Id}$  is the identity operator), and the positively oriented  $n$ -Poncelet polygons  $\{\mathcal{P}(z) : z \in \mathbb{T}\}$  can be written as

$$\mathcal{P}(z) = [z, \tau(z)] \cup [\tau(z), \tau^2(z)] \cup \cdots \cup [\tau^{n-1}(z), z]. \quad (4.3)$$

The map  $\tau : \mathbb{T} \rightarrow \mathbb{T}$ , is also known as the *Poncelet correspondence*, see [21]. Notice that in the construction of  $\tau$  we could start alternatively from an  $n$ -Poncelet curve  $C$  and use its family of  $n$ -Poncelet polygons  $\{\mathcal{P}(z) : z \in \mathbb{T}\}$  to define  $\tau$ . We will assume that  $\tau$  is smooth and

$$\frac{d}{d\theta} \arg \tau(e^{i\theta}) > 0 \text{ for all } \theta \in \mathbb{R}, \quad (4.4)$$

where the argument of  $\tau(e^{i\theta})$  is viewed as a smooth  $\mathbb{R}$ -valued function of  $\theta \in \mathbb{R}$ . The condition (4.4) automatically holds if the family  $\{\mathcal{P}(z) : z \in \mathbb{T}\}$  corresponds to a convex and nonsingular  $n$ -Poncelet curve  $C \subset \mathbb{D}$ .

**Remark 4.3.** The Poncelet correspondence provides a connection between Poncelet curves and discrete dynamical systems and ellipsoidal billiards, see e.g. the work of Dragović and collaborators [1, 20] and Schwarz [60, 67], and in some particular cases is related to the John mapping, see [6].

### 4.3 Envelopes of Chords of Poncelet Polygons

The curve  $C$  can have several connected components. For  $k \in \mathbb{N}$ , we define a curve  $C_k \subset \mathbb{D}$  as the envelope of all chords  $[z, \tau^k(z)]$ , where  $z \in \mathbb{T}$ , the cords connecting every  $k$ th vertex of the polygons. A priori, it is not evident that this definition makes sense. For example, we really should consider the envelope of all lines determined by the chords  $[z, \tau^k(z)]$  since it is not clear that the points of tangency of the line through  $z, \tau^k(z)$  to  $C$  must lie on these chords. This is rather subtle, and our next theorem shows that it is precisely the monotonicity condition (4.4) which implies this. First we will define a dual curve to  $C_k$ , and then we will use this dual to better understand  $C_k$ .

Define a map  $\zeta_k : \mathbb{T} \rightarrow \mathbb{P}^2(\mathbb{R})$  by

$$\zeta_k(z) := \frac{2z \tau^k(z)}{z + \tau^k(z)} = \text{pole of the line containing } [z, \tau^k(z)], \quad (4.5)$$

see (3.25). By construction, if  $z \neq \tau^k(z)$  then  $\zeta_k(z)$  lies outside of the unit disk. Since  $\tau^n = \text{Id}$ , we only need to consider  $1 \leq k \leq n - 1$ . Note that  $\zeta_2$  is related to the pentagram map, see e.g. [66, 67].

**Lemma 4.4.** *For each  $1 \leq k \leq n - 1$ , the map  $\zeta_k : \mathbb{T} \rightarrow \mathbb{P}^2(\mathbb{R})$  is a smooth immersion, and the image  $\zeta_k(\mathbb{T})$  is nonsingular.*

*Proof.* By our assumptions, the map  $\tau : \mathbb{T} \rightarrow \mathbb{T}$  is smooth so that each of the maps  $\zeta_k : \mathbb{T} \rightarrow \mathbb{P}^2(\mathbb{R})$  is also smooth, and the argument of  $\tau(e^{i\theta})$  is a strictly increasing smooth function when viewed as a continuous  $\mathbb{R}$ -valued function of  $\theta \in \mathbb{R}$ . It then also follows that the argument of  $\tau^k(e^{i\theta})$  is a strictly increasing function of  $\theta \in \mathbb{R}$ . As a consequence, the differential of the map  $\zeta_k : \mathbb{T} \rightarrow \mathbb{P}^2(\mathbb{R})$  is nonzero everywhere and hence  $\zeta_k$  is a smooth immersion. Since an immersion is a local embedding, it follows that  $\zeta_k(\mathbb{T})$  is nonsingular.  $\square$

**Definition 4.5.** For each  $1 \leq k \leq n - 1$ , the curve  $C_k$  is the dual of the nonsingular curve  $\zeta_k(\mathbb{T})$ .

Notice that  $C_k$  may have singularities. As usual, cusps of  $C_k$  correspond to tangent lines at inflection points of  $\zeta_k(\mathbb{T})$  and double points of  $C_k$  correspond to lines that are tangent at two distinct points of  $\zeta_k(\mathbb{T})$ , see e.g. Figure 4.5.

**Theorem 4.6.** *For each  $1 \leq k \leq n - 1$ , assumption (4.4) implies that  $C_k \subset \mathbb{D}$ . If*

$$\frac{d}{d\theta} \arg \tau(e^{i\theta}) \geq 0 \text{ for all } \theta \in \mathbb{R}$$

*then  $C_k \subset \overline{\mathbb{D}}$  and can have points on  $\mathbb{T}$  (see Figure 4.4).*

*Finally, if at some  $\theta \in \mathbb{R}$ ,*

$$\frac{d}{d\theta} \arg \tau(e^{i\theta}) < 0$$

*then  $C_k$  has points outside  $\overline{\mathbb{D}}$ .*

*Proof.* It is sufficient to prove the statement for  $k = 1$ .

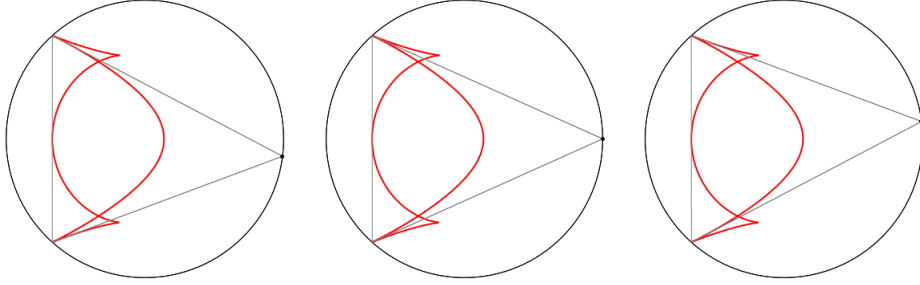


Figure 4.4. A family of 3-Poncelet polygons such that the curve  $C_1$  has a cusp on  $\mathbb{T}$ . The highlighted point on  $\mathbb{T}$  corresponds to  $e^{i\theta}$  for the values  $\theta = -\pi/25, 0$ , and  $\pi/25$ , respectively. The function  $\arg \tau(e^{i\theta})$  is strictly increasing but has a stationary point at  $\theta = 0$ ;  $C_1$  intersects  $\mathbb{T}$ .

The curve  $C_1$  is obtained from the tangent lines to curve  $\zeta_1(\mathbb{T})$  via reciprocation in  $\mathbb{T}$ . In particular,  $C_1$  contains a point outside of  $\overline{\mathbb{D}}$  if and only if there is a tangent line to  $\zeta_1(\mathbb{T})$  that intersects  $\mathbb{T}$  in two distinct points (or alternatively, whose distance to the origin is  $< 1$ ).

In order to simplify notation, denote

$$w = \tau(z), \quad w' = \frac{d}{dz}\tau(z), \quad \dot{w} = \frac{d}{d\theta}\arg \tau(e^{i\theta}).$$

Since  $w \in \mathbb{T}$ ,  $\log w = i \arg w$ , we get that

$$\dot{w} = \frac{zw'}{w}.$$

Recall from (4.4) that  $\dot{w}$  is real valued. Thus, differentiating  $\zeta_1(z) = 2zw/(z + w)$  with  $z = e^{i\theta}$  and  $\zeta_1 = \zeta_1(z)$ , we get that

$$\begin{aligned} \frac{d}{d\theta}\zeta_1 &= \frac{(z+w)(2iz\dot{w} + 2izw) - 2zw(iz + i\dot{w})}{(z+w)^2} \\ &= \frac{2iz^2\dot{w} + 2izw^2}{(z+w)^2} = i\frac{2zw}{z+w}\frac{w + \dot{w}z}{z+w} \end{aligned}$$

$$= i\zeta_1 \frac{w + \dot{w}z}{w + z} = iz \zeta'_1(z).$$

Hence, the parametric equation of the straight line tangent to  $\zeta_1(\mathbb{T})$  at the point  $\zeta_1(e^{i\theta})$  is

$$L(t) = \zeta_1 + it \zeta_1 \frac{w + \dot{w}z}{w + z} = \frac{2zw}{z + w} \left( 1 + it \frac{w + \dot{w}z}{w + z} \right), \quad t \in \mathbb{R}.$$

Notice that  $\dot{w} \in \mathbb{R}$ ,  $z, w \in \mathbb{T}$ , so that  $\bar{z} = \frac{1}{z}$ , similarly for  $w$ . Then

$$\begin{aligned} \overline{L(t)} &= \overline{\frac{2zw}{z + w}} \overline{\left( 1 + it \frac{w + \dot{w}z}{w + z} \right)} \\ &= \frac{2}{z + w} \left( 1 - it \frac{z + \dot{w}w}{w + z} \right), \end{aligned}$$

and hence,

$$|L(t)|^2 = \frac{4zw}{(z + w)^2} \left( 1 + it \frac{w + \dot{w}z}{w + z} \right) \left( 1 - it \frac{z + \dot{w}w}{w + z} \right) = \frac{4wz}{(w + z)^4} (\alpha t^2 + \beta t + \gamma)$$

with

$$\alpha = (w + \dot{w}z)(z + \dot{w}w), \quad \beta = i(w^2 - z^2)(1 - \dot{w}), \quad \gamma = (z + w)^2.$$

This is a quadratic function in  $t$  whose minimum is attained at  $t = -\beta/(2\alpha)$ . Replacing it in the expression for  $|L(t)|^2$  we get that the square of the distance of the tangent line to the origin is

$$\begin{aligned} |L(-\beta/(2\alpha))|^2 &= \frac{4wz}{(w + z)^4} \left( \alpha \left( \frac{-\beta}{2\alpha} \right)^2 + \beta \left( \frac{-\beta}{2\alpha} \right) + \gamma \right) = \frac{4wz}{(w + z)^4} \left( \left( \frac{-\beta}{4\alpha} \right)^2 + \gamma \right) \\ &= \frac{wz}{(z + w)^2} \left( \frac{(w - z)^2(1 - \dot{w})^2 + 4(w + \dot{w}z)(z + \dot{w}w)}{(w + \dot{w}z)(z + \dot{w}w)} \right) \\ &= \frac{wz}{(z + w)^2} \left( \frac{(w + \dot{w}z - z - \dot{w}w)^2 + 4(w + \dot{w}z)(z + \dot{w}w)}{(w + \dot{w}z)(z + \dot{w}w)} \right) \end{aligned}$$

$$\begin{aligned}
&= \frac{wz}{(z+w)^2} \left( \frac{(w+\dot{w}z+z-\dot{w}w)^2}{(w+\dot{w}z)(z+\dot{w}w)} \right) \\
&= \frac{wz}{(z+w)^2} \left( \frac{(1+\dot{w})^2(z+w)^2}{(w+\dot{w}z)(z+\dot{w}w)} \right) \\
&= \frac{zw(1+\dot{w})^2}{(w+\dot{w}z)(z+\dot{w}w)} = \frac{(1+\dot{w})^2}{|z+\dot{w}w|^2}.
\end{aligned}$$

If  $\dot{w} \geq 0$  then by the triangle inequality,

$$|z + \dot{w}w| \leq |z| + |\dot{w}w| = 1 + \dot{w},$$

which shows that the distance is  $\geq 1$ . Moreover, equality holds only when either  $z = w$  or when  $\dot{w} = 0$ . In the same vein, the reversed triangle inequality and the assumption  $\dot{w} < 0$  yields that the distance is  $< 1$ , so that the tangent line intersects the unit circle in two points.  $\square$

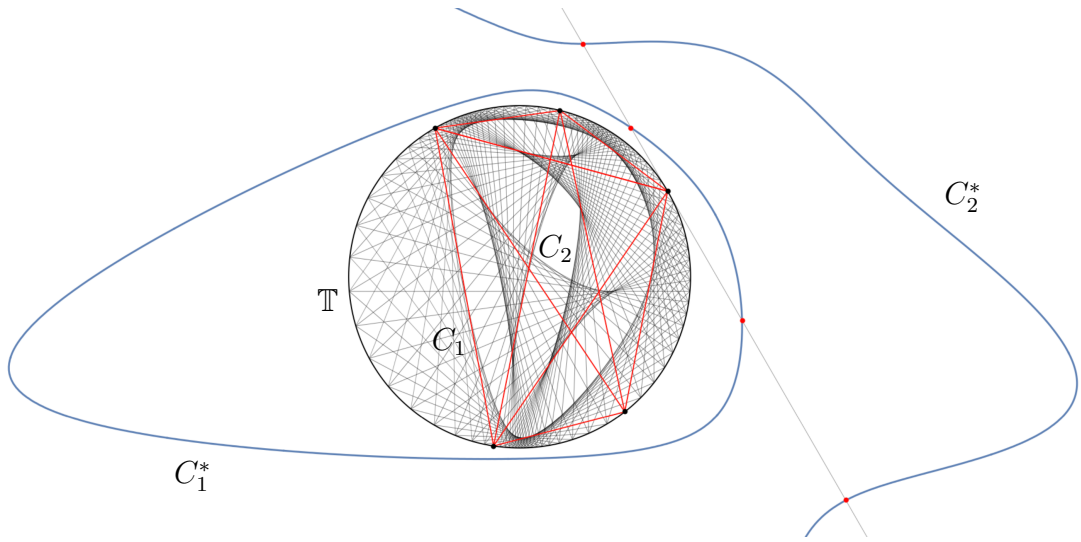


Figure 4.5. The curves  $C_1^*$  and  $C_2^*$  associated to a convex Poncelet curve of rank 5.

**Lemma 4.7.** *For each  $1 \leq k \leq n - 1$ , the map  $\zeta_k : \mathbb{T} \rightarrow \mathbb{P}^2(\mathbb{R})$  is one-to-one, unless  $n = 2k$ , in which case  $\zeta_k$  is two-to-one. Additionally,  $\zeta_k(\mathbb{T}) = \zeta_{n-k}(\mathbb{T})$ .*

*Proof.* The case  $n = 2$  is trivial, so assume  $n \geq 3$ . Let  $z, w \in \mathbb{T}$  such that  $\zeta_k(z) = \zeta_k(w)$ . Then  $[z, \tau^k(z)] = [w, \tau^k(w)]$  and hence either  $z = w$  or  $\tau^k(z) = w$  and  $z = \tau^k(w)$ . The second condition is equivalent to  $\tau^{2k}(z) = z$  which is only possible if  $n = 2k$ . It follows that the map  $\zeta_k$  is one-to-one if  $n \neq 2k$  and two-to-one if  $n = 2k$ .

The last assertion follows from the fact that if  $z \in \mathbb{T}$  and  $w = \tau^k(z)$ , then by definition  $\zeta_k(z)$  is the pole of the line containing  $[z, w]$ . At the same time,  $\tau^{n-k}(w) = \tau^n(z) = z$ , so that  $\zeta_{n-k}(w)$  is the pole of the line containing  $[w, z]$ , which shows that  $\zeta_{n-k}(w) = \zeta_k(z)$ , with  $w = \tau^k(z)$ .  $\square$

This lemma rigorously proves that  $C_{n-k} = -C_k$ , a fact which seems obvious pictorially by considering  $-\mathcal{P}(z)$ . Thus we only need to consider curves  $C_k$  for  $1 \leq k \leq [n/2]$ . The next theorem shows that each such a component  $C_k$  exhibits the Poncelet property:

**Theorem 4.8.** *Assume that  $n \geq 3$  and all  $C_k$ ,  $1 \leq k \leq [n/2]$ , are closed curves in the sense of Definition 4.1. Then, for each  $1 \leq k \leq [n/2]$ , the curve  $C_k \subset \mathbb{D}$  is a Poncelet curve of rank  $n/\gcd(k, n)$ . Moreover, if all Poncelet polygons  $\mathcal{P}(z)$  are convex then the positively oriented Poncelet polygons for  $C_k$  have turning number  $k/\gcd(k, n)$ .*

*Furthermore, if  $d$  is a divisor of  $n$  and  $d \geq 3$ , then the number of curves  $C_k$ ,  $1 \leq k \leq [n/2]$ , that have the  $d$ -Poncelet property is  $\phi(d)/2$ , where  $\phi$  denotes Euler's totient function (i.e.,  $\phi(d)$  counts the positive integers up to  $d$  that are relatively prime to  $d$ ).*

Recall that here we assume that condition (4.4) holds.

*Proof.* For the following, set  $\mathbb{Z}_n := \{0, 1, 2, \dots, n - 1\}$  and view  $\mathbb{Z}_n$  as an additive group, where addition is the usual addition of integers modulo  $n$ . It is an elementary

result in basic group theory that the order of  $k \in \mathbb{Z}_n$  is equal to  $n_k := n/\gcd(k, n)$ .

Here the order of  $k \in \mathbb{Z}_n$  is defined as the smallest positive integer  $m$  such that

$$mk := \underbrace{k + \cdots + k}_{m} = 0 \text{ in } \mathbb{Z}_n.$$

For  $k \in \mathbb{N}$  and  $z \in \mathbb{T}$ , define a polygon with  $n_k$  sides by

$$\mathcal{P}_k(z) := [z, \tau^k(z)] \cup [\tau^k(z), \tau^{2k}(z)] \cup \cdots \cup [\tau^{(n_k-1)k}(z), z]. \quad (4.6)$$

Since  $\tau^n(z) = z$  we can view the exponents in the sequence  $z, \tau^k(z), \tau^{2k}(z)$ , etc., as elements of  $\mathbb{Z}$  or as elements of  $\mathbb{Z}_n$ .

Note that each one of the segments is of the form  $[w, \tau^k(w)]$  for some  $w \in \mathbb{T}$ .

In fact, for any  $0 \leq m \leq n_k - 1$ , we have

$$[\tau^{mk}(z), \tau^{(m+1)k}(z)] = [w, \tau^k(w)], \text{ where } w = \tau^{mk}(z).$$

Thus,  $C_k$  is an  $n_k$ -Poncelet curve with Poncelet polygons  $\mathcal{P}_k(z)$ .

Moreover, if all Poncelet polygons  $\mathcal{P}(z)$  are convex, then for each  $z \in \mathbb{T}$ , the vertices  $z, \tau(z), \dots, \tau^{n-1}(z)$  of  $\mathcal{P}(z)$  are points on  $\mathbb{T}$  in counterclockwise order. Since  $n_k = n/\gcd(k, n) = \min\{m \in \mathbb{N} : mk \text{ is a positive multiple of } n\}$  and

$$\frac{n}{\gcd(k, n)} k = \frac{k}{\gcd(k, n)} n,$$

it follows that the turning number of  $\mathcal{P}_k(z)$  is  $k/\gcd(k, n)$ .

A consequence of the just established fact is that a polygon  $\mathcal{P}_k(z)$  in (4.6) has exactly  $n$  segments if and only if  $\gcd(n, k) = 1$ . Thus, the total number of such polygons is precisely the number of integers  $1 \leq k \leq [n/2]$  with  $\gcd(n, k) = 1$ , which coincides with  $\phi(n)/2$ . More generally, suppose  $d$  is a divisor of  $n$ ,  $d \geq 2$ . A well

known fact is that the number of integers  $1 \leq k \leq [n/2]$  with  $\gcd(n, k) = n/d$  is equal to  $\phi(d)/2$ , which proves the theorem.  $\square$

#### 4.3.1 Complete Poncelet Curves

Let  $\{\mathcal{P}(z) : z \in \mathbb{T}\}$  be a family of *convex*  $n$ -Poncelet polygons such that the Poncelet correspondence  $\tau : \mathbb{T} \rightarrow \mathbb{T}$  is smooth and condition (4.4) holds. Consistent with the hypotheses of Theorem 4.8, we assume that each of the associated Poncelet curves  $C_k$ ,  $1 \leq k \leq [n/2]$ , as constructed in the previous section, is closed (and thus, algebraic) in the sense of Definition 4.1. Moreover, by Theorem 4.6, all  $C_k \subset \mathbb{D}$ .

**Definition 4.9.** Under the assumptions above, the union

$$\mathcal{K}_n := \bigcup_{k=1}^{[n/2]} C_k \subset \mathbb{D} \quad (4.7)$$

is called a *package of Poncelet curves generated by* the family  $\{\mathcal{P}(z) : z \in \mathbb{T}\}$ . If  $\{\mathcal{P}(z) : z \in \mathbb{T}\}$  are the convex Poncelet polygons for a closed curve  $C \subset \mathbb{D}$ , we alternatively say that the package of Poncelet curves is *generated by*  $C$ ; in this case,  $C_1 = C$ .

This terminology was apparently introduced by Mirman, see [55].

Recall that by assumption, every package of Poncelet curves is algebraic, so that there exists a real algebraic curve  $\Gamma$  such  $\mathcal{K}_n \subset \Gamma(\mathbb{R})$ .

**Lemma 4.10.** *Let  $\Gamma$  be any real algebraic curve such that*

$$\mathcal{K}_n = \bigcup_{k=1}^{[n/2]} C_k \subseteq \Gamma(\mathbb{R}). \quad (4.8)$$

*Then the class of  $\Gamma$  is at least  $n - 1$ . If the class of  $\Gamma$  is exactly  $n - 1$ , then (4.8) becomes*

$$\mathcal{K}_n = \bigcup_{k=1}^{[n/2]} C_k = \Gamma(\mathbb{R}). \quad (4.9)$$

*Proof.* First note that every tangent line of one of the curves  $C_k$  is also a tangent line of  $\Gamma(\mathbb{R})$ . Since  $C_k = -C_{n-k}$  it then follows that  $C_k^* \subset \Gamma^*(\mathbb{R})$  for all  $1 \leq k \leq n-1$ .

For every  $z \in \mathbb{T}$ , the line in  $\mathbb{P}^2(\mathbb{R})$  that is tangent to  $\mathbb{T}$  at  $z$  intersects

$$\mathcal{K}_n^* := \bigcup_{k=1}^{[n/2]} C_k^*$$

in exactly  $n-1$  distinct points, namely the polars of the lines containing the diagonals  $[z, \tau^k(z)]$ ,  $k = 1, \dots, n-1$ . Thus, since  $\mathcal{K}_n^* \subseteq \Gamma^*(\mathbb{R})$ , it follows by Bézout's theorem that the degree of  $\Gamma$  must be at least  $n-1$ .

Now suppose that the class of  $\Gamma$  is exactly  $n-1$ . By the argument above, if  $l$  is any line in  $\mathbb{P}^2(\mathbb{R})$  that is tangent to  $\mathbb{T}$ , then  $\mathcal{K}_n^* \cap l = \Gamma^*(\mathbb{R}) \cap l$ . Suppose that  $\mathcal{K}_n \neq \Gamma(\mathbb{R})$  or, equivalently,  $\mathcal{K}_n^* \neq \Gamma^*(\mathbb{R})$ . Let  $p \in \Gamma^*(\mathbb{R}) \setminus \mathcal{K}_n^*$  and let  $l$  be a line containing  $p$  that is tangent to  $\mathbb{T}$ . Then for this line  $l$  we would have  $\mathcal{K}_n^* \cap l \neq \Gamma^*(\mathbb{R}) \cap l$  which is a contradiction. Thus, if the class of  $\Gamma$  is exactly  $n-1$ , then  $\mathcal{K}_n = \Gamma(\mathbb{R})$ .  $\square$

If (4.9) holds, then  $\Gamma(\mathbb{R})$  is a complete Poncelet curve in the sense of the following definition.

**Definition 4.11.** If there exists a real algebraic curve  $\Gamma$  such that (4.9) holds then the set of real points  $\mathcal{K}_n = \Gamma(\mathbb{R}) \subset \mathbb{D}$  of a plane algebraic curve  $\Gamma$  is called a *complete Poncelet curve* (also, a complete Poncelet–Darboux curve) *of rank n* or a *complete n-Poncelet curve* with respect to  $\mathbb{T}$ , generated by the family  $\{\mathcal{P}(z) : z \in \mathbb{T}\}$ .

The dual  $\Gamma^*$  is called the *Darboux curve* for  $\Gamma$ .

Notice that if  $\Gamma(\mathbb{R})$  is a complete Poncelet curve of rank  $n$  then for every  $z \in \mathbb{T}$  there exists an  $n$ -sided polygon  $\mathcal{P}(z)$  inscribed in  $\mathbb{T}$  such that  $z$  is one of these vertices, each of the  $n(n-1)/2$  lines connecting the  $n$  vertices of  $\mathcal{P}(z)$  is tangent to  $\Gamma(\mathbb{R})$ , and each tangent line of  $\Gamma(\mathbb{R})$  containing one of the vertices of the polygon must contain a

side of  $\mathcal{P}(z)$ . Since in this construction we can always replace  $\mathcal{P}(z)$  by the boundary of its convex hull, the convexity assumption on the family  $\{\mathcal{P}(z) : z \in \mathbb{T}\}$  of  $n$ -Poncelet polygons is actually not a restriction and is made for convenience. Any other choice of polygons would simply imply a different enumeration of the components  $C_k$ .

Example 4.12. For  $n = 24$ , if  $\Gamma(\mathbb{R})$  is a complete Poncelet curve, then

$$\Gamma(\mathbb{R}) = \bigcup_{k=1}^{12} C_k,$$

where  $C_1, C_5, C_7$ , and  $C_{11}$  are 24-Poncelet curves,  $C_2$  and  $C_{10}$  are 12-Poncelet curves,  $C_3$  and  $C_9$  are 8-Poncelet curves,  $C_4$  is a 6-Poncelet curve,  $C_6$  is a 4-Poncelet curve,  $C_8$  is a 3-Poncelet curve, and  $C_{12}$  is a 2-Poncelet curve. Note that  $C_{12}$  may consist of a single point, namely in the case when connecting opposite vertices of the inscribed dodecagons all meet in a single point. See Figures ??, 4.7, and 4.8.

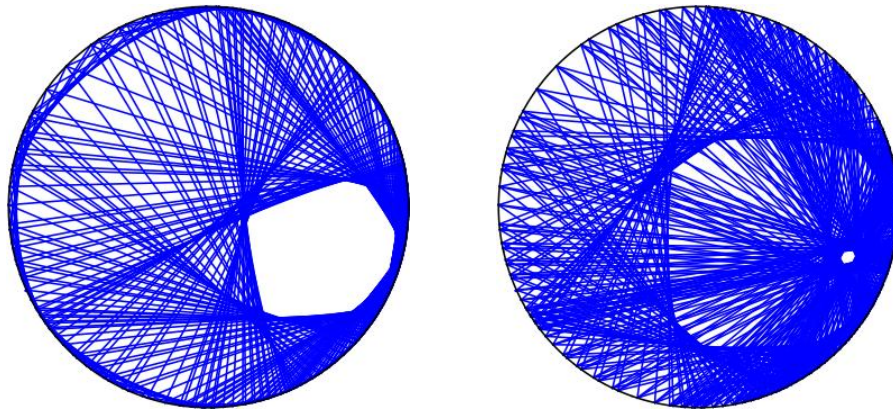


Figure 4.6. On the left,  $C_1$  and  $C_7$  and on the right,  $C_5$  and  $C_{11}$  circumscribe 24-Poncelet curves.

*4.3.1.1 Defining Components.* Note that as  $n$  increases, so do the number of connected components in  $C$ . We will give some of these curves specific names because

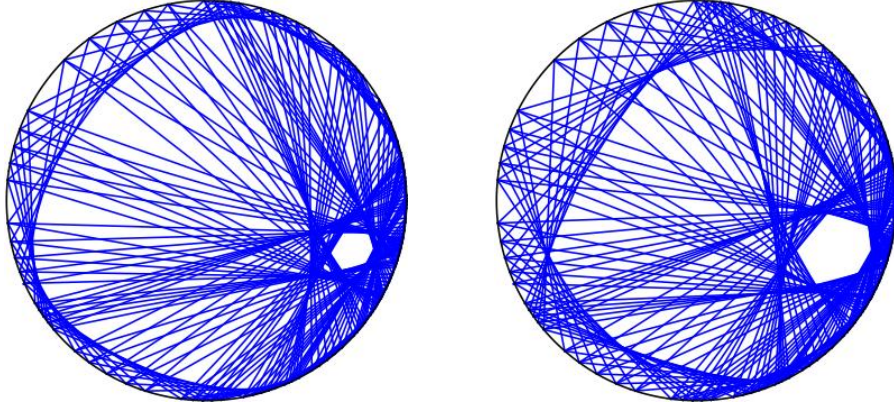


Figure 4.7. On the left,  $C_2$  and  $C_{10}$  are 12-Poncelet curves. On the right,  $C_3$  and  $C_9$  circumscribe 8-Poncelet curves.

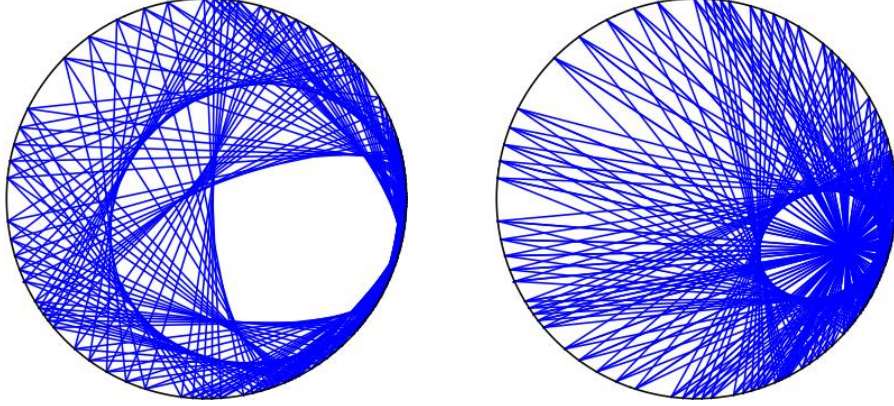


Figure 4.8. On the left,  $C_4$  is a 6-Poncelet curve and  $C_6$  is a 4-Poncelet curve. On the right,  $C_8$  is a 3-Poncelet curve and  $C_{12}$  is a 2-Poncelet curve.

of their geometric interpretations and connections to other maps in the literature. For each of the following, we define the curve with respect to a matrix  $\mathbf{A} \in S_n$ . This means we are defining the curve by first considering the polygons defined by rank one unitary dilations of  $\mathbf{A}$ . The curve  $C$  we previously defined as the envelope of all the diagonals of these polygons, with the individual components  $C_j$  being the envelopes of the diagonals connecting every  $j$ th vertex.

Throughout this dissertation, we will refer to  $C_1$  as the curve defined by the boundary of the numerical range of a matrix in  $S_n$ . We have already noted that  $\zeta_2$  (and thus also  $C_2$ ) is related to Schwartz's pentagram map [66, 67]. As a result, we denote  $C_2$  as the *pentagram curve* of a matrix  $\mathbf{A}$ .

The following theorem will be important for our results in Chapter Six and gives the motivation for calling  $C_3$  the *Brianchon curve* of a matrix  $\mathbf{A}$ .

**Theorem 4.13. (Brianchon)** [9, Theorem 9.15] *If a hexagon circumscribes a nondegenerate conic, then the three principal diagonals are concurrent and distinct.*

*Conversely, if at least five of the sides of a hexagon are in general position (lines are distinct and no subset of three lines has a common point of intersection) and the hexagon has the property that its three principal diagonals are concurrent, then the six sides are tangent to a unique nondegenerate conic.*

Thus in the hexagon case,  $C_3$  being a single point has elliptic implications. As a result, we call  $C_3$  the Brianchon curve in general. We will investigate Brianchon's Theorem in more depth in Chapter Six.

#### 4.4 Mirman's Parametrizations

##### 4.4.1 Mirman's parametrization

Let  $\Gamma$  be a real algebraic curve such that  $\Gamma(\mathbb{R}) \subset \mathbb{D}$ . In this case, we can use reciprocation about  $\mathbb{T}$  to give an alternative parametrization of  $\Gamma^*$  that has been systematically exploited in the work of Mirman and collaborators (see e.g., [55, 57]). Suppose  $\Gamma$  has class  $m$  so that  $\Gamma^*$  is given by an equation  $G(u_1, u_2, u_3) = 0$ , where  $G(u_1, u_2, u_3)$  is a homogenous polynomial of degree  $m$ . Let  $g(u, v) := G(u, v, 1)$  be the dehomogenization. Using the substitution (3.25), define a polynomial

$$P(z_1, z_2) := (z_1 + z_2)^m g\left(\frac{1 + z_1 z_2}{z_1 + z_2}, i \frac{1 - z_1 z_2}{z_1 + z_2}\right). \quad (4.10)$$

Then  $P(z_1, z_2)$  is a symmetric polynomial of (total) degree  $2m$  with complex coefficients. By our discussion above, a point  $\zeta = u + iv \in \mathbb{C}$  in the exterior of  $\mathbb{T}$  lies on  $\Gamma^*(\mathbb{R})$  if and only if the points  $z_1, z_2 \in \mathbb{T}$  given by (3.25) or Figure 4.9 satisfy the equation

$$P(z_1, z_2) = 0. \quad (4.11)$$

We say that in (4.11),  $\Gamma^*$  (or equivalently,  $\Gamma$ ) is written in *tangent coordinates*, and refer to it as *Mirman's parametrization* of the algebraic curve.

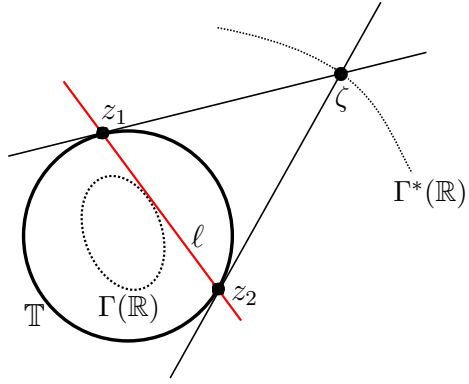


Figure 4.9. A replica of Figure 3.2 for convenience here.

#### 4.4.2 Mirman's parametrization of a package of Poncelet curves

Given a package of Poncelet curves  $\mathcal{K}_n$  generated by a family of Poncelet polygons  $\{\mathcal{P}(z) : z \in \mathbb{T}\}$  (or by a closed curve  $C$ ), we can use Mirman's parametrization to derive an equation for the algebraic curve  $\Gamma$  in the right hand side of (4.8)–(4.9). If  $z = z_1 \in \mathbb{T}$ ,  $w = z_2 \in \mathbb{T}$  are endpoints of a line tangent to  $\Gamma(\mathbb{R})$ , then [55] yields an equation of the form

$$P(z, w) = 0, \quad (4.12)$$

where  $P$  is a polynomial, symmetric in  $z$  and  $w$ .

A crucial consequence of Definition 4.2 is that for every  $w_0 \in \mathbb{T}$  there exist *exactly*  $n - 1$  solutions  $w_1, \dots, w_{n-1}$  of the equation

$$P(w_0, w) = 0, \quad (4.13)$$

namely the other vertices of the Poncelet polygon  $\mathcal{P}(w_0)$ , all of them on  $\mathbb{T}$ , and that they satisfy that

$$P(w_i, w_j) = 0, \quad 0 \leq i < j \leq n - 1. \quad (4.14)$$

This shows that  $P(z, w)$  is of degree at least  $n - 1$  in  $w, z$  (recall that its degree matches the class of  $\Gamma$ , which is consistent with the statement of Lemma 4.8). However,  $P(w_0, w) = 0$  could have other solutions  $w \in \mathbb{C} \setminus \mathbb{T}$ , and in consequence, the actual degree of  $P$  is  $N - 1$ , with  $N \geq n$ .

Denote by  $f_1, \dots, f_{N-1}$  the solutions (with account of multiplicity) of

$$P(0, w) = 0. \quad (4.15)$$

*Proposition 4.14.* *The points  $f_1, \dots, f_{N-1}$ , which are solutions (with account of multiplicity) of (4.15), are the real foci of the curve  $\Gamma$ .*

*Proof.* As it was pointed out, the equation

$$g(u, v) = 0$$

of the dual curve (in the affine coordinates) can be obtained from (4.12) using the substitution (3.27), with

$$u = \frac{\zeta + \hat{\zeta}}{2}, \quad v = \frac{\zeta - \hat{\zeta}}{2i}.$$

according to which  $z = z(\zeta, \hat{\zeta})$ ,  $w = w(\zeta, \hat{\zeta})$ . The resulting equation should be homogenized to a curve in  $\mathbb{P}^2(\mathbb{C})$  with its equation obtained by taking  $\zeta \rightarrow \zeta/t$ ,

$t \in \mathbb{C}$ . As it follows from Equation (4.2), foci of  $\Gamma$  are solutions of the equation

$$g\left(\frac{1}{t}, \frac{i}{t}\right) = 0.$$

We see that

$$u = \frac{\zeta + \hat{\zeta}}{2} = \frac{1}{t}, \quad v = \frac{\zeta - \hat{\zeta}}{2i} = \frac{i}{t}$$

implies that  $\zeta = 0$  and  $\hat{\zeta} = 2/t$ . If we fix the branch of the square root in (3.27) by  $\sqrt{-1} = i$ , then in this case  $z = 0$ ,  $w = t$  so that the foci of  $\Gamma$  are precisely the solutions of the equation  $P(0, t) = 0$ .  $\square$

An important consequence of the discussion in [57, Section 5] (see in particular Lemma 5.1.2) is the following result:

Theorem 4.15. *Let  $n \in \mathbb{N}$ ,  $n \geq 3$ . With the notation above and up to a multiplicative constant,*

$$P(z, w) = \frac{w \Phi_{N-1}(w) \Phi_{N-1}^*(z) - z \Phi_{N-1}(z) \Phi_{N-1}^*(w)}{w - z}, \quad (4.16)$$

where

$$\Phi_{N-1}(z) = \Phi_{N-1}(z; f_1, \dots, f_{N-1}). \quad (4.17)$$

Thus, the real foci  $f_j$  of  $\Gamma$  are precisely the zeros of  $\Phi_{N-1}(z)$ .

Furthermore, we have the relation

$$N = n + 2m + d, \quad (4.18)$$

where  $m$  is the number of real foci  $f_j$  (accounted with multiplicity) that lie in the exterior of  $\mathbb{T}$  and  $d$  is the number of real foci  $f_j$  (accounted with multiplicity) that lie on  $\mathbb{T}$ .

In particular, if all real foci  $f_j$  are in  $\mathbb{D}$ , then  $N = n$ .

Since the right hand side in (4.16) is a Bezoutian of the polynomials  $\Phi_{N-1}$  and  $\Phi_{N-1}^*$ , we say that  $P(z, w)$  is written in a *Bezoutian form*.

*Proof.* Formula (4.16) has been proved in [57], see Theorem 1.1 and equation (20) therein. Relation (4.18) for  $d = 0$  also follows from [57, Lemma 5.1.2]. Thus, we only need to consider  $d > 0$ .

Suppose  $f_j$  is a real focus such that  $|f_j| = 1$ . Then  $\overline{f_j} = 1/f_j$  and we easily find that

$$P(z, w) = \text{const } (z - f_j)(w - \overline{f_j})\tilde{P}(z, w),$$

where  $\tilde{P}(z, w)$  is the polynomial as given by (4.16) with  $\Phi_{N-1}(z)$  replaced by  $\tilde{\Phi}_{N-2}(z) := \Phi_{N-2}(z; f_1, \dots, f_{j-1}, f_{j+1}, \dots, f_{N-1})$ . If we had exactly  $d$  foci on the unit circle, the degree of  $\tilde{P}(z, w)$  would be  $N - d$ , and by [57, Lemma 5.1.2], the number of solutions of the equation  $\tilde{P}(w_0, w) = 0$  on the unit circle satisfies  $N - d = n + 2m$ . Thus, (4.18) holds.  $\square$

#### 4.4.2.1 From the Bezoutian form to Poncelet curves.

As we have just seen, the Poncelet property of a curve implies that its Mirman's parametrization can be written in a Bezoutian form. This motivates us to analyze the converse: is a Poncelet curve associated to any symmetric polynomial in a Bezoutian form? This approach is tempting since the only data necessary to generate such polynomials is the collections of foci  $f_j$ 's.

Let  $P(z, w)$  be a symmetric polynomial in  $z, w$ , given by (4.16)–(4.17). Clearly, representation (4.16) is sufficient for property (4.14) to hold. This does not mean however that  $P(z, w) = 0$  automatically parametrizes a Poncelet curve. A necessary condition for that is, for instance, that for every  $z \in \mathbb{T}$ , the equation  $P(z, w) = 0$  has the same number of solutions on  $\mathbb{T}$ . Mirman showed in [55, Thm. 1] that this holds if  $d = 0$  and

$$1 + \sum_{j=1}^{N-1} \frac{1 - |f_j|^2}{|z - f_j|^2} > 0 \quad \text{for all } z \in \mathbb{T}. \quad (4.19)$$

More precisely, (4.19) implies that for each  $z \in \mathbb{T}$ , the equation  $P(z, w) = 0$  has exactly  $n - 1 = N - 2m - 1$  distinct solutions  $w \in \mathbb{T}$  (notice that it is automatically satisfied if all  $f_j \in \mathbb{D}$ ). For such polynomials  $P(z, w)$  we can then define a family of  $n$ -Poncelet polygons by

$$\mathcal{P}(z) := \partial(\text{conv}\{w \in \mathbb{T} : P(z, w) = 0\})$$

that generate the package of Poncelet curves  $C_1, \dots, C_{[n/2]}$ ; here and in what follows we denote the convex hull of the set  $S$  by  $\text{conv}(S)$ .

Since  $P(z, w)$  is a symmetric polynomial in  $z$  and  $w$ , it can be written in the form  $P(z, w) = h(z + w, zw)$ . If we set

$$g(u, v) := \bar{\zeta}^{N-1} h\left(\frac{2}{\bar{\zeta}}, \frac{\zeta}{\bar{\zeta}}\right) \quad \text{with } \zeta = u + iv, \bar{\zeta} = u - iv,$$

then  $g(u, v)$  is a polynomial with real coefficients of degree  $N - 1$ . Fujimura (see [24]) expressed  $g(u, v)$  as a polynomial in  $\zeta$  and  $\bar{\zeta}$ , where the coefficients are given by explicit formulas in the elementary symmetric functions (and their complex conjugates) of the  $f_j$ 's. She only stated these formulas in the case when  $m = d = 0$ , but her arguments work in general. Let  $G(u_1, u_2, u_3)$  denote the homogenization of  $g(u, v)$  as usual. Then the real algebraic curve given by  $G(u_1, u_2, u_3) = 0$  is the dual of a real algebraic curve  $\Gamma$  of class  $N - 1$  whose real foci are the  $f_j$ 's. By construction, we have

$$\bigcup_{k=1}^{[n/2]} C_k \subseteq \Gamma(\mathbb{R}).$$

We cannot ensure in general that this inclusion is not strict. Neither can we assure that the  $C_k$ 's will be Poncelet curves, in the sense of Definition 4.2.

Moreover, Mirman [55, Remark 1] stated (without proof) that  $C_1$  is always convex. In the following example we show that this is false in general, if  $m > 0$ .

Example 4.16. Consider a family of examples with  $P(z, w)$  given by (4.16)–(4.17), where  $N = 5$  and

$$\Phi_4(z) = \Phi_4(z; 0, 0, 0, a), \quad a \in \mathbb{C} \setminus \mathbb{T}.$$

In this case, the corresponding polynomial  $g(u, v)$  is of the form

$$\begin{aligned} g(u, v) = & (a^2 - 1)v^4 + 2((a^2 - 1)u^2 - 2au - 2a^2 + 6)v^2 \\ & + ((a^2 - 1)u^4 - 8au^3 + (12 - 4a^2)u^2 + 16au - 16). \end{aligned}$$

It is easy to show that  $g(u, v)$  is an irreducible polynomial (over  $\mathbb{C}$ ) by looking at its Newton polygon which is the convex hull of the lattice points  $(0, 0)$ ,  $(4, 0)$ , and  $(0, 4)$ . The method of showing (absolute) irreducibility of polynomials in several variables via Newton polytopes is nicely explained in [25]. Notice that  $g(u, v)$  can be viewed as quadratic polynomial in  $v^2$ . Thus it is relatively easy to carry out explicit calculations to study  $\Gamma^*(\mathbb{R})$ .

In particular,

- $\Gamma^*(\mathbb{R})$  is nonsingular and a disjoint union of two nested “ovals” in  $\overline{\mathbb{C}}$ .
- If  $|a| < 1$ , then both components of  $\Gamma^*(\mathbb{R})$  lie in the exterior of  $\mathbb{T}$  (which means that  $\Gamma(\mathbb{R}) \subset \mathbb{D}$ ). Furthermore, if  $|a| \leq \sqrt{3 - \sqrt{6}} \approx 0.741964$ , then neither of the two components of  $\Gamma^*(\mathbb{R})$  has inflection points (so,  $\Gamma(\mathbb{R})$  has no cusps). If  $\sqrt{3 - \sqrt{6}} < |a| < 1$ , then the larger component of  $\Gamma^*(\mathbb{R})$  has inflection points, see Figure 4.10, left.
- If  $1 \leq |a| \leq 5/3$ , then one component of  $\Gamma^*(\mathbb{R})$  intersects  $\mathbb{T}$ , see Figure 4.10, right.

- If  $|a| > 5/3$ , then one component of  $\Gamma^*(\mathbb{R})$  lies in the exterior and the other lies in the interior of  $\mathbb{T}$  (so, the same is true for  $\Gamma(\mathbb{R})$ ). Furthermore, if  $|a| \geq \sqrt{3 + \sqrt{6}} \approx 2.33441$ , then neither of the two components of  $\Gamma^*(\mathbb{R})$  has inflection points, see Figure 4.11. If  $5/3 < |a| < \sqrt{3 + \sqrt{6}}$ , then the component of  $\Gamma^*(\mathbb{R})$  that lies in the exterior of  $\mathbb{T}$  has inflection points.

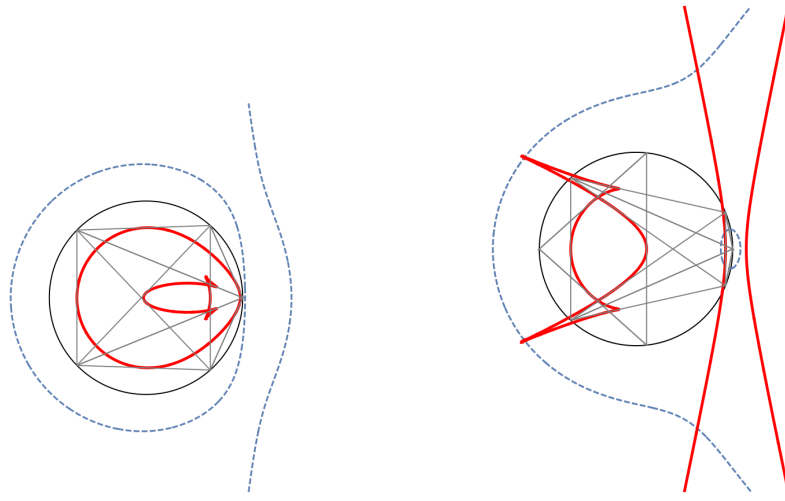


Figure 4.10. Illustration for Example 4.16: curve  $\Gamma(\mathbb{R})$  (solid lines) and its dual  $\Gamma^*(\mathbb{R})$ , dotted lines, for  $a = 0.9$  (left) and  $a = 1.5$ , in which case Mirman's condition (4.19) is not satisfied (right). Notice that in this situation  $\Gamma(\mathbb{R})$  is tangent both to triangles and pentagons.

Notice that Mirman's condition (4.19) to generate Poncelet curves is satisfied whenever  $|a| < 1$  or  $|a| > 5/3$ . For  $|a| < 1$ , we obtain a package of two 5-Poncelet curves  $C_1$  and  $C_2$  with  $C_1 \cup C_2 = \Gamma(\mathbb{R})$ . In this case,  $C_1$  is nonsingular and equal to the boundary of the convex hull of  $\Gamma(\mathbb{R})$ . Furthermore, if  $|a| \leq \sqrt{3 - \sqrt{6}}$ , then  $C_2$  is also nonsingular and convex since its dual  $C_2^*$  has no inflection points.

For  $|a| > 5/3$ , the situation is more surprising and we obtain a package consisting of a single 3-Poncelet curve  $C_1$  with  $C_1 \neq \Gamma(\mathbb{R})$ , see Figure 4.11. If  $|a| \geq \sqrt{3 + \sqrt{6}}$ , then  $C_1$  is nonsingular and convex since its dual  $C_1^*$  has no inflection points. How-

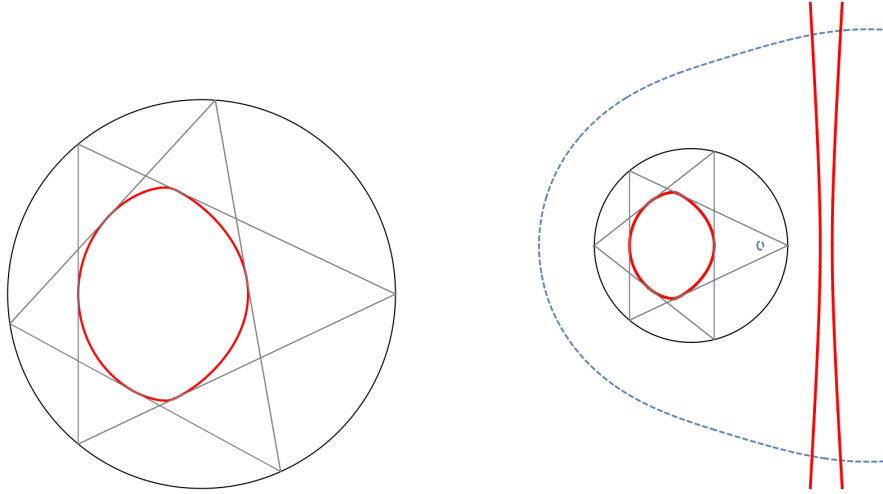


Figure 4.11. Illustration for Example 4.16: a nonsingular 3-Poncelet curve  $C_1$  (left) and the corresponding algebraic curve  $\Gamma(\mathbb{R})$  (solid lines) and its dual  $\Gamma^*(\mathbb{R})$ , dotted lines, for  $a = 2.4$ . Curve  $C_1$  for  $a = 2$  appears in Figure 4.3, right.

ever, if  $5/3 < |a| < \sqrt{3 + \sqrt{6}}$ , then  $C_1$  is singular since  $C_1^*$  has inflection points which correspond to cusp singularities of  $C_1$ .

**Example 4.17.** Another common misconception is that in the package of Poncelet curves  $C_1$  encloses the rest of the curves  $C_k$ . This is definitely the case if the starting point is a family of convex Poncelet polygons  $\{\mathcal{P}(z) : z \in \mathbb{T}\}$ , as in Definition 4.9. However, if we construct our curves from the representation (4.16)–(4.17), satisfying (4.19), this is not always true. The situation with  $N = 7$ ,

$$\Phi_6(z) = \Phi_6(z; 0, 0, 0, 0, 0, a)$$

and  $a = 1.41$  is illustrated in Figure 4.12.

In the next chapter, we will see Mirman's parametrizations again in the context of iterating through the foci of a curve inside  $\mathbb{D}$  rather than through the foci of the circumscribing polygons. The equations and terminology used above will be the basis that we build upon in these inner iterations.

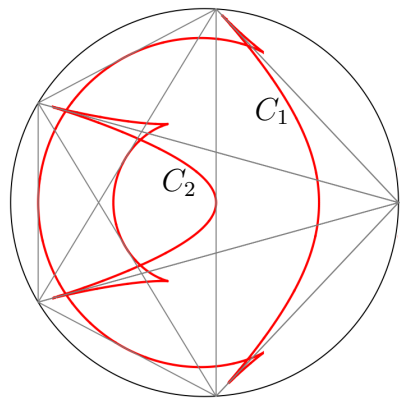


Figure 4.12. Illustration for Example 4.17: curves  $C_1$  and  $C_2$  have a non-empty intersection.

## CHAPTER FIVE

### Constructing Complete Poncelet Curves with Given Foci

A majority of this chapter is submitted for publication as Markus Hunziker, Andrei Martínez-Finkelshtein, Taylor Poe, and Brian Simanek, *Poncelet-Darboux, Kippenhahn, and Szegő: interactions between projective geometry, matrices and orthogonal polynomials*, Preprint, 2021.

In this chapter, we gather all the knowledge accumulated so far to analyze minimal class complete  $n$ -Poncelet curves  $\Gamma$  in the sense of the Definition 4.11. In particular, we show that they are characterized by either one of these properties:

- $\Gamma$  is of class  $n - 1$ ;
- all real foci of  $\Gamma$  are inside the unit disk  $\mathbb{D}$ .

Moreover, in this case the set of foci  $f_1, \dots, f_{n-1}$  determines  $\Gamma$  completely, so that this is a bijection between points in  $\mathbb{D}^{n-1}$  and complete  $n$ -Poncelet curves. The curve  $\Gamma$  can be reconstructed from its real foci. We describe three approaches to this problem; all three can be formulated in terms of the paraorthogonal extension of the set  $f_1, \dots, f_{n-1}$ .

Recall that the paraorthogonal extension (see Definition 3.4) consists in applying the Szegő recursion as in Equation (3.8) with  $\Phi_{n-1}(z) = \Phi_{n-1}(z; f_1, \dots, f_{n-1})$  and obtaining the 1-parametric family of points  $\mathcal{Z}_n^\lambda = \{z_{n,1}^\lambda, \dots, z_{n,n}^\lambda\}$  on  $\mathbb{T}$  as the zeros of the resulting paraorthogonal polynomials of degree  $n$ . As our next result shows, the sets  $\mathcal{Z}_n^\lambda$  are identified by the same Blaschke product with zeros at  $f_j$ 's and, at the same time, are eigenvalues of a 1-parametric family of unitary dilations (see Section 3.3.3) of the CMV matrix  $\mathcal{G}^{(n-1)} \in \mathcal{S}_{n-1}$  associated with  $\Phi_{n-1}(z)$ . In short, all these approaches are completely equivalent.

### 5.1 Three Equivalent Realizations

Theorem 5.1. Let  $\Gamma$  be a plane real algebraic curve such that  $\Gamma(\mathbb{R})$  is a complete  $n$ -Poncelet curve ( $n \geq 3$ ) with respect to  $\mathbb{T}$ , generated by a family of convex Poncelet polygons  $\mathcal{P}(z)$  (see Definition 4.11), so that

$$\Gamma(\mathbb{R}) = \bigcup_{k=1}^{[n/2]} C_k.$$

Then  $\Gamma$  is of minimal class (that is, of class  $n - 1$ ) if and only if all real foci are contained the unit disk  $\mathbb{D}$ . In this case,  $C_1$  is a convex curve, real foci  $f_1, \dots, f_{n-1}$  of  $\Gamma$  (enumerated with account of multiplicity) determine  $\Gamma$ , and for every set of points  $f_1, \dots, f_{n-1}$  in  $\mathbb{D}$ , not necessarily all distinct, there exists a (unique) algebraic  $n$ -Poncelet curve  $\Gamma$  of class  $n - 1$  with real foci precisely at  $f_1, \dots, f_{n-1}$ . Such a curve  $\Gamma$  is completely determined by its set of real points  $\Gamma(\mathbb{R})$ .

There are three equivalent realizations of the complete  $n$ -Poncelet curve  $\Gamma$  of class  $n - 1$ :

(i)  $\Gamma(\mathbb{R})$  is the envelope of the closed polygons supported on the paraorthogonal extension (see Definition 3.4) of the set  $f_1, \dots, f_{n-1}$ .

(ii) The Blaschke product

$$B_n(z) = z \frac{\Phi_{n-1}(z)}{\Phi_{n-1}^*(z)}, \quad \Phi_{n-1}(z) = \Phi_{n-1}(z; f_1, \dots, f_{n-1}), \quad (5.1)$$

identifies the set of points  $\mathcal{Z}^\lambda = \{z_1^\lambda, \dots, z_n^\lambda\}$  on  $\mathbb{T}$  (see Definition 3.5) in such a way that  $\Gamma(\mathbb{R})$  is the envelope of the closed polygons supported on  $\mathcal{Z}^\lambda$ .

(iii) there is a matrix  $\mathbf{A} \in \mathcal{S}_{n-1}$  with its spectrum equal to the set  $f_1, \dots, f_{n-1}$  (and hence,  $\mathbf{A}$  unique up to unitary equivalence) such that

$$\text{conv}(\Gamma(\mathbb{R})) = \partial W(\mathbf{A}).$$

The equation of the dual curve  $\Gamma^*$  in  $\mathbb{P}^2(\mathbb{C})$  is given by

$$G_{\mathbf{A}}(u_1, u_2, u_3) = 0,$$

where  $G_{\mathbf{A}}(u_1, u_2, u_3)$  was defined in (3.17). As for a matrix  $\mathbf{A}$ , we can take the cut-off CMV matrix  $\mathcal{G}^{(n-1)}$  corresponding to the polynomial  $\Phi_{n-1}(z; f_1, \dots, f_{n-1})$ .

Furthermore, each set  $\mathcal{Z}^\lambda = \{z_1^\lambda, \dots, z_n^\lambda\}$  of eigenvalues of a 1-parametric family of unitary dilations of matrix  $\mathbf{A}$  in (i) is identified by the Blaschke product (5.1).

Recall also that the eigenvalues of the matrix correspond to the zeros of its characteristic polynomial, which for the unitary dilations of CMV matrices are POPUC. Thus the set  $\mathcal{Z}^\lambda$  is simultaneously the zero set of a POPUC, the eigenvalue set of a unitary dilation of  $\mathbf{A} \in S_n$ , and a preimage set identified by the Blaschke product.

*Proof.* We first show that such a curve  $\Gamma$  of minimal class  $n - 1$  is completely determined by its set of real points  $\Gamma(\mathbb{R})$ . Let  $\tilde{\Gamma}$  be the real algebraic curve such that  $\tilde{\Gamma}^*$  is the intersection of all real algebraic curves containing  $\Gamma(\mathbb{R})^*$ . Note that  $\tilde{\Gamma}^* \subseteq \Gamma^*$  and  $\tilde{\Gamma}^*(\mathbb{R}) = \Gamma^*(\mathbb{R})$ . If  $\tilde{G}(u_1, u_2, u_3)$  and  $G(u_1, u_2, u_3)$  are the homogenous polynomials of minimal degree defining  $\tilde{\Gamma}^*$  and  $\Gamma^*$ , respectively, then  $\tilde{G}(u_1, u_2, u_3)$  divides  $G(u_1, u_2, u_3)$ . By Lemma 4.10, the class of the curve  $\tilde{\Gamma}$  is  $n - 1$ , which means that  $\tilde{G}(u_1, u_2, u_3)$  has degree  $n - 1$ . Since  $\tilde{G}(u_1, u_2, u_3)$  divides  $G(u_1, u_2, u_3)$  and since  $G(u_1, u_2, u_3)$  also has degree  $n - 1$ , we have  $G(u_1, u_2, u_3) = c\tilde{G}(u_1, u_2, u_3)$ , where  $c$  is a nonzero constant. Thus,  $\Gamma^* = \tilde{\Gamma}^*$  and hence  $\Gamma = \tilde{\Gamma}$ . Since  $\tilde{\Gamma}$  is completely determined by  $\Gamma(\mathbb{R})$ , so is  $\Gamma$ .

Let  $P(z, w) = 0$  be Mirman's parametrization of the complete  $n$ -Poncelet curve  $\Gamma$ , as explained in Section 4.4. By Theorem 4.15,  $\Gamma$  is of class  $n - 1$  if and only if  $N = n$ , that is,  $m = d = 0$  (in other words, when all real foci are in  $\mathbb{D}$ ).

Let  $f_1, \dots, f_{n-1}$  be the real foci of a complete  $n$ -Poncelet curve  $\Gamma$  of class  $n - 1$ . Again by Theorem 4.15, its Mirman's parametrization is, up to a multiplicative

constant,

$$P(z, w) = \frac{w \Phi_{n-1}(w) \Phi_{n-1}^*(z) - z \Phi_{n-1}(z) \Phi_{n-1}^*(w)}{w - z}, \quad (5.2)$$

with  $\Phi_{n-1}$  defined in (5.1). In particular, it means that for any pairs of points  $z, w \in \mathbb{T}$  satisfying  $P(z, w) = 0$  it holds that

$$B_n(z) = B_n(w), \quad \text{with} \quad B_n(z) = z \frac{\Phi_{n-1}(z)}{\Phi_{n-1}^*(z)},$$

i.e.,  $z, w$  are identified by  $B_n(z)$ . As we have seen in Section 3.2, this is equivalent to being  $z, w$  paraorthogonal extensions of  $\Phi_{n-1}(z)$ . Since  $|B_n(z)| = 1$  for  $z \in \mathbb{T}$ , there exists  $\lambda \in \mathbb{T}$  such that

$$z, w \in \mathcal{Z}^\lambda = \{z_1^\lambda, \dots, z_n^\lambda\},$$

the set of solutions of  $B_n(z) = \bar{\lambda}$ . Hence, by our discussion in Section 3.3.3.1, for each  $\lambda \in \mathbb{T}$ , points from  $\mathcal{Z}^\lambda$  are also the eigenvalues of a rank one unitary dilation of the  $(n-1) \times (n-1)$  cutoff CMV matrix  $\mathbf{A}$  whose eigenvalues are  $\{f_j\}_{j=1}^{n-1}$ . From [54] (see also Section 3.3.2) it follows that the unitary equivalence class of  $\mathbf{A}$  is also uniquely determined by  $f_1, \dots, f_{n-1}$  and as a representative of this class we can take  $\mathbf{A} = \mathcal{G}^{(n-1)}(\alpha_0, \dots, \alpha_{n-1})$ , where the Verblunsky coefficients are determined by  $\Phi_{n-1}(z)$  using the inverse Szegő recursion: with notation (3.1) and (3.7),

$$\Phi_{n-1}(z) = \Phi_{n-1}(z; f_1, \dots, f_{n-1}) = \Phi_n^{(\alpha_0, \dots, \alpha_{n-1})}(z).$$

Let

$$\mathcal{P}(z) := \partial (\text{conv}\{w \in \mathbb{T} : P(z, w) = 0\});$$

by the previous observation, this family coincides with

$$\{\partial (\text{conv}(\mathcal{Z}^\lambda)) : \lambda \in \mathbb{T}\}.$$

Direct calculations (see also [73, formula (6.10)]) show that

$$\frac{d}{d\theta} \arg B(e^{i\theta}) = \frac{d}{d\theta} \arg \bar{\lambda} = 1 + \sum_{j=1}^{n-1} \frac{1 - |f_j|^2}{|z - f_j|^2} > 0$$

(see also an alternative expression in terms of orthonormal OPUC in [50, formula (10.8)]). The Inverse Function Theorem shows that the Poncelet correspondence  $\tau$  for  $\{\mathcal{P}(z) : z \in \mathbb{T}\}$  is strictly increasing, is smooth and satisfies (4.4). In consequence, the associated Poncelet curves  $\{C_1, \dots, C_{[n/2]}\}$  constructed in Section 4.3, make up the package of Poncelet curves generated by  $\mathbf{A}$  in the sense described in [54]. Therefore, we may apply what is stated in [54, page 130], namely that (5.2) is the Mirman parametrization of a complete  $n$ -Poncelet curve  $\Gamma$ . It follows also that  $\Gamma$  is an algebraic curve of class  $n - 1$  with real foci  $\{f_j\}_{j=1}^{n-1}$  (see Proposition 4.14). Our construction also shows the equivalence of (i) and (ii).

It was proved in [28] that

$$W(\mathbf{A}) = \bigcap_{\lambda \in \mathbb{T}} \text{conv}(\mathcal{Z}^\lambda). \quad (5.3)$$

This shows, in particular, that  $\partial W(\mathbf{A})$  coincides with the component  $C_1$  in the package of Poncelet curves (4.9); our earlier considerations imply that  $C_1$  is also the convex hull of  $\Gamma(\mathbb{R})$  (and thus, is a convex curve). If  $\Gamma'$  is the curve whose existence is guaranteed by Kippenhahn's Theorem (see Theorem 2.3), then since the convex hull of  $\Gamma'(\mathbb{R})$  is  $\partial W(\mathbf{A})$ , it follows from Bezout's Theorem that  $\Gamma = \Gamma'$ . The content of Section 4.1.2 implies that the equation for the dual curve of  $\Gamma$  is

$$G_{\mathbf{A}}(u_1, u_2, u_3) = 0, \quad (5.4)$$

where  $G_{\mathbf{A}}$  was defined in (3.17), as claimed. We have thus demonstrated that  $\Gamma$  can be realized by the description in (iii). The fact that each set of eigenvalues of

a 1-parametric family of unitary dilations of  $\mathbf{A}$  in (iii) is identified by the Blaschke product  $B_n$  is the direct consequence of (3.15).

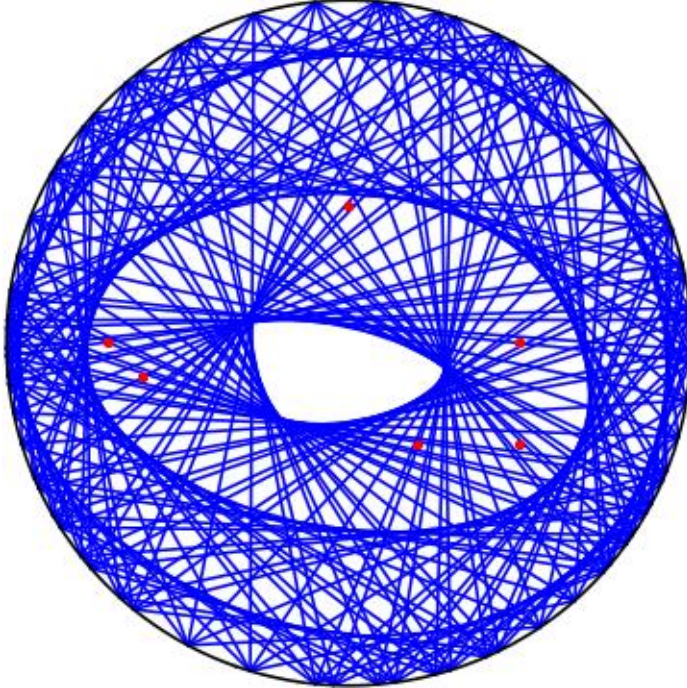


Figure 5.1. These Poncelet heptagons can be equivalently realized by a degree-7 normalized Blaschke product, the paraorthogonal extension for an OPUC  $\Phi_6(z)$ , and the numerical range of unitary dilations of a cutoff CMV matrix  $A \in S_6$ .  $\Phi_6(z)$  is the characteristic polynomial of  $A$ , and  $B_7(z) = \frac{z\Phi_6(z)}{\Phi_6^*(z)}$

To show that  $\Gamma$  is the unique curve with the desired properties, we suppose that  $\tilde{\Gamma}$  is another complete  $n$ -Poncelet curve of class  $n - 1$  with real foci  $\{f_j\}_{j=1}^{n-1}$ . Let  $\tilde{G}(u_1, u_2, u_3) = 0$  be the equation of  $\tilde{\Gamma}^*$ . Then

$$G_{\mathbf{A}}(1, i, f_j) = 0 = \tilde{G}(1, i, f_j), \quad j = 1, 2, \dots, n - 1.$$

Since  $G_{\mathbf{A}}(1, i, z)$  and  $\tilde{G}(1, i, z)$  are both polynomials of degree (at most)  $n - 1$  and have  $n - 1$  zeros in common, it follows that they must be scalar multiples of one another and hence they define the same curve. This means  $\Gamma^* = \tilde{\Gamma}^*$  and so  $\Gamma = \tilde{\Gamma}$ .  $\square$

Thus we can construct a complete  $n$ -Poncelet curve of class  $n - 1$  given the set of foci of the curve. Note, however, that this does not necessarily mean that the curve will be an ellipse. We will explore this more in Section 5.2 as well as the specific cases of  $n = 2, 3, 4, 5, 6$  in Section 5.3 and Chapter Six and Chapter Seven.

**Remark 5.2.** (a) In Theorem 5.1 we assume that  $\Gamma$  is a complete  $n$ -Poncelet curve *and* is of class  $n - 1$ . We conjecture that this assumption is superfluous, and the results in Theorem 5.1 can be established *for any* complete Poncelet curve  $\Gamma$ . In particular, it would imply that all real foci of such a curve are in  $\mathbb{D}$ . Notice that in general for a real algebraic curve  $\Gamma$ , the fact that  $\Gamma(\mathbb{R}) \subset \mathbb{D}$  does not imply that its real foci are in  $\mathbb{D}$ . A simple example [59] is the curve given by the equation

$$(x_1^2 + x_2^2 - x_3^2/2) ((x_1 - 2)^2 + x_2^2 + x_3^2) = 0$$

with real foci at  $(0 : 0 : 1)$  and  $(2 : 0 : 1)$ .

(b) It was established in [55] that the  $n$ -Poncelet property of a convex curve of class  $n - 1$  characterizes this curve as being a boundary of  $W(\mathbf{A})$  for some  $\mathbf{A} \in \mathcal{S}_{n-1}$ . The assumption on its class is essential as a counterexample in [55, Example 1 on p. 131] to a conjecture of Gau and Wu [28, Conjecture 5.1] shows; see also the discussion in [30] on p. 184.

Curiously, the counterexample that appears in [57], constructed by violating the assumption that all  $f_j$ 's are in  $\mathbb{D}$ , is wrong. Namely, the authors consider the case of  $\Phi_4(z; 0, 0, 0, a) = z^3(z - a)$ ,  $a > 1$ , and the corresponding curve with Mirman's parametrization (4.16). In [57], they take  $a = 2$ , but the resulting Poncelet curve is not convex! In fact, it is depicted in Figure 4.3, right. However,

for a correct counterexample it is sufficient to use  $a > \sqrt{3 + \sqrt{6}}$ , see our detailed discussion in Example 4.16.

- (c) Construction (ii) was extensively explored in the works [13, 14]. Its equivalence with (ii) was proved in [54].
- (d) Property (6.15) characterizes the class  $S_{n-1}$ : as it was shown in [28, Theorem 4.4], a contraction  $\mathbf{A} \in \mathbb{C}^{(n-1) \times (n-1)}$  (i.e.  $\|\mathbf{A}\| \leq 1$ ) is in  $S_{n-1}$  if and only if  $W(\mathbf{A})$  in  $\mathbb{D}$  has the Poncelet property.

### 5.1.1 Composition of Blaschke Products and Factorization of OPUC

As noted in Chapter Three, orthogonal polynomials and Blaschke products relate naturally by definition. Using results from [11], the following theorem appears in [42] further connecting finite Blaschke products and OPUC. This result will be particularly useful in Chapter Six.

**Theorem 5.3.** *Let  $n = jk$  and  $B_n(z)$  be a regular Blaschke product, i.e.  $B_n(z) = \frac{z\Phi_{n-1}(z)}{\Phi_{n-1}^*(z)}$ . Then  $B_n(z)$  can be expressed as a composition of two regular Blaschke products  $B_j(B_k(z))$  (with the degree of  $B_m$  equal to  $m$ ) if and only if  $\Phi_{n-1}(z)$  factors as*

$$\Phi_{n-1}(z) = \Phi_{k-1}(z) \prod_{m=1}^{j-1} \mathcal{S}_{\bar{a}_m}(\Phi_{k-1}(z))$$

*for some  $\Phi_{k-1}(z)$  having all of its zeros in  $\mathbb{D}$  and some  $\{a_1, \dots, a_{j-1}\} \in \mathbb{D}^{j-1}$ . If this factorization holds, then the zeros of  $\Phi_{k-1}(z)$  are the zeros of  $B_k(z)/z$  and  $\{a_1, \dots, a_{j-1}\}$  is the zero set of  $B_j(z)/z$ .*

*Proof.* Let  $B_n(z) = B_j(B_k(z))$ . Then

$$B_j(z) = \frac{z(z - a_1)\dots(z - a_{j-1})}{(1 - \overline{a_1}z)\dots(1 - \overline{a_{j-1}}z)}$$

for some  $\{a_1, \dots, a_{j-1}\} \in \mathbb{D}^{j-1}$ . If

$$B_k(z) = \frac{z\Phi_{k-1}(z)}{\Phi_{k-1}^*(z)},$$

then

$$\begin{aligned} B_n(z) &= B_j \left( \frac{z\Phi_{k-1}(z)}{\Phi_{k-1}^*(z)} \right) \\ &= \frac{z\Phi_{k-1}(z)(z\Phi_{k-1}(z) - a_1\Phi_{k-1}^*(z)) \cdots (z\Phi_{k-1}(z) - a_{j-1}\Phi_{k-1}^*(z))}{\Phi_{k-1}^*(z)(\Phi_{k-1}^*(z) - \bar{a}_1 z\Phi_{k-1}(z)) \cdots (\Phi_{k-1}^*(z) - \bar{a}_{j-1} z\Phi_{k-1}(z))} \\ &= \frac{z\Phi_{k-1}(z)\mathcal{S}_{\bar{a}_1}(\Phi_{k-1}(z)) \cdots \mathcal{S}_{\bar{a}_{j-1}}(\Phi_{k-1}(z))}{\Phi_{k-1}^*(z)\mathcal{T}_{\bar{a}_1}(\Phi_{k-1}^*(z)) \cdots \mathcal{T}_{\bar{a}_{j-1}}(\Phi_{k-1}^*(z))} \end{aligned}$$

and hence  $\Phi_{n-1}(z)$  has the desired factorization. Reversing this reasoning shows the converse statement.  $\square$

### 5.2 Mirman's Circular Iterations

Our goal in the following chapters will be to use Theorem 5.1 to classify matrices in  $S_n$  with elliptic numerical ranges given the foci of the numerical range ellipse rather than the set of all the foci of  $C$ . Notice that the theorem is also stated for general curves, so some other conditions will be required in the elliptic case. We will explore this more in later sections for some particular values of  $n$ . Recall Darboux's result: if a component  $C_j$  of a complete  $n$ -Poncelet curve as in Equation (4.9) is an ellipse and has  $n$ -Poncelet property (notice that here both  $n$  are the same) then  $C$  is a union of  $[n/2]$  disjoint ellipses (also known as a package of ellipses). Using the terminology introduced in Section 4.1.1, this is equivalent to assuming that the curve  $C_j$  is the envelope of polygons  $\mathcal{P}_j(z)$  as defined in (4.6), with  $\gcd(j, n) = 1$ . In this section we want to explore these ideas further and analyze the case of a component  $C_j$  being an

ellipse. This situation, especially when the convex component  $C_1$  is assumed to be an ellipse, has attracted interest before, see e.g. [5, 8, 10, 11, 12, 13, 26, 29, 36, 51, 56].

We will use Mirman's iterations to find a condition that determines if a set of points are the foci of a Poncelet curve  $C$ . As we will see, Mirman's iterations provide a necessary but not sufficient condition in the elliptic case. As it could be expected, for an ellipse, Mirman's parametrization  $P(z, w) = 0$ , described in the previous section, has a more explicit form. It was derived by Mirman [55, 56] that if  $f_1, f_2 \in \mathbb{D}$  are the foci of  $C_j$  and  $s$  is the length of its minor semiaxis, then the straight line  $\ell$  joining two points,  $z, w \in \mathbb{T}$ , is tangent to  $C_j$  if and only if  $z, w$  satisfy the equation  $q(z, w) = 0$ , where

$$q(z, w) = q(z, w; f_1, f_2, s) := (w + b_1(z; f_1))(w + b_1(z; f_2)) - \frac{4s^2zw}{\Phi_2^*(z; f_1, f_2)}, \quad (5.5)$$

see the notation in (3.1), (3.2), (3.13). If  $C_j$  is degenerated to a point ( $f_1 = f_2, s = 0$ ), then we need to replace the expression above by

$$q(z, w) = q(z, w; f_1, f_1, 0) = q(z, w; f_1) := w + b_1(z; f_1). \quad (5.6)$$

In the non-degenerate case ( $C_j$  is not a point) the Poncelet correspondence  $\tau$  is correctly defined. Algebraically, it means that for  $z \in \mathbb{T}$ , the equation  $q(z, w; f_1, f_2, b) = 0$  is quadratic in  $w$  and has two solutions, the endpoints of the tangents to  $C_j$  starting at  $z$  and ending on  $\mathbb{T}$  (namely,  $\tau(z)$  and  $\tau^{-1}(z)$ ). This allows us to define an iterative process (that we call the *circular Mirman's iteration*) as follows:

Start from  $w_0 \in \mathbb{T}$  and define  $w_1 \in \mathbb{T}$  as one of the two solutions of  $q(w_0, w; f_1, f_2, s) = 0$ .

For  $i = 1, 2, \dots$ , choose as  $w_{i+1}$  the solution of  $q(w_i, w; f_1, f_2, s) = 0$  such that  $w_{i+1} \neq w_{i-1}$ .

Clearly,  $C_j$  has an  $n$ -Poncelet property if and only if  $w_n = w_0$ , and  $n$  is the smallest natural number for which equality holds (in other words, if the orbit of the circular Mirman's iteration has length  $n$ ).

The advantage of the algebraic interpretation of the iteration  $\tau^k(z)$  is that we no longer need to assume  $z \in \mathbb{T}$  (in which case the geometric interpretation is less obvious).

Reasoning as in the case of Mirman's parametrization (see Section 4.4), we see that replacing  $w_0 = 0$  in  $q(w_0, w; f_1, f_2, s) = 0$  yields the foci of  $C_j$ ; in other words, starting in Mirman's iterations with  $w_0 = 0$  necessarily yields either  $w_1 = f_1$  or  $w_1 = f_2$ . So, we can define the iterative process (let us call it the *inner Mirman's iteration*) as follows:

Start from  $w_0 = 0$ , define  $w_1 \in \{f_1, f_2\}$  and for  $i = 1, 2, \dots$ , choose as  $w_{i+1}$  the solution of  $q(w_i, w; f_1, f_2, s) = 0$  such that  $w_{i+1} \neq w_{i-1}$ .

Assume that  $C_j$  has the  $n$ -Poncelet property and let  $f_1, \dots, f_{n-1}$  be the set of points in  $\mathbb{D}$  generated by this iterative process. According to Theorem 5.1, there exists a unique algebraic  $n$ -Poncelet curve  $\Gamma$  of class  $n - 1$  with real foci precisely at  $f_1, \dots, f_{n-1}$ , and let  $P(z, w) = 0$  be its Mirman's parametrization. The following result was proved in [55] and is a simple consequence of Bézout's theorem:

*Theorem 5.4.* *Under the assumptions above,  $q(z, w; f_1, f_2, s)$  divides  $P(z, w)$ . Moreover, in the decomposition (4.9), each component  $C_k$  is an ellipse, and they are all disjoint. The ellipse  $C_{[n/2]}$  is degenerate (a point) if  $n$  is even. If we denote by  $f_{2k-1}$  and  $f_{2k}$  the foci of  $C_k$ , and by  $s_k$  its minor semiaxis, then*

$$P(z, w; f_1, \dots, f_{n-1}) = \prod_{k=1}^{[n/2]} q(z, w; f_{2k-1}, f_{2k}, s_k); \quad (5.7)$$

*if  $n$  is even, we take  $f_{n-1} = f_n$ ,  $s_{[n/2]} = 0$ .*

Comparing this statement with Theorem 2.2 in the Introduction, we see that Mirman in fact reproved Darboux's result while being unaware of his work!

### 5.2.1 Nonelliptic packages with elliptic components

An assumption of Theorem 5.4 is that the curve  $\Gamma$  is of class exactly  $n - 1$ , as the following construction shows. With  $f_1, \dots, f_{n-1}$  being the points in  $\mathbb{D}$  generated by inner Mirman's iterations for  $C_j$ , let

$$b_n(z) = b_n(z; 0, f_1, \dots, f_{n-1}) = \frac{z\Phi_{n-1}(z)}{\Phi_{n-1}^*(z)}, \quad \Phi_{n-1}(z) = \Phi_n(z; f_1, \dots, f_{n-1}).$$

Pick arbitrary points  $g_1, \dots, g_{m-1} \in \mathbb{D}$ , define

$$B_m(z) = b_m(z; 0, g_1, \dots, g_{m-1}) = \frac{z\Phi_{m-1}(z)}{\Phi_{m-1}^*(z)}, \quad \Phi_{m-1}(z) = \Phi_{m-1}(z; g_1, \dots, g_{m-1}),$$

and consider the composition

$$D_{mn}(z) = (B_m \circ b_n)(z) = B_m(b_n(z)),$$

which is again a Blaschke product with  $D_{mn}(0) = 0$ . Then the envelope of polygons supported on solutions of  $D_{mn}(z) = \bar{\lambda}$ ,  $\lambda \in \mathbb{T}$ , is a complete  $mn$ -Poncelet curve  $\tilde{\Gamma}$  of class  $mn - 1$ . One of its components is the  $n$ -Poncelet ellipse  $C_j$ . However, as we have seen, the inner Mirman's iteration for  $C_j$  generates only  $n - 1$  values,  $f_1, \dots, f_{n-1}$ , among them, the two foci of this ellipse. All these values are a subset of the real foci of  $\tilde{\Gamma}$ , and by considerations above and by Theorem 5.4, these will be foci of a package of  $[n/2]$  ellipses, all components of  $\tilde{\Gamma}$ . However, this does not mean that *the whole* curve  $\tilde{\Gamma}$  is a package of Poncelet ellipses.

Example 5.5. Let  $n = 3$ ,  $f_1, f_2 \in \mathbb{D}$ ,  $g_1, \dots, g_{m-1} \in \mathbb{D}$  ( $m \geq 2$ ), and as above,

$$D_{3m}(z) = (B_m \circ b_3)(z), \quad b_3(z) = b_3(z; 0, f_1, f_2), \quad B_m(z) = b_m(z; 0, g_1, \dots, g_{m-1}).$$

Then the envelope of polygons supported on solutions of  $D_{3n}(z) = \bar{\lambda}$ ,  $\lambda \in \mathbb{T}$ , contains a 3-Poncelet ellipse with foci  $f_1$  and  $f_2$ , whose minor semiaxis is

$$s^2 = \frac{1 - |f_1|^2 - |f_2|^2 + |f_1 f_2|^2}{4}$$

(use (5.7) with  $n = 3, m = 1$ ). Notice that the inner Mirman iteration for that ellipse yields only  $f_1$  and  $f_2$ .

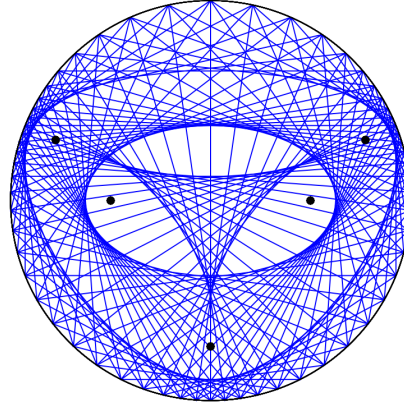


Figure 5.2. Illustration for Example 5.5, with  $f_1 = -f_2 = 1/2$  and  $g_1 = i/2$  ( $m = 2$ ).

A simple consequence of our considerations is the following

**Theorem 5.6.** *Let  $\Gamma$  be a complete  $n$ -Poncelet curve of class  $n - 1$ ,  $C_j$  be an elliptic component of the decomposition (4.9), and assume that the maximal set generated by Mirman's inner iteration corresponding to  $C_j$  contains only  $m - 1$  distinct values  $w_1, \dots, w_{m-1}$ ,  $m \leq n$ . Then*

- *$n$  is divisible by  $m$ ;*

- $\{w_1, \dots, w_{m-1}\} \subset \{f_1, \dots, f_{n-1}\}$ , and  $w_j$  are foci of a package of  $[m/2]$  ellipses, all of them components of  $\Gamma$ .

For instance, if  $n$  is prime, then the existence of any elliptic component in  $\Gamma(\mathbb{R})$  forces all  $C_k$ 's to be ellipses (it is a package of ellipses).

Using the above and Theorem 5.3, we have the following lemmas, which we will use in Chapter Six.

**Lemma 5.7.** *Let  $B_{2m}(z)$  be a regular Blaschke product that decomposes as*

$$B_{2m}(z) = B_m(B_2(z)). \quad (5.8)$$

*Then if  $\mathcal{P}(z)$  is the polygon with vertices at  $\mathcal{Z}^\lambda$ , the solution set to  $B_{2m}(z) = \lambda$ , then the main diagonals of  $\mathcal{P}(z)$  meet at a single point, the zero of  $\frac{B_{2m}(z)}{z}$ . Equivalently, if  $\phi_{2m-1}(z)$  factors as*

$$\Phi_1(z) \prod_{j=1}^{m-1} \mathcal{S}_{a_j}(\Phi_1(z)), \quad (5.9)$$

*then the main diagonals of the polygons identified by the paraorthogonal extension of  $\phi_{2m-1}(z)$  meet at  $\overline{\Phi_1(0)}$ , the conjugate of the first Verblunsky coefficient in the factorization.*

Lemma 5.7 is a rephrasing of [11, Corollary 5.8], and the following lemma is also a rephrasing of [11, Corollary 5.10].

**Lemma 5.8.** *Let  $B_{3m}(z)$  be a regular Blaschke product that decomposes as*

$$B_{3m}(z) = B_m(B_3(z)). \quad (5.10)$$

*Then if  $P(z)$  is the polygon with vertices at  $\mathcal{Z}^\lambda$ , the solution set to  $B_{3m}(z) = \lambda$ , then the vertices of  $P(z)$  can be divided into  $m$  triangles that circumscribe a Poncelet-3 ellipse. The foci of this Poncelet-3 ellipse are the zeros of  $\frac{B_3(z)}{z}$ . Equivalently, if*

$\phi_{3m-1}(z)$  factors as

$$\Phi_2(z) \prod_{j=1}^{m-1} \mathcal{S}_{a_j}(\Phi_2(z)), \quad (5.11)$$

then vertices of the polygons identified by the paraorthogonal extension of  $\phi_{3m-1}(z)$  meet at the zeros of  $\Phi_2(z)$ .

See Figure 5.2.

### 5.2.2 Mirman's System

We can reformulate Mirman's iteration by observing the independent term in (5.5) and applying Vieta's formulas: given a value  $z$ , the two solutions  $w'$  and  $w''$  of  $q(z, w; f_1, f_2, s) = 0$  satisfy

$$w'w'' = b_1(z; f_1)b_1(z; f_2) = b_2(z; f_1, f_2).$$

In particular, in the circular Mirman iteration,

$$w_{i+1}w_{i-1} = b_2(w_i; f_1, f_2), \quad i = 1, 2, \dots \quad (5.12)$$

This is a three term recurrence relation that has an advantage of not requiring knowledge of value  $s$  of the semiaxis. It needs two initial values, for which we could use  $w_0$  and  $w_1$ . However, notice that it is necessary to know  $s$  in order to calculate  $w_1$ . Obviously, since all  $w_i$ 's are on  $\mathbb{T}$ , formulas (5.12) generate  $w_{i+1}$  from  $(w_{i-1}, w_i)$  for all  $i \in \mathbb{N}$ .

As before, relaxing the assumptions we still can use the iterations (5.12); however, in the present situation there are two additional moments to address:

- The iteration breaks down when  $w_{j-1} = 0$ ;
- for that reason, we cannot use  $w_0 = 0$  and  $w_1 = f_1$  (or  $w_1 = f_2$ ) to initialize the process; we need to calculate a third value, a solution of  $q(w_1, w; f_1, f_2, s) = 0$ ,

$w_2 \neq 0$ . Notice that

$$q(f_i, w; f_1, f_2, s) = w \left( w + b_1(f_i; f_j) - \frac{4s^2 f_i}{\Phi_2^*(f_i; f_1, f_2)} \right), \quad i \neq j, \quad i, j \in \{1, 2\},$$

so we can initialize the inner Mirman iterations explicitly by

$$w_1 = f_i \in \{f_1, f_2\}, \quad w_2 = -b_1(f_i; f_j) + \frac{4s^2 f_i}{\Phi_2^*(f_i; f_1, f_2)}, \quad i \neq j, \quad i, j \in \{1, 2\}. \quad (5.13)$$

As it was observed, the value of  $s$  is necessary to calculate  $w_2$ .

Note also that satisfying Mirman's system is a necessary but not sufficient condition for a set  $\{f_1, \dots, f_{n-1}\}$  to be the foci of a package of Poncelet ellipses. As we will see in the following chapters, Mirman's system yields both trivial solutions (some  $f_j = 0$ ) and solutions outside  $\bar{\mathbb{D}}$ . Mirman's system also gives solutions with the initial  $f_1, f_2$  as foci of smaller ellipses in the package rather than foci of the numerical range ellipse. Thus Mirman's system alone is not enough to specify the entire set of foci of  $C$  given only  $f_1, f_2$ , the desired foci of  $C_1$ .

### 5.3 Examples

#### 5.3.1 Poncelet Triangles

Poncelet triangles have been explored thoroughly, see e.g. [13]. The question of finding  $\mathbf{A} \in S_2$  with an elliptic numerical range and foci  $f_1, f_2$  is rather straightforward given the Elliptical range theorem, see e.g. [13, Chapter 6], [41, §1.3] or [51].

Theorem 5.9 (Elliptical Range Theorem). *If  $n = 2$  and  $\mathbf{A}$  is a  $2 \times 2$  matrix, then  $W(\mathbf{A})$  is an ellipse with eigenvalues  $f_1$  and  $f_2$  as foci, and the minor axis of length*

$$\sqrt{\text{tr}(\mathbf{A}^* \mathbf{A}) - |f_1|^2 - |f_2|^2}.$$

Equivalently, if  $B_3(z)$  is a regular Blaschke product with  $f_1, f_2$  zeros of  $\frac{B_3(z)}{z}$ , then the polygons identified by  $\mathcal{Z}^\lambda$  circumscribe a Poncelet-3 ellipse given by the equation

$$|z - f_1| + |z - f_2| = |1 - \overline{f_1}f_2|. \quad (5.14)$$

See [13, Theorem 2.9, Corollary 5.8] as well as [13, Chapters 2-5] for more details.

Finally, [54, Section 12] provides the OPUC equivalence of Poncelet triangles. Given  $f_1, f_2$ , define  $\Phi_2(z) = (z - f_1)(z - f_2)$ . Then the triangles formed by the paraorthogonal extensions of  $\Phi_2(z)$  form Poncelet triangles that circumscribe an ellipse with foci  $f_1, f_2$ . Equivalently, from  $\Phi_2(z)$  we can define a CMV matrix  $\mathbf{A} \in S_2$  whose characteristic polynomial is  $\Phi_2(z)$ . Then  $W(\mathbf{A})$  is an ellipse with foci  $f_1, f_2$  and the eigenvalues of the rank one unitary dilations of  $\mathbf{A}$  are the vertices of the circumscribing triangles.

Recall also that Chapple discovered that a circle  $E \in \mathbb{D}$  with center at  $f_1 \in \mathbb{D}$  is circumscribed by infinitely many triangles with vertices of  $\mathbb{T}$  if and only if the radius of the circle is

$$r = \frac{1 - |f_1|^2}{2}. \quad (5.15)$$

Using (5.14) above with  $f_1 = f_2$ , one recovers this formula.

---

**Algorithm 5.1** Find a matrix  $\mathbf{A} \in S_2$  with an elliptic numerical range and foci  $f_1, f_2$

**Input:**  $f_1, f_2$ .

- 1: Define  $\Phi_2(z) = (z - f_1)(z - f_2)$
- 2:  $-\overline{\alpha_1} = f_1 f_2$
- 3: Perform inverse Szegő recursion to recover  $\Phi_0(z)$ .
- 4:  $-\overline{\alpha_0} = \Phi_1(0) = \frac{(f_1 f_2 (\overline{f_1} + \overline{f_2}) - f_1 - f_2)}{1 - |f_1 f_2|^2}$

**Output:**

$$\mathbf{A} = \begin{pmatrix} \overline{\alpha_0} & \overline{\alpha_1} \rho_0 \\ \rho_0 & -\overline{\alpha_1} \alpha_0 \end{pmatrix}, \quad \rho_n = \sqrt{1 - |\alpha_n|^2} \quad (5.16)$$


---

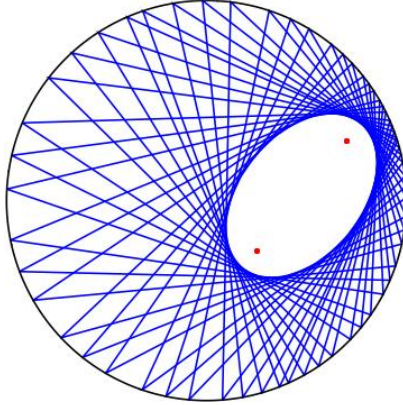


Figure 5.3. Poncelet-3 ellipse with foci  $0.25 - 0.25i$  and  $0.7 + 0.3i$  as in Example 5.10

Example 5.10. Find the Poncelet 3-ellipse with foci  $f_1 = 0.25 - 0.25i$  and  $f_2 = 0.7 + 0.3i$ .

We begin with

$$\Phi_2(z) = (z - 0.25 + 0.25i)(z - 0.7 - 0.3i)$$

and  $-\overline{\alpha_1} = (0.25 - 0.25i)(0.7 + 0.3i) = 0.25 - 0.1i$ . Then

$$\overline{\alpha_0} = \frac{(0.25 - 0.1i)(0.95 - 0.05i) - 0.95 - 0.05i}{1 - 0.0525} = -0.757256 - 0.166227i.$$

Then  $\rho_0 = 0.631611$  and  $\rho_1 = 0.963068$ , so the desired CMV matrix is

$$\mathbf{A} = \begin{pmatrix} -0.757256 - 0.166227i & 0.631611(-0.25 + 0.1i) \\ 0.631611 & (0.25 - 0.1i)(-0.757256 - 0.166227i) \end{pmatrix}$$

whose numerical range is depicted in Figure 5.3.

### 5.3.2 Toy Version

Although Theorem 5.1 is stated for  $n \geq 3$ , its “toy version” for  $n = 2$  also holds:

Proposition 5.11. *Let  $f \in \mathbb{D}$ , and for  $\lambda \in \mathbb{T}$  define*

$$z_{\pm}^{\lambda} = \frac{1}{2} \left( f - \overline{f}\lambda \pm \sqrt{(f - \overline{f}\lambda)^2 + 4\lambda} \right) \in \mathbb{T},$$

*zeros of  $\Phi_2^{(\bar{f}, \lambda)}(z) = z(z - f) - \bar{\lambda}(1 - \bar{f}z)$ , or equivalently, eigenvalues of the  $2 \times 2$  cut-off CMV matrix*

$$\mathcal{G}^{(2)} = \mathcal{G}^{(2)}(\bar{f}, \lambda) = \begin{pmatrix} f & \bar{\lambda}\sqrt{1 - |f|^2} \\ \sqrt{1 - |f|^2} & -\bar{f}\lambda \end{pmatrix}.$$

*Then for every  $\lambda \in \mathbb{T}$ , the straight segment joining  $z_-^{\lambda}$  and  $z_+^{\lambda}$  passes through  $f$ .*

In terms of finite Blaschke products, this is equivalent to the way a regular degree-2 Blaschke product identifies chords through  $\mathbb{T}$  that all intersect at the zero of  $\frac{B_2(z)}{z}$ . See the proof in [13, Theorem 4.1], for instance.

For higher degree  $n$ , these characterizations naturally become more complex as the number of connected components of  $C$  increases. In Chapter Six, we will apply Theorem 5.1 to the cases of Poncelet Quadrilaterals and Hexagons. In Chapter Seven, we will use Section 5.2 to characterize Poncelet Pentagons.

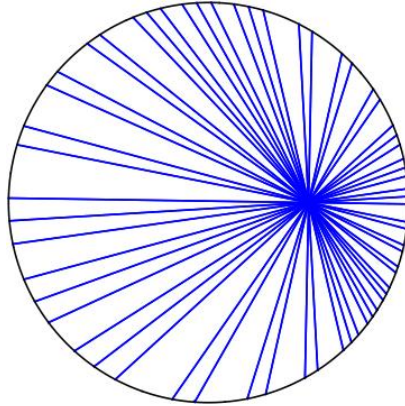


Figure 5.4. Line segments through  $f_1 = 0.5$ .

## CHAPTER SIX

### Quadrilateral and Hexagonal Cases

A majority of this chapter is submitted for publication as Markus Hunziker, Andrei Martíez-Finkelshtein, Taylor Poe, and Brian Simanek, *On foci of ellipses inscribed in cyclic polygons*, Preprint, 2021.

We saw in Chapter Five that OPUC, finite Blaschke products, and numerical ranges of matrices in  $S_n$  give equivalent realizations of Poncelet ellipses. In particular, in this chapter we will see how OPUC results and terminology unify previous results using numerical ranges and Blaschke products and even allow us to reconstruct Mirman's iterations. For example, much of the following section will restate results from [37] in OPUC terms and, in many cases, give clarity to the relationships described therein. As composite numbers, four and six both factor, giving opportunity for degree-4 and -6 Blaschke products to decompose. In this sense, much of the analysis will be similar for quadrilaterals and hexagons.

#### *6.1 Poncelet Quadrilaterals*

##### *6.1.1 Packages of Poncelet-4 Ellipses*

In this section, we will characterize matrices in  $S_3$  whose numerical ranges are bounded by ellipses, or equivalently by [22, 43] with an elliptic component as there are only two components in the curve  $C$ . Many of these results first appeared in [24, 37] (see also [44]). We provide the orthogonal polynomial versions of their results, new proofs, and some extensions of their work.

Gorkin and Wagner [37, Theorem 3.3] showed that  $\mathbf{A} \in S_3$  has a numerical range that is an elliptical disk if and only if there are regular Blaschke products  $B_2(z), D_2(z)$  of degree 2 such that

$$B_4(z) = \frac{z \det(zI - \mathbf{A})}{\det(zI - \mathbf{A})^*} = B_2(D_2(z)). \quad (6.1)$$

The foci of the ellipse  $f_1, f_2$ , as stated before, are eigenvalues of  $\mathbf{A}$  and zeros of  $\frac{B_4(z)}{z}$ .

Gorkin and Wagner in [37, Proposition 3.7, Corollary 3.8] furthered Fujimura's results by finding a formula for the third zero of  $\det(zI - \mathbf{A})$  given  $f_1, f_2$ . They also proved that the diagonals of every circumscribing quadrilateral intersect at this third zero [37][Corollary 3.9].

The following theorem uses Theorem 5.3 to give an OPUC version of Fujimura's result.

**Theorem 6.1.** *Suppose  $\mathbf{A} \in S_3$ . The numerical range of  $\mathbf{A}$  is an elliptical disk if and only if there exist  $a, b \in \mathbb{D}$  so that*

$$\det(zI - \mathbf{A}) = \Phi_1(z; a)\Phi_2(z; a, b).$$

*If this condition holds, then the Pentagram curve is the single point  $\bar{a}$  and the foci of  $\partial W(\mathbf{A})$  are the zeros of  $\Phi_2(z; a, b)$ .*

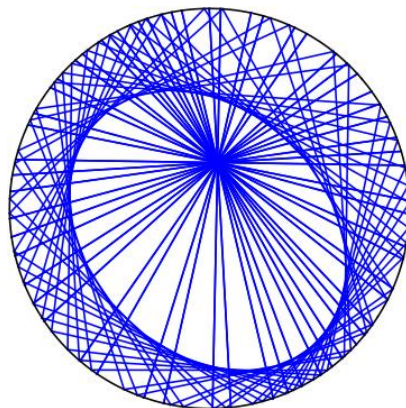


Figure 6.1. A Poncelet-4 ellipse given by  $\phi_3(z) = \Phi_0(z; 0.04 + 0.23i)\Phi_1(z; 0.04 + 0.23i, -0.25i)$ .

Theorem 6.1 uses the factorization (or equivalently, decomposition) described in Lemma 5.7. In this case, this diagonal point is also  $C_2$ , which we labeled in Section 4.3.1.1 as the Pentagram curve. Thus in the quadrilateral case, we call this the *Pentagram point* of the ellipse  $E$ .

This OPUC statement brings light to some subtleties from Fujimura, Gorkin, and Wagner's work. Gorkin and Wagner's formula for recovering the unique third zero where the main diagonals intersect is precisely the formula given by the inverse Szegő recursion. This point, the Pentagram point, is the zero of  $\frac{D_2(z)}{z}$ , the inner Blaschke product in the composition. Then the foci of the ellipse bounding the numerical range must be the other two zeros of  $\frac{B_4(z)}{z}$ . As stated in the theorem, the OPUC perspective shows that the Pentagram point is the conjugate of the first Verblunsky coefficient, and the foci are the zeros of  $\Phi_2(z; a, b)$ .

Theorem 6.1 gives us a new interpretation of the algorithm for finding a matrix in  $S_3$  with elliptic numerical range and two prescribed foci (such an algorithm can be found in [37]). Indeed, given  $\{f_1, f_2\} \in \mathbb{D}^2$ , consider the polynomial  $\Phi_2(z) = (z - f_1)(z - f_2)$ . Perform the Inverse Szegő recursion to obtain a degree 1 monic polynomial  $\Phi_1(z; \bar{f}_3)$  whose zero  $f_3$  is in  $\mathbb{D}$ . The  $3 \times 3$  cutoff CMV matrix with eigenvalues at  $\{f_1, f_2, f_3\}$  has the desired property.

In this case,

$$\Phi_1(z) = z + \frac{(f_1 f_2 (\bar{f}_1 + \bar{f}_2) - f_1 - f_2)}{1 - |f_1 f_2|^2}$$

and

$$-\overline{\beta_0} = \Phi_1(0) = \frac{(f_1 f_2 (\bar{f}_1 + \bar{f}_2) - f_1 - f_2)}{1 - |f_1 f_2|^2}, \quad (6.3)$$

precisely Gorkin and Wagner's formula.

---

**Algorithm 6.1** Find a matrix  $\mathbf{A} \in S_3$  with an elliptic numerical range and foci  $f_1, f_2$ .

---

**Input:**  $f_1, f_2$ .

- 1: Define  $\Phi_2(z) = (z - f_1)(z - f_2)$
- 2:  $-\overline{\beta_1} = f_1 f_2$
- 3: Perform inverse Szegő recursion to recover  $\Phi_1(z)$ .
- 4:  $-\overline{\beta_0} = \Phi_1(0)$
- 5:  $\det\{zI - \mathbf{A}\} = (z - f_1)(z - f_2)(z - \beta_0)$
- 6:  $-\overline{\alpha_2} = -f_1 f_2 \beta_0$
- 7: Perform inverse Szegő recursion to recover  $\alpha_1, \alpha_0$  **Output:**

$$\mathbf{A} = \begin{pmatrix} \overline{\alpha_0} & \overline{\alpha_1} \rho_0 & \rho_1 \rho_0 \\ \rho_0 & -\overline{\alpha_1} \alpha_0 & -\rho_1 \alpha_0 \\ 0 & \overline{\alpha_2} \rho_1 & -\overline{\alpha_2} \alpha_1 \end{pmatrix}, \quad \rho_n = \sqrt{1 - |\alpha_n|^2} \quad (6.2)$$


---

### 6.1.2 Specified Combinations of Foci

These results also allow us to find a matrix  $\mathbf{A} \in S_3$  with a single prescribed focus and main Pentagram point and to find a one-parameter family of matrices in  $S_3$  with the same Pentagram point and whose numerical ranges are elliptical disks.

Theorem 6.2. *Given  $\{f_1, f_3\} \in \mathbb{D}^2$ , there exists a unique  $3 \times 3$  cutoff CMV matrix whose numerical range is bounded by an ellipse with one focus at  $f_1$  and such that the Pentagram curve is the single point  $\{f_3\}$ .*

*Proof.* By Theorem 6.1, this amounts to showing that we can find  $b \in \mathbb{D}$  such that  $\Phi_2(z; \bar{f}_2, b)$  vanishes at  $f_1$ . Then

$$\Phi_2(z; f_3, b) = z(z - f_3) - \bar{b}(1 - z\bar{f}_3) \quad (6.4)$$

and

$$\Phi_2(f_1; f_3, b) = 0 = f_1(f_1 - f_3) - \bar{b}(1 - f_1\bar{f}_3). \quad (6.5)$$

Thus

$$\bar{b} = \frac{f_1 \Phi_1(f_1; f_3)}{\Phi_1^*(f_1; f_3)} = \frac{f_1(f_1 - f_3)}{1 - \bar{f}_3 f_1}$$

(see also [72]). □

From this, we see that the preimages of  $D_2(z; f_3) = \bar{b}$  are the foci of the ellipse. Recall  $b$  is the second Verblunsky coefficient of  $\Phi_2(z)$  and  $D_2(z)$  is the inner Blaschke product in the decomposition, where the zero of  $\frac{D_2(z)}{z}$  is the Pentagram point.

One can also find an  $\mathbf{A}_\alpha \in S_3$  with  $\partial W(\mathbf{A}_\alpha)$  an ellipse and whose Pentagram curve is a specified point but with no specified foci. Since this is a weaker set of conditions than was used in Theorem 6.2, one expects that we will have many solutions to this problem. Rather than a unique matrix as in Theorem 6.2, fixing the Pentagram point yields a family of matrices in  $S_3$  parametrized by the second Verblunsky coefficient of  $\Phi_2(z; a, b)$ .

*Proposition 6.3.* *Given  $\alpha_0 \in \mathbb{D}$ , there exists a one-parameter family  $\mathbf{A}_\alpha \in S_3$ ,  $\alpha \in \mathbb{D}$  such that for each  $\mathbf{A}_\alpha$ ,  $\partial W(\mathbf{A}_\alpha)$  is an ellipse and the Pentagram point of  $\mathbf{A}_\alpha$  is  $\alpha_0$ .*

*Proof.* Suppose  $\alpha_0$  is given and consider the polynomial  $\Phi_1(z; \bar{\alpha}_0)$ . For any  $\alpha \in \mathbb{D}$ , consider  $\Phi_2(z; \bar{\alpha}_0, \alpha)$  and define

$$\phi_3(z) = \Phi_1(z; \bar{\alpha}_0)\Phi_2(z; \bar{\alpha}_0, \alpha).$$

Thinking of  $\phi_3(z)$  as an OPUC and applying the inverse Szegő recursion allows us to recover the Verblunsky coefficients of  $\phi_3(z)$  and thus define a cutoff CMV matrix,  $\mathbf{A}_\alpha \in S_3$ , whose characteristic polynomial is  $\phi_3(z)$ . As  $\phi_3(z)$  factors into a degree one and degree two OPUC related by the Szegő recursion, Theorem 6.1 implies that  $\partial W(\mathbf{A}_\alpha)$  is an ellipse and the Pentagram point of  $\mathbf{A}_\alpha$  is  $\alpha_0$ . □

See Figure 6.2 for an example of Proposition 6.3.

#### 6.1.3 Mirman's Iterations for the Quadrilateral Case

Now suppose we have an  $\mathbf{A} \in S_3$  with numerical range given by an elliptical disk. Suppose that the foci of the ellipse bounding that elliptical disk are  $\{f_1, f_2\}$

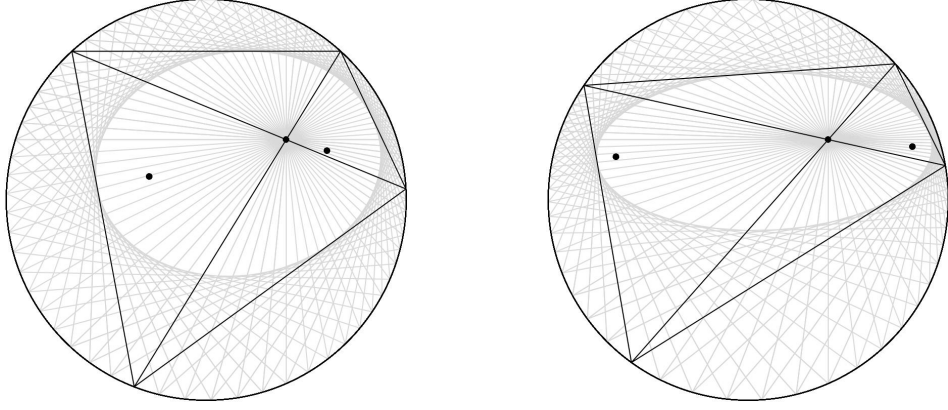


Figure 6.2. Two Poncelet 4-ellipses with the same Pentagram point,  $0.4 + 0.3i$ .

and the Pentagram point of that ellipse is  $\{f_3\}$ . Then

$$\det(zI - \mathbf{A}) = (z - f_1)(z - f_2)(z - f_3).$$

By Theorem 6.1, we also have

$$\det(zI - \mathbf{A}) = (z - f_3)(z(z - f_3) - b(1 - \bar{f}_3 z))$$

for some  $b \in \mathbb{D}$ . Evaluating both of these expressions at 0 and equating them shows  $b = -f_1 f_2$ . It follows that

$$(z - f_1)(z - f_2) = z(z - f_3) + f_1 f_2(1 - \bar{f}_3 z) = z^2 + z(-f_3 - f_1 f_2 \bar{f}_3) + f_1 f_2. \quad (6.6)$$

If we replace  $z$  by  $f_3$  in (6.6), we get

$$(f_3 - f_1)(f_3 - f_2) = f_1 f_2(1 - |f_3|^2). \quad (6.7)$$

If we look at the reversed polynomials in (6.6) and replace  $z$  by  $f_3$ , we get

$$(1 - \bar{f}_1 f_3)(1 - \bar{f}_2 f_3) = 1 - |f_3|^2. \quad (6.8)$$

If we divide (6.7) by (6.8), we recover the Mirman system:  $f_1 f_2 = B_2(f_3; f_1, f_2)$ .

Solving for  $f_3$  yields the familiar formula for  $f_3$  in terms of  $f_1, f_2$  (recall 6.3):

$$f_3 = \frac{f_1 + f_2 - f_2|f_1|^2 - f_1|f_2|^2}{1 - |f_1 f_2|^2}.$$

Notice that we have recovered something that the Mirman system does not give us. One can verify that  $f_3 = 0$  is a solution to the Mirman system, but this does not (in general) give us the matrix in  $S_3$  with elliptical numerical range. Our calculations using OPUC eliminate this extraneous solution.

#### 6.1.4 Examples of Poncelet Quadrilaterals

Note that the following examples do contain numerical approximations. Some values are rounded for spacing and convenience.

Example 6.4. Find the CMV matrix whose numerical range is bounded by the Poncelet-4 ellipse with foci  $f_1 = 0.4 + 0.2i$  and  $f_2 = -0.7i$ .

Using Algorithm 6.1 and Equation 6.3, we find that  $f_3 = -0.226164 + 0.507761i$ .

Then

$$\phi_3(z) = (z - 0.4 - 0.2i)(z + 0.7i)(z + 0.226164 - 0.507761i)$$

and  $-\overline{\alpha_2} = 0.14 - 0.28i$ . Then by the inverse Szegő recursion we recover  $\alpha_1, \alpha_0$  and find

$$\mathbf{A} = \begin{pmatrix} -0.460317 - 0.595761i & -0.148852 - 0.334188i & 0.547118 \\ 0.658162 & -0.40661 - 0.0989909i & 0.382653 - 0.495246i \\ 0 & 0.831282 & 0.226164 - 0.507761i \end{pmatrix},$$

see Figure 6.3.

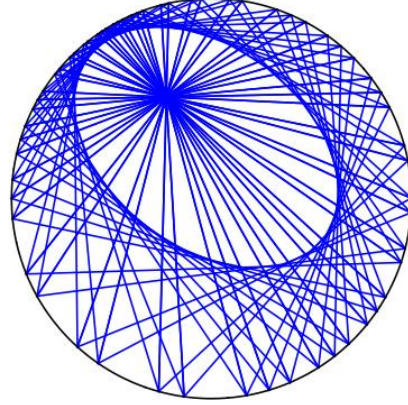


Figure 6.3. The numerical range of  $\mathbf{A}$  in Example 6.4.

Example 6.5. Find the CMV matrix whose pentagram point is  $f_3 = 0.7 + 0.13i$  whose numerical range is bounded by an ellipse, one of the foci of which is  $f_1 = 0.2 - 0.3i$ .

Using Theorem 6.2 and Equation 6.1.2, we see that

$$f_2 = \frac{(0.2 - 0.3i)(0.2 - 0.3i - 0.7 - 0.13i)}{1 - (0.7 - 0.13i)(0.2 - 0.3i)} = -0.220821 + 0.129159i.$$

Then  $\phi_3(z) = (z + 0.220821 - 0.129159i)(z - 0.2 - 0.3i)(z - 0.7 - 0.13i)$  and  $-\bar{\alpha}_3 = -0.0157618 + 0.0637506i$ . Then by the inverse Szegő recursion, we see that

$$\mathbf{A} = \begin{pmatrix} -0.7 - 0.13i & -0.00301946 - 0.0915823i & 0.696207 \\ 0.702211 & -0.0199646 - 0.090735i & 0.694015 - 0.128888i \\ 0 & 0.99145 & 0.00429993 - 0.13042i \end{pmatrix},$$

see Figure 6.4.

Example 6.6. Find the CMV matrix whose numerical range is bounded by a circle with pentagram point  $f_3 = -0.3333i$ .

For the numerical range to be bounded by a circle, we know the characteristic polynomial of the desired  $\mathbf{A} \in S_3$  must factor as  $\Phi_2(z)\Phi_1(z)$  where

$$\Phi_2(z) = (z - a)^2$$

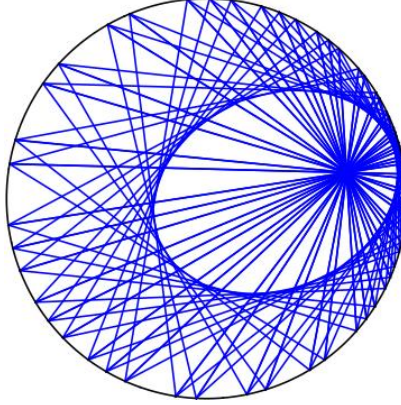


Figure 6.4. The numerical range of  $\mathbf{A}$  in Example 6.5.

as the foci coincide (i.e.  $f_1 = f_2 = f$ ). As  $\Phi_2(z)$  must relate to  $\Phi_1(z)$  by the Szegő recursion, we also know

$$\Phi_2(z) = z(z - f_3) - \overline{\beta_1}(1 - \overline{f_3}z) = z^2 + (\overline{\beta_1 f_3} - f_3)z - \overline{\beta_1}.$$

To guarantee the double root, the discriminant of  $\Phi_2(z)$  must be zero, i.e.

$$(\overline{\beta_1 f_3} - f_3)^2 - 4\overline{\beta_1} = 0.$$

Using the quadratic formula to solve for  $\overline{\beta_1}$ , we see that

$$\overline{\beta_1} = \frac{-2 + |f_3|^2 \pm 2\sqrt{1 - |f_3|^2}}{\overline{f_3}^2}.$$

As the center must be inside  $\mathbb{D}$ , we choose the positive root. Equipped with  $\beta_0 = 0.3333i$  and  $\beta_1 = 0.029431$ , we find  $\phi_3(z) = z(z - 0.3333i) - 0.029431(1 + 0.3333iz)$  and  $-\overline{\alpha_2} = -0.000980935i$ . Performing inverse Szegő recursion, we find that

$$\mathbf{A} = \begin{pmatrix} 0.171555i & 0.169011i & 0.970569 \\ 0.985175 & -0.029431 & 0.169011i \\ 0 & 0.985175 & 0.171555i \end{pmatrix}.$$

Alternatively, we could have used the fact that the center is a double root of

$$\frac{z(z - f_3)}{1 - \overline{f_3}z} - \overline{\alpha_1} = 0$$

or equivalently, a zero of the derivative of the Blaschke product. Figure 6.5 depicts this example.

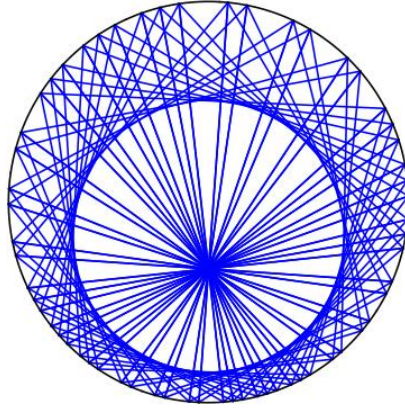


Figure 6.5. The numerical range of  $A$  in Example 6.6.

### 6.2 Poncelet Hexagons

In this section, we will consider curves that are realized as the envelope of line segments joining vertices of hexagons inscribed in the unit circle (see Section 3.4.4 for a rigorous discussion of envelopes of cyclic polygons) and characterize matrices in  $S_5$  with elliptic numerical ranges and prescribed foci. In many ways, the hexagon case will parallel the quadrilateral case. The main differences arise from the hexagons yielding three ellipses, one degenerate, where the package in the quadrilateral case contained only two components. Recall the names and interpretations of each component (see Section 4.3): the largest one (outer) formed by connecting adjacent eigenvalues of the unitary dilations is the *Poncelet curve*, the middle compo-

nent formed by joining alternate eigenvalues is the *Pentagram curve*, and the smallest component formed by joining opposite eigenvalues is the *Brianchon curve*.

### 6.2.1 Elliptic Components for Hexagons

As in the quadrilateral case, our analysis begins with results from [11] which we restate in OPUC terms. First, we consider analogous conditions for the Pentagram curve of  $\mathcal{G}^{(5)}$  to be an ellipse.

Theorem 6.7. *Let  $\mathcal{G}^{(5)}$  be a cut-off CMV matrix and*

$$\Phi_5(z) := \det(zI_5 - \mathcal{G}^{(5)}).$$

*The following are equivalent.*

- (i) *the Pentagram curve of  $\mathcal{G}^{(5)}$  is an ellipse;*
- (ii) *there exist regular Blaschke products  $\{B_j\}_{j=2}^3$  with  $\deg(B_j) = j$  such that*

$$\frac{z\Phi_5(z)}{\Phi_5^*(z)} = B_2(B_3(z))$$

- (iii) *there exist  $\alpha_0, \alpha_1, \alpha_2 \in \mathbb{D}$  so that*

$$\Phi_5(z) = \Phi_2(z; \alpha_0, \alpha_1)\Phi_3(z; \alpha_0, \alpha_1, \alpha_2).$$

*If any of these conditions hold, then the foci of the Pentagram curve are the zeros of  $B_3(z)/z$  or equivalently, the zeros of  $\Phi_2(z; \alpha_0, \alpha_1)$ .*

Similarly, the following theorem gives the conditions for which the Brianchon curve of  $\mathcal{G}^{(5)}$  is a single point.

Theorem 6.8. *If we retain the notation from Theorem 6.7, then the following are equivalent:*

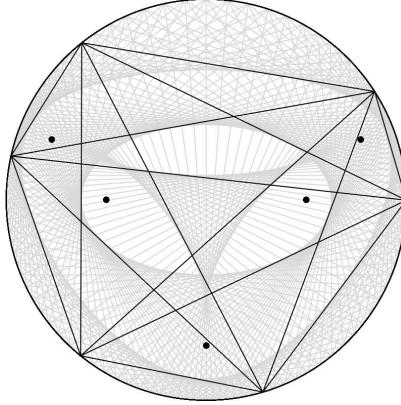


Figure 6.6. A 6-Poncelet curve such that the Pentagram curve is an ellipse but the Brianchon curve is not a single point.

- (i) the Brianchon curve of  $\mathcal{G}^{(5)}$  is a single point;
- (ii) there exist regular Blaschke products  $\{B_j\}_{j=2}^3$  with  $\deg(B_j) = j$  such that

$$\frac{z\Phi_5(z)}{\Phi_5^*(z)} = B_3(B_2(z))$$

- (iii) there exist  $\alpha_0, \alpha_1, \gamma_1 \in \mathbb{D}$  so that

$$\Phi_5(z) = \Phi_1(z; \alpha_0)\Phi_2(z; \alpha_0, \alpha_1)\Phi_2(z; \alpha_0, \gamma_1).$$

If any of these conditions hold, then the Brianchon point is the zero of  $B_2(z)/z$  and the zero of  $\Phi_1(z; \alpha_0)$ .

The equivalence of (i) and (ii) in both theorems is proven in [11][Corollary 5.10, Corollary 5.8]. The equivalence of (ii) and (iii) in both theorems follows from Theorem 5.3.

By comparing Theorem 6.8 with Theorem 6.1, one arrives at the following result.

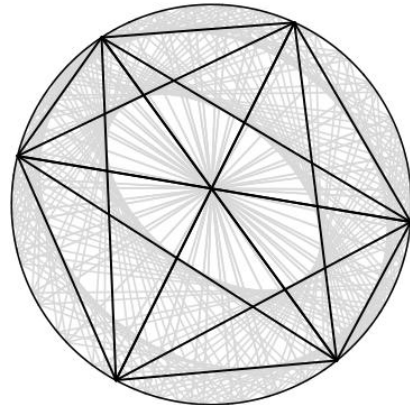


Figure 6.7. A 6-Poncelet curve such that the Brianchon curve is a degenerate ellipse but the Pentagram curve is not an ellipse.

Corollary 6.9. Let  $\mathbf{A} \in S_5$  have eigenvalues  $\{f_j\}_{j=1}^5$ . Suppose the Brianchon curve of  $\mathbf{A}$  is the point  $f_5$ . Then  $\{f_j\}_{j=1}^4$  can be labelled in such a way that both of the following conditions hold:

- (i)  $f_5$  is the Pentagram point of the Poncelet 4-ellipse with foci at  $f_1$  and  $f_4$ ;
- (ii)  $f_5$  is the Pentagram point of the Poncelet 4-ellipse with foci at  $f_2$  and  $f_3$ .

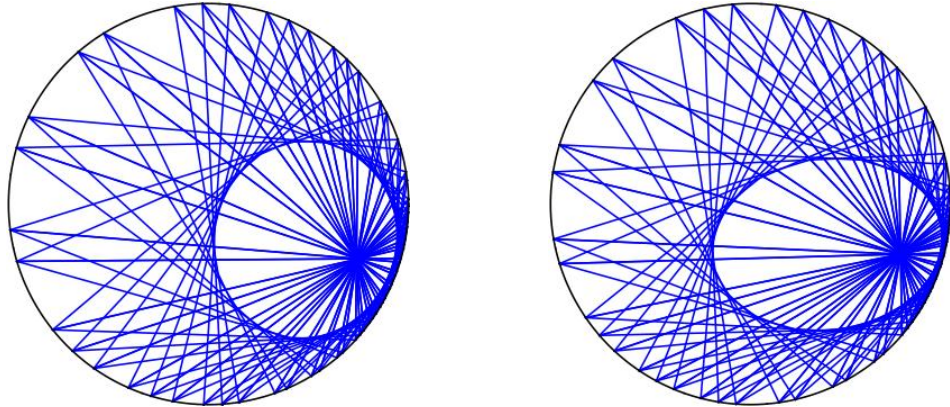


Figure 6.8. Using the foci from Example 6.17, the figure on the left represents Corollary 6.9 (i) and the figure on the right represents Corollary 6.9 (ii).

### 6.2.2 Package of Poncelet-6 Ellipses

Combining Theorem 6.7 and Theorem 6.8, we can prove the following.

Theorem 6.10. *If we retain the notation from Theorem 6.7, then the following are equivalent*

- (i) *The Poncelet curve associated with  $\mathcal{G}^{(5)}$  is an ellipse.*
- (ii) *There exist regular Blaschke products  $\{B_j\}_{j=2}^3$  with  $\deg(B_j) = j$  and regular Blaschke products  $\{D_j\}_{j=2}^3$  with  $\deg(D_j) = j$  such that*

$$\frac{z\Phi_5(z)}{\Phi_5^*(z)} = B_3(B_2(z)) = D_2(D_3(z)).$$

- (iii) *The Pentagram curve of  $\mathcal{G}^{(5)}$  is an ellipse and the Brianchon curve of  $\mathcal{G}^{(5)}$  is a single point.*

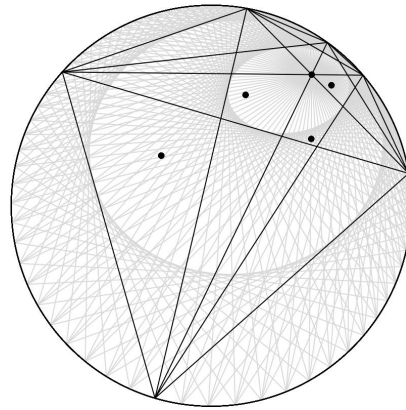


Figure 6.9. A Poncelet 6-ellipse along with the Pentagram ellipse and Brianchon point.

*Proof.* The equivalence of (ii) and (iii) is an immediate consequence of Theorems 6.7 and 6.8. The fact that (i) implies (iii) is a result of Darboux (see [43, Theorem B]). To see that (iii) implies (i), we will make use of the dual curve described in Section

3.4.2. Notice that Chapter Four implies that if  $C_1$ ,  $C_2$ , or  $C_3$  is an algebraic curve of degree 1 or 2, then the same is true of the corresponding component of the dual curve and vice versa (counting a single point as having degree 1). The dual curve in this case has degree 5 (see [24, Section 3]). Thus, if the Brianchon curve has degree 1 and the Pentagram curve has degree 2, then the Poncelet curve has degree 2, which means it is an ellipse.  $\square$

By Theorem 6.7 and Theorem 6.8, the decomposition in (ii) implies

$$\Phi_5(z) = \Phi_1(z; \alpha_0)\Phi_2(z; \alpha_0, \alpha_1)\Phi_2(z; \alpha_0, \gamma_1) = \Phi_2(z; \alpha_0, \alpha_1)\Phi_3(z; \alpha_0, \alpha_1, \alpha_2). \quad (6.9)$$

which allows us to state the following result for characterizing a matrix  $\mathbf{A} \in S_5$  with elliptic numerical range and given foci in terms of OPUC. Theorem 2.4 tells us that such an ellipse exists and is the unique Poncelet 5-ellipse with foci at  $f_1$  and  $f_2$ . We will find a cutoff CMV matrix whose numerical range is bounded by an ellipse with foci at  $\{f_1, f_2\}$ , whose Pentagram curve is an ellipse (whose foci will be called  $\{f_3, f_4\}$ ), and whose Brianchon curve is a single point (that we will call  $f_5$ ).

*Theorem 6.11. A matrix  $\mathbf{A} \in S_5$  with eigenvalues  $\{f_j\}_{j=1}^5$  satisfies all of the following conditions*

- (i)  $W(\mathbf{A})$  is an elliptical disk
- (ii) the foci of  $\partial W(\mathbf{A})$  are  $\{f_1, f_2\}$
- (iii) the foci of the Pentagram curve are  $\{f_3, f_4\}$
- (iv) the Brianchon curve is the single point  $f_5$

if and only if the complex numbers  $\{f_j\}_{j=1}^5$  satisfy

$$\{f_3, f_4\} = \left\{ \frac{f_5 - f_2}{1 - f_2 \bar{f}_5}, \frac{f_5 - f_1}{1 - f_1 \bar{f}_5} \right\} \quad (6.10)$$

as sets and

$$\begin{aligned} f_3 + f_4 + f_1 f_2 f_5 \bar{f}_4 \bar{f}_3 &= f_1 + f_2 + f_5 \\ f_3 f_4 + f_1 f_2 f_5 (\bar{f}_4 + \bar{f}_3) &= f_1 f_2 + f_2 f_5 + f_1 f_5 \end{aligned} \tag{6.11}$$

Recall that Theorem 6.8 and Theorem 6.10 show that if  $W(\mathbf{A})$  is bounded by an ellipse, then the characteristic polynomial factors in a certain way (in terms of OPUC) and the degree 1 polynomial in that factorization vanishes at the Brianchon point. To prove Theorem 6.11, we require the following refinement of that result, which tells us about the zeros of the remaining polynomials in that factorization.

**Lemma 6.12.** *Suppose  $\mathbf{A} \in S_5$  is such that  $W(\mathbf{A})$  is an elliptical disk and the eigenvalues of  $\mathbf{A}$  are  $\{f_j\}_{j=1}^5$ . Suppose the foci of  $\partial W(\mathbf{A})$  are  $\{f_1, f_2\}$ , the foci of the Pentagram curve are  $\{f_3, f_4\}$ , and the Brianchon point is  $f_5$ . Write*

$$\det(zI_5 - \mathbf{A}) = \Phi_1(z; \alpha_0)\Phi_2(z; \alpha_0, \alpha_1)\Phi_2(z; \alpha_0, \gamma_1)$$

as in Theorem 6.8. If  $\Phi_2(f_1; \alpha_0, \alpha_1) = 0$ , then  $\Phi_2(f_2; \alpha_0, \gamma_1) = 0$ .

*Proof.* Suppose  $\Phi_2(f_1; \alpha_0, \alpha_1) = 0$  and  $\Phi_2(f_2; \alpha_0, \gamma_1) \neq 0$ . Then  $\Phi_2(f_2; \alpha_0, \alpha_1) = 0$  and hence  $\Phi_2(f_3; \alpha_0, \gamma_1) = \Phi_2(f_4; \alpha_0, \gamma_1) = 0$  since OPUC are determined by their Verblunsky coefficients and vice versa.

Since  $\Phi_2(f_2; \alpha_0, \alpha_1) = 0$ , we can write

$$(z - f_5)(z - f_1)(z - f_2) = \Phi_1(z; \alpha_0)\Phi_2(z; \alpha_0, \alpha_1).$$

This means  $\{f_1, f_2, f_5\}$  are the eigenvalues of some  $\mathbf{A} \in S_3$  that satisfies the hypotheses of Theorem 6.1. Applying the Mirman system in the  $N = 4$  case shows

$$f_1 f_2 = B_2(f_5; f_1, f_2)$$

The Mirman system in the case  $n = 6$  shows shows  $f_3 f_4 = B_2(f_5; f_1, f_2)$  and hence  $f_1 f_2 = f_3 f_4$ . Since  $f_3, f_4$  are the zeros of  $\Phi_2(z; \alpha_0, \gamma_1)$  and  $\gamma_1 = -\overline{\Phi_2(0; \alpha_0, \gamma_1)}$ , we conclude that  $\gamma_1 = \alpha_1$ , which implies  $\Phi_2(z; \alpha_0, \gamma_1) = \Phi_2(z; \alpha_0, \alpha_1)$ . It follows that  $\Phi_2(f_2; \alpha_0, \gamma_1) = 0$ , which gives us a contradiction.  $\square$

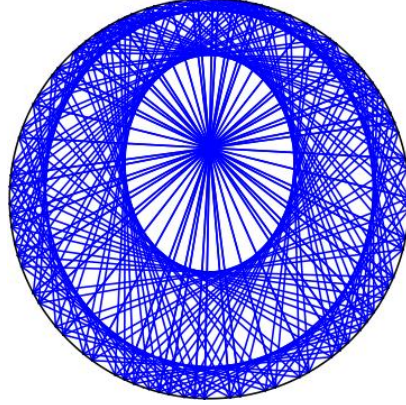


Figure 6.10. A family of Poncelet hexagons. The foci of the ellipse bounding  $C_1$  are  $f_1 = -0.3i$  and  $f_2 = 0.4i$ .

*Proof of Theorem 6.11* Theorem 6.7 states that the foci of the Pentagram ellipse will be the zeros of  $\Phi_2(z; \alpha_0, \alpha_1)$ . Thus, the foci of the Poncelet curve and the Brianchon point must be the zeros of  $\Phi_3(z; \alpha_0, \alpha_1, \alpha_2)$ . The product of these zeros is then  $\bar{\alpha}_2$  and hence we have

$$z(z - f_3)(z - f_4) - f_1 f_2 f_5(1 - \bar{f}_3 z)(1 - \bar{f}_4 z) = (z - f_1)(z - f_2)(z - f_5) \quad (6.12)$$

Expanding each expression yields

$$\begin{aligned} & z^3 - (f_3 + f_4 + f_1 f_2 f_5 \overline{f_3 f_4}) z^2 + (f_3 f_4 + f_1 f_2 f_5 (\bar{f}_3 + \bar{f}_4)) z - f_1 f_2 f_5 \\ &= z^3 - (f_1 + f_2 + f_5) z^2 + (f_1 f_2 + f_1 f_5 + f_2 f_5) z - f_1 f_2 f_5 \end{aligned} \quad (6.13)$$

Equating coefficients of  $z$  and  $z^2$  in (6.12) tells us that (6.11) must hold.

One can perform a similar calculation invoking Theorem 6.8, which states that the Brianchon point must be the zero of  $\Phi_1(z; \alpha_0)$ , and using Lemma 6.12. Without loss of generality,

$$\begin{aligned} z(z - f_5) + f_1 f_4 (1 - \bar{f}_5 z) &= (z - f_1)(z - f_4) \\ z^2 - (f_5 + f_1 f_4 \bar{f}_5)z + f_1 f_4 &= z^2 - (f_1 + f_4)z + f_1 f_4 \end{aligned} \tag{6.14}$$

and similarly for  $f_2, f_3$ . By equating coefficients of  $z$ , we see that

$$\begin{aligned} f_5 + f_1 f_4 \bar{f}_5 &= f_1 + f_4 \\ f_4 &= \frac{f_1 - f_5}{1 - f_1 \bar{f}_5} \end{aligned} \tag{6.15}$$

we find that (6.10) must hold.

For the converse statement, the above calculations show that if (6.10) and (6.11) hold, then the conditions (iii) in Theorems 6.7 and 6.8 are satisfied (by equating coefficients of polynomials). Theorem 6.10 then implies that the cutoff CMV matrix  $\mathcal{G}^{(5)}$  with eigenvalues  $\{f_j\}_{j=1}^5$  has numerical range that is bounded by an ellipse, has Pentagram curve that is an ellipse with foci  $\{f_3, f_4\}$ , and has Brianchon point  $\{f_5\}$ . The foci of  $\partial W(\mathcal{G}^{(5)})$  are eigenvalues of  $\mathcal{G}^{(5)}$  (see Chapter Five). By [55, Corollary 4], we know that one can partition the eigenvalues of  $\mathcal{G}^{(5)}$  into the Brianchon point, the foci of the Pentagram curve, and the foci of the boundary of the numerical range. Thus, by elimination it must be that the foci of  $\partial W(\mathcal{G}^{(5)})$  are  $\{f_1, f_2\}$ .

□

### 6.2.3 Mirman's Iterations for the Hexagon Case

Recall that the Mirman system in the  $N = 6$  case is

---

**Algorithm 6.2** Find a matrix  $\mathbf{A} \in S_5$  with an elliptic numerical range and foci  $f_1, f_2$ .

---

**Input:**  $f_1, f_2$ .

- 1: Find the unique solution  $f_5 \in \mathbb{D}$  to 6.11 by substituting 6.10.
- 2: Define  $f_3, f_4$  by 6.10.
- 3: Define  $\Phi_5(z) = (z - f_1)(z - f_2)(z - f_3)(z - f_4)(z - f_5) = \det\{z\mathbf{I} - \mathbf{A}\}$ .
- 4:  $-\overline{\alpha_4} = \Phi_5(0)$ .
- 5: Perform inverse Szegő recursion to recover  $\alpha_3, \alpha_2, \alpha_1, \alpha_0$ .

**Output:**

$$\mathbf{A} := \begin{pmatrix} \overline{\alpha_0} & \overline{\alpha_1}\rho_0 & \rho_1\rho_0 & 0 & 0 \\ \rho_0 & -\frac{\overline{\alpha_1}\alpha_0}{\overline{\alpha_2}\rho_1} & -\frac{\rho_1\alpha_0}{\overline{\alpha_2}\alpha_1} & 0 & 0 \\ 0 & \frac{\overline{\alpha_2}\rho_1}{\rho_2\rho_1} & -\frac{\rho_2\alpha_1}{\overline{\alpha_3}\alpha_2} & -\frac{\overline{\alpha_3}\rho_2}{\overline{\alpha_4}\rho_3} & -\frac{\rho_3\alpha_2}{\overline{\alpha_4}\alpha_3} \\ 0 & 0 & 0 & -\frac{\overline{\alpha_3}\alpha_2}{\overline{\alpha_4}\alpha_3} & -\frac{\rho_3\alpha_2}{\overline{\alpha_4}\alpha_3} \end{pmatrix}, \quad \rho_n = \sqrt{1 - |\alpha_n|^2} \quad (6.16)$$


---

$$f_1f_5 = B_2(f_3; f_1, f_2), \quad f_3f_4 = B_2(f_5; f_1, f_2), \quad f_2f_5 = B_2(f_4; f_1, f_2). \quad (6.17)$$

The conditions (6.10) and (6.11) allow us to recover these relations. Substitute  $z$  for  $f_3$  in (6.12) to obtain

$$(f_3 - f_1)(f_3 - f_2) = \frac{f_1f_2f_5(1 - |f_3|^2)(1 - f_3\bar{f}_4)}{f_5 - f_3}. \quad (6.18)$$

If we replace  $z$  by  $f_3$  in the reversed polynomials from (6.12), then we obtain

$$(1 - \bar{f}_1f_3)(1 - \bar{f}_2f_3) = \frac{(1 - |f_3|^2)(1 - f_3\bar{f}_4)}{1 - \bar{f}_5f_3}. \quad (6.19)$$

If we divide (6.18) by (6.19), and use (6.10), we find  $B_2(f_3; f_1, f_2) = f_1f_5$ . Similar reasoning can be used to derive  $B_2(f_4; f_1, f_2) = f_2f_5$ . Replacing  $z$  by  $f_5$  in (6.12) tells us that

$$\frac{f_5(f_5 - f_4)(f_5 - f_3)}{(1 - \bar{f}_4f_5)(1 - \bar{f}_3f_5)} = f_1f_2f_5.$$

If we assume  $f_1f_2f_5 \neq 0$  and we substitute the relations (6.10) for  $f_3$  and  $f_4$  (for an appropriate choice of which to call  $f_3$  and which to call  $f_4$ ), then we find

$$(1 - \bar{f}_2 f_5)(1 - \bar{f}_1 f_5) = (1 - \bar{f}_5 f_2)(1 - \bar{f}_5 f_1).$$

In other words  $(1 - \bar{f}_2 f_5)(1 - \bar{f}_1 f_5) \in \mathbb{R}$ . If we use this fact, then multiplying the expressions in (6.10) gives  $B_2(f_5; f_1, f_2) = f_3 f_4$ .

#### 6.2.4 Specified Elliptic Components in the Package of Hexagons

If one is given  $(f_1, f_2) \in \mathbb{D}^2$ , the construction in Section 6.2.2 above shows how to find an  $\mathbf{A} \in S_5$  so that  $\partial W(\mathbf{A})$  is an ellipse with foci at  $f_1$  and  $f_2$ . Similar to the quadrilateral case, we can consider the case of determining  $\mathbf{A} \in S_5$  with elliptic numerical range and prescribed foci of either the Pentagram ellipse or prescribed Brianchon point. First we will consider  $\mathbf{A} \in S_5$  with  $\partial W(\mathbf{A})$  an ellipse and whose Pentagram curve has prescribed foci (Theorem 6.10 assures us that if the Poncelet curve of  $\mathbf{A}$  is an ellipse, then so is its Pentagram curve).

##### 6.2.4.1 Fixed Pentagram Curve.

Theorem 6.13. *Given  $(f_3, f_4) \in \mathbb{D}^2$ , there exists a unique (up to unitary conjugation)  $\mathbf{A} \in S_5$  so that  $\partial W(\mathbf{A})$  is an ellipse and the Pentagram curve of  $\mathbf{A}$  is an ellipse with foci at  $f_3$  and  $f_4$ .*

One can interpret this result more geometrically. As we will prove in Lemma 6.14, given  $f_3, f_4$ , there is a unique Poncelet 3-ellipse with foci at  $f_3$  and  $f_4$ . The circumscribed triangles (that are inscribed in  $\partial\mathbb{D}$ ) must then be paired to produce the vertices of hexagons that will form the envelope of the desired Poncelet ellipse. In this context, the problem boils down to finding a point in  $\mathbb{D}$  (which will become the Brianchon point) so that for each circumscribed triangle the three chords through the vertices of that triangle and this chosen point all end in the vertices of another triangle.

Our proof of Theorem 6.13 requires the following two lemmas.

**Lemma 6.14.** *Given two triangles inscribed in  $\partial\mathbb{D}$  with interlacing vertices, there is a unique ellipse that is inscribed in both of them.*

*Proof.* By [31, Theorem 3.1], we know that there exists a unique cutoff CMV matrix  $\mathcal{G}^{(2)}$  whose numerical range is circumscribed by the two triangles. By the Elliptical Range Theorem (Theorem 5.9), we know that this numerical range is bounded by an ellipse with the desired properties. Uniqueness follows from the uniqueness statement in [31, Theorem 3.1] and the fact that every Poncelet 3-ellipse can be realized as boundary of the numerical range of some  $2 \times 2$  cutoff CMV matrix (see Theorem 2.4).  $\square$

**Remark.** Note that Lemma 6.14 is related to Wendroff's Theorem for POPUC (see [54, Theorem 8] or [2]).

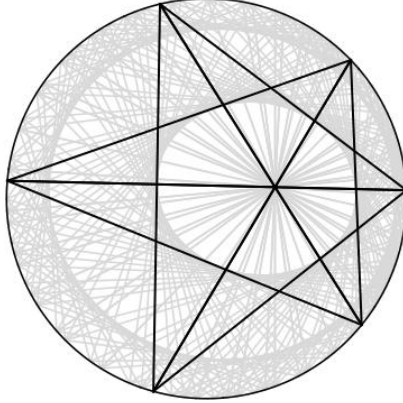


Figure 6.11. An example of a family of Poncelet hexagons circumscribing an ellipse with specified pentagram ellipse foci. The details of this construction are given in Example 6.20.

**Lemma 6.15.** *Let  $\{\Phi_3^{(\lambda)}\}_{\lambda \in \partial\mathbb{D}}$  be the collection of degree 3 POPUC for the same degree 2 OPUC. Label the zeros of  $\Phi_3^{(\lambda)}(z)$  as  $\{z_j^{(\lambda)}\}_{j=1}^3$ . For each  $\lambda \in \partial\mathbb{D}$  there exists a unique  $\tau \in \partial\mathbb{D}$  so that the line segments joining  $z_j^{(\lambda)}$  to  $z_j^{(\tau)}$  all meet in a single point independent of  $j$  (this assumes an appropriate labeling of the zeros  $\{z_j^{(\lambda)}\}_{j=1}^3$ ).*

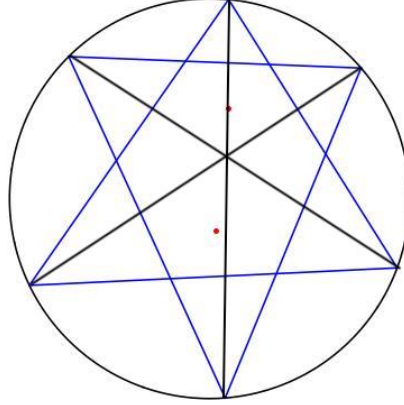


Figure 6.12. As in Lemma 6.15, here the line segments joining  $z_j^i$  and  $z_j^{-i}$  all meet at a single point.

*Proof.* For each  $\tau$ , let  $z_1^{(\tau)}$  be the zero that lies between  $z_2^{(\lambda)}$  and  $z_3^{(\lambda)}$ , let  $z_2^{(\tau)}$  be the zero that lies between  $z_3^{(\lambda)}$  and  $z_1^{(\lambda)}$ , and let  $z_3^{(\tau)}$  be the zero that lies between  $z_1^{(\lambda)}$  and  $z_2^{(\lambda)}$ . Let  $L_j^{(\tau)}$  be the line segment that joins  $z_j^{(\lambda)}$  to  $z_j^{(\tau)}$  for  $j = 1, 2, 3$ .

Given  $\{z_j^{(\lambda)}\}_{j=1}^3$ , start with  $\tau = \lambda$  and move  $\tau$  around  $\mathbb{T}$  counterclockwise. As this happens, consider  $\eta_j(\tau) := L_1^{(\tau)} \cap L_j^{(\tau)}$  for  $j = 2, 3$  and notice that both of these points are in  $L_1^{(\tau)}$ . Define

$$d_j(\tau) = \frac{|z_1^{(\lambda)} - \eta_j(\tau)|}{|L_1^{(\tau)}|}, \quad j = 2, 3.$$

Initially,  $d_3(\tau)$  is close to 0 and  $d_2(\tau)$  is close to 1. As  $\tau$  nears the end of its trip around  $\mathbb{T}$ , it holds that  $d_2(\tau)$  is close to 0 and  $d_3(\tau)$  is close to 1. Thus, by the Intermediate Value Theorem, there must be a value of  $\tau$  such that  $d_2(\tau) = d_3(\tau)$  as desired. One can see by inspection that this choice of  $\tau$  is unique.  $\square$

*Proof of Theorem 6.13* Suppose  $(f_3, f_4) \in \mathbb{D}^2$  are given. Consider the Poncelet 3-ellipse with foci at  $f_3$  and  $f_4$  (call it  $E$ ). Pick any triangle  $T^{(\lambda)}$  that is inscribed in  $\partial\mathbb{D}$  and circumscribed about  $E$ . By Lemma 6.15, there exists a unique second such triangle  $T^{(\tau)}$  such that the line segments joining opposite vertices meet in a single

point. By Brianchon's Theorem, there is an ellipse inscribed in the hexagon whose vertices are the vertices of  $T^{(\tau)}$  and  $T^{(\lambda)}$ . Call this ellipse  $E'$  and suppose its foci are  $f_1$  and  $f_2$ .

From what we already know, the ellipse  $E'$  is the unique Poncelet 6-ellipse with foci at  $f_1$  and  $f_2$ , and Theorem 2.4 tells us that it is associated to a matrix in  $S_5$ . For this matrix, the associated Pentagram curve must be an ellipse and the associated Brianchon curve must be a single point. This Pentagram ellipse is a Poncelet 3-ellipse and must be inscribed in the triangles  $T^{(\lambda)}$  and  $T^{(\tau)}$ . By Lemma 6.14, that ellipse must be  $E$ .

□

*6.2.4.2 Fixed Brianchon Point.* Our next result is an analog of Theorem 6.13 for the Brianchon curve. Specifically, we will show that one can find  $\mathbf{A} \in S_5$  so that  $\partial W(\mathbf{A})$  is an ellipse and the Brianchon curve is a single predetermined point. The main difference between Theorem 6.16 and Theorem 6.13 is the lack of uniqueness.

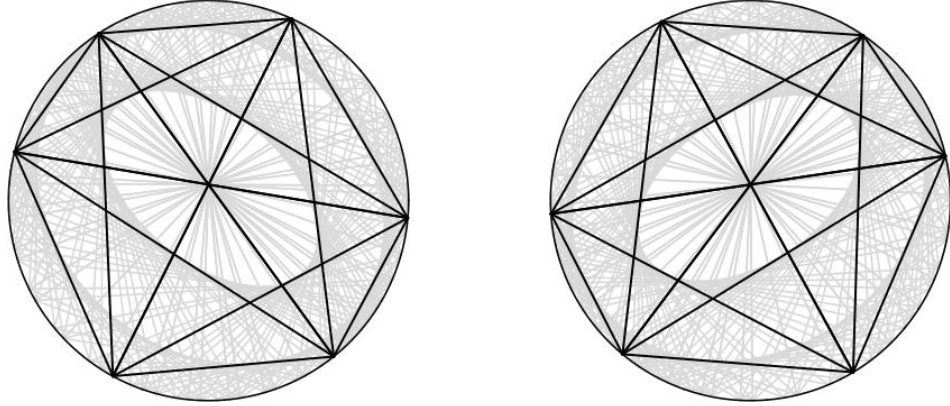


Figure 6.13. Two Poncelet 6-ellipses with the same Brianchon point,  $0.08i$ . Example 6.18 describes the creation of the left figure. The figure on the right was created by conjugating  $f_1$  in Example 6.18 and repeating the same process.

Theorem 6.16. Given  $f_5 \in \mathbb{D}$ , there exists a  $5 \times 5$  cutoff CMV matrix  $\mathbf{A}$  so that  $\partial W(\mathbf{A})$  is an ellipse and the Brianchon curve of  $\mathbf{A}$  is the single point  $f_5$ . Furthermore, the set of all possible  $5 \times 5$  cutoff CMV matrices with this property is naturally parametrized by an open triangle.

*Proof.* Suppose  $f_5 \in \mathbb{D}$  is given. Consider the set of all lines passing through  $f_5$ . Each line intersects  $\mathbb{T}$  in two places. One can choose three distinct lines, thus specifying 6 distinct points of  $\mathbb{T}$ , labeled cyclically as  $v_j$  for  $j = 1, 2, \dots, 6$ . By Brianchon's Theorem, there is an ellipse inscribed in the hexagon whose vertices are  $\{v_j\}_{j=1}^6$ . Call this ellipse  $E$  and its foci  $f_1$  and  $f_2$ . By Theorem 6.11,  $E$  is the boundary of  $W(\mathbf{A})$  for some  $\mathbf{A} \in S_5$ . Thus, the Poncelet curve and Pentagram curve of  $\mathbf{A}$  are ellipses and the Brianchon curve of  $\mathbf{A}$  is a single point, which we see must be  $f_5$  as desired.

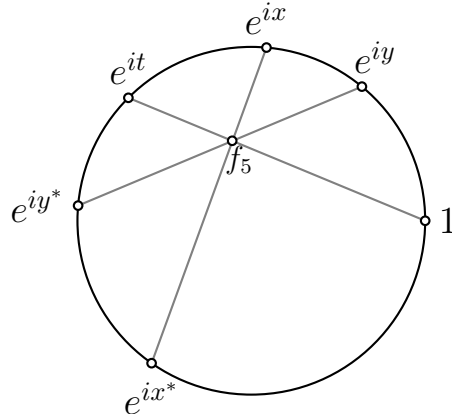


Figure 6.14. Given  $f_5$  and the line through  $1, f_5$ , varying  $x, y$  such that  $0 < x < y < t$  parametrizes the set of all  $\mathbf{A} \in S_5$  with elliptic numerical range and Brianchon curve  $f_5$ .

Note that the above procedure yields a well-defined map from collections of distinct triples of lines through  $f_5$  to matrices in  $S_5$  whose numerical range is an elliptical disk and whose Brianchon point is  $f_5$ . To see this, suppose one starts with three distinct lines through  $f_5$ . This produces six points on the unit circle by the above procedure. Connecting alternate points forms two triangles that must be

tangent to the Pentagram ellipse of the matrix we seek. By Lemma 6.14, there is only one possible choice for such an ellipse, so its foci  $f_3, f_4$  are a well-defined output. By Theorem 6.11 and Equation (6.10), we can calculate the foci  $f_1, f_2$  of the Poncelet curve of this matrix. Thus, the eigenvalues  $\{f_j\}_{j=1}^5$  of the matrix we seek are a computable quantity from any three distinct lines through  $f_5$ . Since the eigenvalues determine the matrix in  $S_5$ , this means the map is well-defined.

To make this map a bijection, we restrict it to triples of lines through  $f_5$  for which one of them also passes through 1. Given any  $\mathbf{A} \in S_5$  with  $W(\mathbf{A})$  an elliptical disk and Brianchon point  $f_5$ , there exists a hexagon that circumscribes  $\partial W(\mathbf{A})$  for which 1 is a vertex, so the restricted map is onto. To show that it is injective, suppose  $H$  is a hexagon inscribed in  $\mathbb{T}$  with one vertex at 1 and  $E$  is an ellipse that is tangent to every edge of  $H$ . From any given point on  $\mathbb{T}$  (in particular, the point 1), there are only two tangents to  $E$  through that point. This implies  $H$  is the unique hexagon that includes 1 and has the required tangency properties. Thus, our restricted map uniquely determines the numerical range of the matrix and hence uniquely determines the matrix itself.

Suppose that the line through 1 and  $f_5$  also intersects  $\mathbb{T}$  at  $e^{it}$ . We have shown that the space of all  $5 \times 5$  CMV matrices with the desired property is naturally parametrized by  $\{(x, y) : 0 < x < y < t\}$ , which is an open triangle.  $\square$

Recall that one can specify an elliptic component without requiring an elliptic numerical range. In this respect, Theorem 6.8 reveals an interesting phenomenon. Suppose we are given an  $\mathbf{A} \in S_5$  whose Brianchon curve is a point and whose Pentagram curve is not an ellipse (it is easy to find such  $\mathbf{A}$ ). Take a rank one unitary dilation  $\mathbf{U}_1$  of  $\mathbf{A}$  and look at the hexagon with vertices at the eigenvalues of  $\mathbf{U}_1$ . The diagonals of this hexagon meet in a single point (which is the Brianchon curve of  $\mathbf{A}$ ), so by Brianchon's Theorem there exists an ellipse  $E_1$  inscribed in this hexagon. By construction, the ellipse  $E_1$  is a Poncelet 6-ellipse, so there is in fact an infinite family

of hexagons  $\{H_\lambda\}$  inscribed in  $\partial\mathbb{D}$  and circumscribed about  $E_1$ . On the other hand, one can look at any other rank one unitary dilation of  $\mathbf{A}$  and repeat this process. This gives a second infinite family of hexagons, each of which is circumscribed in  $\partial\mathbb{D}$  and has its diagonals meeting at the point that is the Brianchon curve of  $\mathbf{A}$ . But these two families of hexagons cannot be the same, for that would imply that the numerical range of  $\mathbf{A}$  is bounded by an ellipse and we know it is not.

#### 6.2.5 Examples of Poncelet Hexagons

Note that the following examples contain numerical approximations and rounded decimals.

Example 6.17. Find the CMV matrix whose numerical range is bounded by a Poncelet 6-ellipse with foci  $f_1 = 0.5$  and  $f_2 = -0.25i$ .

Using Algorithm 6.2 and equations (6.11) and (6.10), we find

$$f_5 = 0.75 - 0.25i$$

$$f_3 = 0.769231 - 0.153846i$$

$$f_4 = 0.461538 - 0.37962i.$$

Then  $\Phi_5(z) = (z - 0.5)(z + 0.25i)(z - 0.75 + 0.25i)(z - 0.769231 + 0.153846i)(z - 0.461538 + 0.37962i)$  and by evaluating  $\Phi_4(0)$  and iterating the inverse Szegő recursion, we find that

$$\overline{\alpha_4} = -0.0384615 - 0.0192308i \quad \overline{\alpha_3} = 0.0433494 + 0.247499i$$

$$\overline{\alpha_2} = 0.31094 - 0.589024i \quad \overline{\alpha_1} = -0.741589 + 0.539706i$$

$$\overline{\alpha_0} = 0.942959 - 0.280341i,$$

see Figure 6.15.

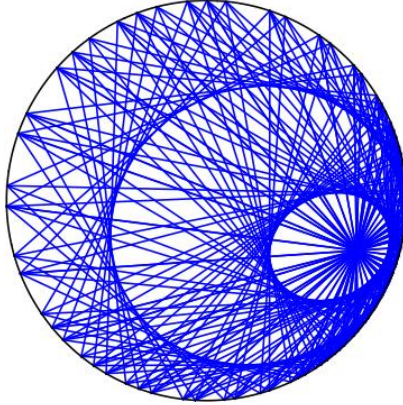


Figure 6.15. The numerical range, pentagram curve, and brianchon point of  $\mathbf{A}$  in Example 6.17.

Example 6.18. Find a CMV matrix whose numerical range is bounded by an ellipse and whose Brianchon point is  $f_5 = 0.08i$ .

We will begin similarly as we did in Example 6.17, only this time we will specify  $f_5$  and a freely chosen  $f_1$  by Theorem 6.16. If we let  $f_1 = 0.4 - 0.3i$ , then we can use Equation (6.11) to find that  $f_2 = -0.379796 + 0.346536i$ . Then using Equation (6.10), we find that

$$f_3 = 0.398802 - 0.261673i, \quad f_4 = 0.378659 + 0.382927i.$$

Then we can find  $\Phi_5(z)$  and through the inverse Szegő recursion find that

$$\overline{\alpha_4} = 0.00199259 - 0.00489244i \quad \overline{\alpha_3} = 0.0601849 + 0.0277636i$$

$$\overline{\alpha_2} = -0.0732452 - 0.0197404i \quad \overline{\alpha_1} = 0.103798 - 0.463977i$$

$$\overline{\alpha_0} = -0.0735574 + 0.22168i,$$

see Figure 6.16. Then with these Verblunsky coefficients we can find a CMV matrix with Brianchon point  $0.08i$  and whose numerical range is bounded by an elliptical disk.

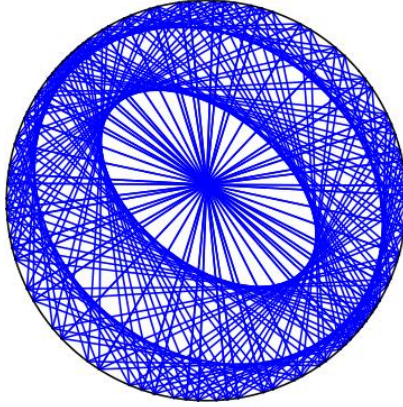


Figure 6.16. The numerical range, pentagram curve, and briancon point of  $A$  in Example 6.18.

Example 6.19. Consider the concentric circles studied by Chapple. The circle is circumscribed by equilateral triangles. If we want to create a family of Poncelet hexagons whose pentagram curve is this circle centered at zero and whose Poncelet curve circumscribes a circle also, we begin with  $f_3 = f_4 = 0$ , and we define the family of Poncelet triangles defined by the OPUC  $\phi_3(z) = z^3$ . By the process outlined in the proof of Lemma 6.15, we see that the lines joining the vertices of the triangles formed by  $\lambda = e^{\pi i \frac{24}{25}}$  and  $\tau = e^{\pi i}$  all intersect at  $f_5 = 0$ . Then  $f_1 = f_2 = 0$  and we see a curve with three circular components all centered at zero circumscribed by Poncelet hexagons, see Figure 6.17.

Example 6.20. Find the CMV matrix whose pentagram curve is an ellipse with foci  $f_3 = 0.5$  and  $f_4 = 0.1i$  and whose numerical range is an ellipse.

First we use Section 5.3, Algorithm 5.1 to form the family of Poncelet triangles that circumscribe an ellipse with the given foci. Then  $\phi_3(z) = z(z - 0.5)(z - 0.1i)$ . As described in the proof of Lemma 6.15, we find a pair of triangles with the chords connecting opposite vertices all meeting at a single point (see Figure 6.18), in this case  $f_5 = 0.342517 + 0.0571291i$ . Then using Equation (6.10), we solve for  $f_1, f_2$  and find that  $f_1 = 0.34556 - 0.0312132i$  and  $f_2 = -0.187428 + 0.0753949i$ . With all five

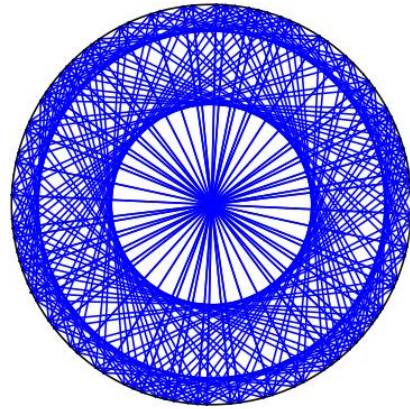


Figure 6.17. The numerical range, pentagram curve, and briancon point of  $A$  in Example 6.19.

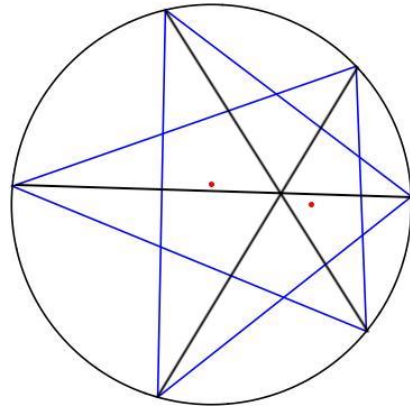


Figure 6.18. The triangles circumscribing the ellipse with foci  $0.5$  and  $0.1i$  with the line segments joining the respective vertices of the triangles meeting at a single point.

foci, we can write down  $\Phi_5(z)$  and perform inverse Szegő recursion. This gives us

$$\overline{\alpha_4} = -0.000368094 - 0.001160003i \quad \overline{\alpha_3} = 0.0145382 - 0.001909878i$$

$$\overline{\alpha_2} = -0.0247788 + 0.0547175i \quad \overline{\alpha_1} = -0.247165 - 0.144148i$$

$$\overline{\alpha_0} = 0.789865 + 0.0924397i,$$

see Figure 6.19.

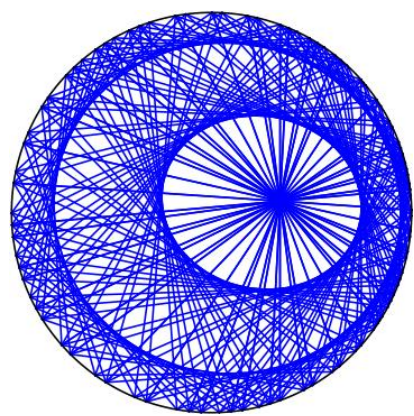


Figure 6.19. The numerical range, Pentagram curve, and Brianchon point of  $\mathbf{A}$  in Example 6.20.

## CHAPTER SEVEN

### Pentagonal Case

A majority of this chapter is submitted for publication as Markus Hunziker, Andrei Martíez-Finkelshtein, Taylor Poe, and Brian Simanek, *On foci of ellipses inscribed in cyclic polygons*, Preprint, 2021.

The situation when  $n = 5$ , where  $n$  is the number of sides of the circumscribing Poncelet polygons, is considerably different than the cases  $n = 4, 6$ . One can see that there exist matrices  $\mathbf{A} \in S_4$  for which  $W(\mathbf{A})$  is an elliptical disk by considering a single  $4 \times 4$  Jordan block with eigenvalue 0. By 2.4, we know that given  $f_1, f_2$ , there is a matrix in  $S_4$  whose numerical range is bounded by an ellipse with these foci. However, our approach to finding all such matrices cannot be the same as in the previous chapter. In particular, it will not be possible to consider compositions of Blaschke products as in the previous sections, which partially explains why this case has been studied less often in the literature (see [26]). Instead, we will revisit the Mirman system and prove a structure theorem about the set of possible solutions. In this setting, the system of equations has multiple solutions and our next result describes their relative placement in the plane.

#### *7.1 Mirman's Iterations for the Pentagon Case*

Theorem 7.1. *Let  $f_1, f_2 \in \mathbb{D}$ ,  $f_1 f_2 \neq 0$  and set  $\Phi_2(z) = (z - f_1)(z - f_2)$ . The system*

$$\begin{aligned}\frac{\Phi_2(z)}{\Phi_2^*(z)} &= wf_1, \\ \frac{\Phi_2(w)}{\Phi_2^*(w)} &= zf_2\end{aligned}\tag{7.1}$$

*has exactly 5 distinct solution pairs  $(z, w) \in \mathbb{C}^2$ : four of them are in  $\mathbb{D}^2$ :  $(0, f_2)$ ,  $(f_1, 0)$ ,  $(z_1, w_1)$ ,  $(z_2, w_2)$ , and exactly one solution  $(z_3, w_3)$  satisfies  $|z_3| > 1$ ,  $|w_3| > 1$ .*

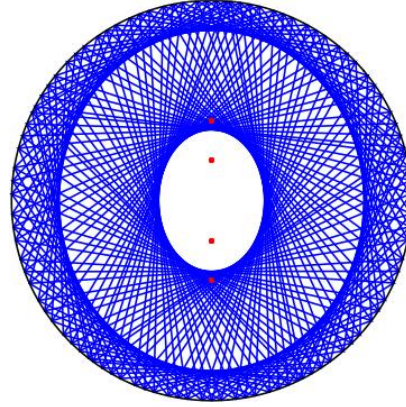


Figure 7.1. A family of Poncelet pentagons.

Moreover,

i) It holds that

$$\frac{z_1 - f_2}{w_1 - f_1} = \frac{z_2 - f_2}{w_2 - f_1} = \frac{z_3 - f_2}{w_3 - f_1} = \frac{f_1 \Phi_2^*(f_2)}{f_2 \Phi_2^*(f_1)},$$

ii) The points  $f_1$ ,  $w_1$ ,  $w_2$  and  $w_3$  are collinear, i.e.

$$\frac{w_i - f_1}{w_j - f_1} \in \mathbb{R}, \quad i, j \in \{1, 2, 3\}, \quad i \neq j.$$

and the points  $f_2$ ,  $z_1$ ,  $z_2$  and  $z_3$  are collinear, i.e.

$$\frac{z_i - f_2}{z_j - f_2} \in \mathbb{R}, \quad i, j \in \{1, 2, 3\}, \quad i \neq j.$$

*Proof.* Let us denote

$$g_1(z) = \frac{1}{f_1} \frac{(z - f_1)(z - f_2)}{(1 - z\bar{f}_1)(1 - z\bar{f}_2)}, \quad g_2(z) = \frac{1}{f_2} \frac{(z - f_1)(z - f_2)}{(1 - z\bar{f}_1)(1 - z\bar{f}_2)},$$

so that (7.1) takes the form  $g_1(z) = w$ ,  $g_2(w) = z$ . From here, we get that (7.1) implies that

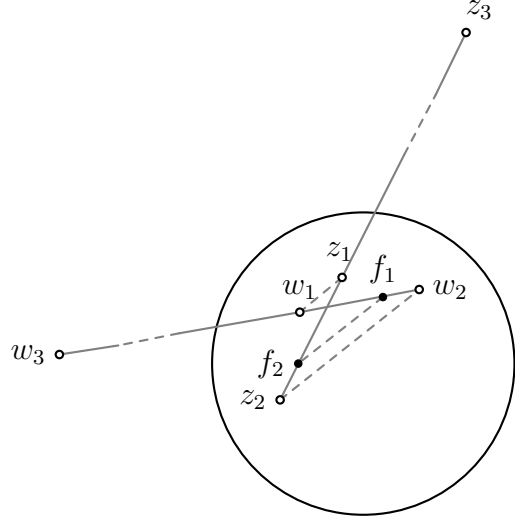


Figure 7.2. Collinearity of the points  $f_1$ ,  $f_2$ ,  $z_j$ 's and  $w_j$ 's, as explained in Theorem 7.1.

$$\begin{aligned} g_2 \circ g_1(z) &= z, \\ g_1 \circ g_2(w) &= w. \end{aligned} \tag{7.2}$$

We claim that both  $g_2 \circ g_1$  and  $g_1 \circ g_2$  have 4 fixed points inside  $\mathbb{D}$ . Indeed, consider  $g_2 \circ g_1$  (same analysis for  $g_1 \circ g_2$ ). Recall that a Blaschke product is analytic in  $\mathbb{D}$ , maps  $\mathbb{T} \rightarrow \mathbb{T}$ ,  $\mathbb{D} \rightarrow \mathbb{D}$  and exterior of  $\mathbb{D}$  onto its exterior. So,

$$|z| = 1 \Rightarrow |g_1(z)| > 1 \Rightarrow |g_2(g_1(z))| > 1.$$

By Rouché's theorem,  $g_2 \circ g_1(z) - z$  and  $g_2 \circ g_1(z)$  have the same number of zeros in  $\mathbb{D}$ ; it is straightforward to check that  $g_2 \circ g_1$  vanishes at 4 points in  $\mathbb{D}$ .

Finally, we claim that the statement of the proposition is equivalent to the just established fact that both  $g_2 \circ g_1$  and  $g_1 \circ g_2$  have 4 fixed points inside  $\mathbb{D}$ .

Indeed, the 4 pairs of solutions of (7.1) satisfy (7.2). Reciprocally, let  $z$  be a fixed point of  $g_2 \circ g_1$  and denote  $\tau = g_1(z)$ . Then  $g_2(\tau) = g_2(g_1(z)) = z$ , and in consequence,  $g_1(g_2(\tau)) = g_1(z) = \tau$ , meaning that  $\tau = g_1(z)$  is a fixed point of  $g_1 \circ g_2$ .

This shows that the fixed points  $z$  and  $w$  of  $g_2 \circ g_1$  and  $g_1 \circ g_2$  can be paired  $(z, w)$  in such a way that (7.1) holds.

Now we prove the statement about the remaining solution, this time in  $(\mathbb{C} \setminus \overline{\mathbb{D}})^2$ .

The identity

$$\frac{(1/\bar{z} - f_1)(1/\bar{z} - f_2)}{(1 - \bar{f}_1/\bar{z})(1 - \bar{f}_2/\bar{z})} = \frac{1}{\frac{(z-f_1)(z-f_2)}{(1-z\bar{f}_1)(1-z\bar{f}_2)}} \quad (7.3)$$

allows us to reduce the analysis of (7.1) in  $(\mathbb{C} \setminus \overline{\mathbb{D}})^2$  to the equivalent system

$$\begin{aligned} \frac{(z - f_1)(z - f_2)}{(1 - z\bar{f}_1)(1 - z\bar{f}_2)} &= \frac{w}{\bar{f}_1}, \\ \frac{(w - f_1)(w - f_2)}{(1 - w\bar{f}_1)(1 - w\bar{f}_2)} &= \frac{z}{\bar{f}_2} \end{aligned} \quad (7.4)$$

for  $(z, w) \in \mathbb{D}^2$  (we return to the actual solutions outside by the mapping  $z \mapsto 1/\bar{z}$ ,  $w \mapsto 1/\bar{w}$ ). The advantage of working in  $\mathbb{D}$  is that again we can use the fixed point argument and Rouché's Theorem. Indeed, as before, define

$$h_1(z) = \bar{f}_1 \frac{(z - f_1)(z - f_2)}{(1 - z\bar{f}_1)(1 - z\bar{f}_2)}, \quad h_2(z) = \bar{f}_2 \frac{(z - f_1)(z - f_2)}{(1 - z\bar{f}_1)(1 - z\bar{f}_2)},$$

and look for fixed points of  $h_1 \circ h_2$  and  $h_2 \circ h_1$ . This time

$$|z| = 1 \Rightarrow |h_1(z)| < 1 \Rightarrow |h_2(h_1(z))| < 1,$$

and by Rouché's Theorem,  $h_2 \circ h_1(z) - z$  and  $f(z) = z$  have the same number of zeros in  $\mathbb{D}$ , that is, exactly one.

To prove the statements about colinearity, evaluate Mirman's equation (see (5.5)) with  $x = f_1$  and again with  $y = f_2$  to define the linear functions

$$\begin{aligned} z(t) &= \frac{f_2 - f_1}{1 - f_1\bar{f}_2} + \frac{4f_1}{(1 - |f_1|^2)(1 - f_1\bar{f}_2)}t \\ w(t) &= \frac{f_1 - f_2}{1 - f_2\bar{f}_1} + \frac{4f_2}{(1 - |f_2|^2)(1 - f_2\bar{f}_1)}t \end{aligned} \quad (7.5)$$

Replacing (7.5) in (7.1) gives us two polynomials in the variable  $t$ ,

$$\Phi_2(z(t)) - w(t)f_1\Phi_2^*(z(t)), \quad \Phi_2(w(t)) - z(t)f_2\Phi_2^*(w(t)).$$

It is a straightforward calculation to verify that these two polynomials are scalar multiples of each other so any zero of one is a zero of the other. Notice that both of these polynomials have degree 3. One can also check by hand that if  $t_z$  is such that  $z(t_z) = 0$ , then  $w(t_z) \neq f_2$ . Similarly, if  $t_w$  is such that  $w(t_w) = 0$ , then  $z(t_w) \neq f_1$ . Thus, the three zeros  $\{t_j\}_{j=1}^3$  of

$$Y(t) := \Phi_2(z(t)) - w(t)f_1\Phi_2^*(z(t)) \tag{7.6}$$

will be such that  $(z(t_j), w(t_j))$  is a solution to the system (7.1) other than  $(0, f_2)$  and  $(f_1, 0)$ . Thus we can say  $(z_j, w_j) = (z(t_j), w(t_j))$ . If we set  $t_0 = \frac{1}{4}(1 - |f_1|^2)(1 - |f_2|^2)$  and observe that  $z(t_0) = f_2$  and  $w(t_0) = f_1$ , then a short calculation shows

$$\frac{z_j - f_2}{w_j - f_1} = \frac{z(t_j) - z(t_0)}{w(t_j) - w(t_0)} = \frac{f_1\Phi_2^*(f_2)}{f_2\Phi_2^*(f_1)}.$$

This proves claim (i) of the theorem.

To prove claim (ii), it suffices to show that each  $t_j \in \mathbb{R}$ . To this end, a calculation reveals that if we divide the polynomial  $Y(t)$  in (7.6) by its leading coefficient, then we obtain a monic degree 3 polynomial with real coefficients.

Recall (5.5)

$$q(x, y; t) := \left( y + \frac{x - f_1}{1 - \overline{f}_1 x} \right) \left( y + \frac{x - f_2}{1 - \overline{f}_2 x} \right) - \frac{4txy}{(1 - \overline{f}_1 x)(1 - \overline{f}_2 x)}.$$

There exist two distinguished matrices  $\mathbf{A}_1, \mathbf{A}_2 \in S_4$  such that  $\mathbf{A}_1$  has numerical range bounded by an ellipse with foci at  $\{f_1, f_2\}$  and the Pentagram curve of  $\mathbf{A}_2$  is

an ellipse with foci at  $\{f_1, f_2\}$ . Let us denote the eigenvalues of  $\mathbf{A}_j$  by  $\{f_1, f_2, z_j, w_j\}$  for  $j = 1, 2$ . Then from [43, Section 5] (and also [55, Equations 29–32]) we know that there exist positive real numbers  $b_1$  and  $b_2$  so that

$$q(f_2, z_j; b_j^2) = q(w_j, f_1; b_j^2) = q(z_j, w_j; b_j^2) = 0$$

for  $j = 1, 2$ . In fact,  $b_j$  is the length of the minor semiaxis of the ellipse associated with  $\mathbf{A}_j$  whose foci are  $\{f_1, f_2\}$  (see [55]).

Using  $q(f_2, z_j; b_j^2) = q(w_j, f_1; b_j^2) = 0$  and the formulas (7.5), we find that  $z_j = z(b_j^2)$  and  $w_j = w(b_j^2)$ . A short calculation shows (recall  $t_0 = (1 - |f_1|^2)(1 - |f_2|^2)/4$ )

$$q(z(t), w(t); t) = \frac{Y(t)(t - t_0)}{C_{f_1, f_2} \Phi_2^*(z(t))},$$

where  $C_{f_1, f_2} = \frac{-f_1 t_0}{f_2}$ . Thus the zeros of  $Y(t)$  are also zeros of  $q(z(t), w(t); t)$ .

If  $t_0$  were a zero of  $Y(t)$ , then  $z = z(t_0)$  and  $w = w(t_0)$  would satisfy (7.1). However, we have seen that  $z(t_0) = f_2$  and  $w(t_0) = f_1$ , giving  $0 = \Phi_2(f_2) = f_1^2$ , which is nonzero by assumption, so  $Y(t_0) \neq 0$ .

Thus the zeros of  $Y(t)$  are zeros of  $q(z(t), w(t); t)$  distinct from  $t_0$ . We know that  $q(z(t), w(t); t)$  has zeros at  $t = b_1^2$  and  $t = b_2^2$  so these must be zeros of  $Y(t)$  as well. This gives us two real zeros of  $Y(t)$ . Our earlier observation implies that  $Y(t)$  has either one or three real zeros, so all zeros of  $Y(t)$  are real as desired.  $\square$

Notice that Theorem 7.1 implies that each line  $\ell_j$  passing through  $\{z_j, w_j\}$  for  $j = 1, 2, 3$  is parallel to the line through  $\{f_1, f_2\}$ . For  $j = 1, 2$ , one can obtain this same conclusion from the fact that the ellipses  $C_1$  and  $C_2$  corresponding to a matrix  $\mathbf{A} \in S_4$  are in the same package (see [57]). The fact that this same conclusion applies to  $\ell_3$  is a new result. From these observations, we see that if one knows  $\{f_j\}_{j=1}^2$  and  $\{z_j\}_{j=1}^3$ , then one can find  $\{w_j\}_{j=1}^3$  using only a picture (see Figure 7.2).

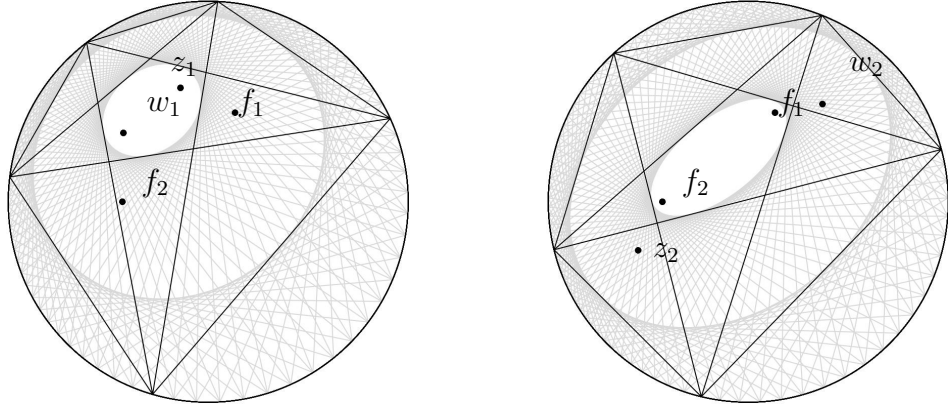


Figure 7.3. Pairs  $(z_1, w_1)$  and  $(z_2, w_2)$  as foci of the Pentagram and the Poncelet ellipses, respectively.

### 7.2 Geometric Interpretations of the Solutions

The solutions to the Mirman system in this setting have a geometric interpretation. Given  $\{f_1, f_2\} \in \mathbb{D}^2$ , we have just seen that there are three nontrivial solution pairs  $(z, w)$  to the Mirman system and we denote them by  $(z_1, w_1)$ ,  $(z_2, w_2)$ , and  $(z_3, w_3)$ . One of the solution pairs in  $\mathbb{D}^2$  (say  $(z_1, w_1)$ ) will be such that the  $4 \times 4$  cutoff CMV matrix with eigenvalues  $\{f_1, f_2, z_1, w_1\}$  will have numerical range bounded by an ellipse with foci at  $f_1$  and  $f_2$ , and the Pentagram curve of this matrix will be an ellipse with foci at  $z_1$  and  $w_1$ . For the other solution pair in  $\mathbb{D}^2$  (say  $(z_2, w_2)$ ), it will be true that the  $4 \times 4$  cutoff CMV matrix with eigenvalues  $\{f_1, f_2, z_2, w_2\}$  has numerical range bounded by an ellipse with foci at  $z_2$  and  $w_2$ , and the Pentagram curve of this matrix will be an ellipse with foci at  $f_1$  and  $f_2$ , see Figure 7.3. The geometric interpretation of the solution  $(z_3, w_3) \in (\mathbb{C} \setminus \bar{\mathbb{D}})^2$  is not clear.

Let  $z(t)$ ,  $w(t)$ , and  $Y(t)$  be as in Section 7.1. As stated before,  $Y(t)$  (once divided by its leading coefficient) is a monic degree three polynomial with real coefficients and three real roots. Call these roots  $t_1, t_2, t_3$  and note that  $t_1, t_2, t_3$  must all be distinct as Mirman's iterations give two semiaxis lengths, each of a different

Poncelet-5 ellipse, and a solution outside the disk. Then as the zeros of  $Y(t)$  are real and distinct, we can order them  $t_1 < t_2 < t_3$ .

As  $0 < |f_1|, |f_2| < 1$ , the coefficients of  $Y(t)$  are continuous functions of  $f_1, f_2$ . Likewise, the roots of a cubic are continuous. Thus  $t_1, t_2, t_3$  are continuous functions of  $f_1, f_2$ . Experimentally, given  $f_1, f_2$ , the solution  $t_1$  corresponds to the  $\mathbf{A}_1 \in S_5$  whose Pentagram curve is an ellipse with foci  $f_1, f_2$ ;  $t_2$  corresponds to the  $\mathbf{A}_2 \in S_5$  whose numerical range is bounded by a Poncelet-5 ellipse with foci  $f_1, f_2$ ; and  $t_3$  yields  $(z_3, w_3) \notin \mathbb{D}$ . It remains to show that these geometric interpretations are continuous as  $f_1, f_2$  change.

Consider  $t_3$ . For a given  $f_1, f_2$ ,  $t_3$  gives solutions  $z(t_3) = z_3$  and  $w(t_3) = w_3$  to (7.1) where  $|z_3|, |w_3| > 1$ . So  $z_3$  and  $w_3$  vary continuously with  $t_3, f_1, f_2$ . If  $z_3$  (and similarly  $w_3$ ) could move continuously to the interior of the disc, then for some  $t_3, f_1, f_2$ ,  $|z_3| = 1$ . But by Theorem 7.1,  $|z_j| \neq 1$  for any  $j$ . Thus  $z_3, w_3$  must stay outside the disc, and  $t_3$  always corresponds to the solution outside the disc.

Next consider  $t_2$ . We know  $z(t_2) = z_2$  and  $w(t_2) = w_2$  are continuous functions of  $f_1, f_2$ . Consider the matrix  $\mathbf{A}$  whose eigenvalues are  $f_1, f_2, z_2, w_2$ . Then as  $f_1, f_2$  vary continuously,  $\mathbf{A}$  varies continuously as well. The numerical range of a matrix is defined to be  $W(\mathbf{A}) = \{\langle x, \mathbf{A}x \rangle : x \in \mathbb{C}^n, \|x\| = 1\}$ . As  $\langle x, \mathbf{A}x \rangle$  is a continuous function of  $x$ , by continuity  $t_2$  corresponds to the Poncelet-5 ellipse (the boundary of  $W(\mathbf{A})$ ).

Then given  $t_1 < t_2 < t_3$ , since  $t_3$  yields  $z_3, w_3$  outside the disk and  $t_2$  is the length of the minor semi-axis of the elliptic disk with foci  $f_1, f_2$  bounding the numerical range of a matrix  $\mathbf{A}_2 \in S_5$ , by process of elimination we see  $t_1$  must be the length of the minor semi-axis of the ellipse with foci  $f_1, f_2$  bounding the Pentagram curve of a matrix  $\mathbf{A}_1 \in S_5$ .

### 7.3 Examples of Poncelet Pentagons

With the results from the previous two sections, we can now algorithmically find  $\mathbf{A} \in S_4$  with elliptic numerical range and given foci. Note the calculations in the following examples are numerically approximated, and decimals have been rounded for convenience.

---

**Algorithm 7.1** Find a matrix  $\mathbf{A} \in S_4$  with an elliptic numerical range and foci  $f_1, f_2$

**Input:**  $f_1, f_2$ .

- 1: Define  $\Phi_2(z) = (z - f_1)(z - f_2)$  and  $z(t), w(t)$  as in (7.5).
- 2: Define  $Y(t)$  as in (7.6).
- 3: Find the zeros of  $Y(t)$  and label them in increasing order
- 4: By Section 7.2,  $t_2$  corresponds to the matrix  $\mathbf{A} \in S_4$  whose numerical range is an elliptical disk.
- 5: Find  $z(t_2), w(t_2)$ .
- 6:  $\phi_4(z) = (z - f_1)(z - f_2)(z - z(t_2))(z - w(t_2))$  is the characteristic polynomial of  $A$ .
- 7: Use  $-\bar{\alpha}_3 = \phi_4(0)$  to perform inverse Szegő recursion to recover  $\alpha_2, \alpha_1, \alpha_0$ .

**Output:**

$$\mathbf{A} := \begin{pmatrix} \bar{\alpha}_0 & \bar{\alpha}_1 \rho_0 & \rho_1 \rho_0 & 0 \\ \rho_0 & -\bar{\alpha}_1 \alpha_0 & -\bar{\rho}_1 \alpha_0 & 0 \\ 0 & \bar{\alpha}_2 \rho_1 & -\bar{\alpha}_2 \alpha_1 & \bar{\alpha}_3 \rho_2 \\ 0 & \rho_2 \rho_1 & -\rho_2 \alpha_1 & -\bar{\alpha}_3 \alpha_2 \end{pmatrix}, \quad \rho_n = \sqrt{1 - |\alpha_n|^2} \quad (7.7)$$


---

Example 7.2. Find the CMV matrix whose numerical range is bounded by an ellipse with foci  $f_1 = 0.3 - 0.4i$  and  $f_2 = 0.2i$ .

We define  $\Phi_2(z) = (z - 0.3 + 0.4i)(z - 0.2i)$  and

$$z(t) = -0.246154 + 0.569231i + (1.36752 - 2.05128)t,$$

$$w(t) = 0.307692 - 0.5384632i - (0.042735 - 0.769231i)t.$$

Then we can find  $Y(t)$ . Solving  $Y(t) = 0$ , we see  $t_1 = 0.0451748, t_2 = 0.50213, t_3 = 25.7102$ . Then by the results in Section 7.2,  $t_2$  will give the elliptic disk with the desired foci. Then

$$z(0.50213) = 0.44052 - 0.46078i,$$

$$w(0.50213) = 286234 - 0.152208i,$$

and

$$\Phi_4(z) = (z - 0.3 + 0.4i)(z - 0.2i)(z - 0.44052 + 0.46078i)(z - 286234 + 0.152208i)$$

with  $\overline{\alpha_3} = 0.286234 + 0.152208i$ . Then by the inverse Szegő recursion, we see that

$$\overline{\alpha_2} = 0.44052 + 0.46078i,$$

$$\overline{\alpha_1} = -0.2i,$$

$$\overline{\alpha_0} = -0.3 + 0.4i,$$

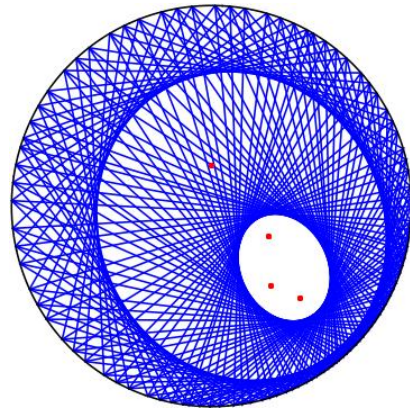


Figure 7.4. The numerical range and pentagram curve of  $A$  in Example 7.2.

and the desired CMV matrix is  $\mathbf{A} =$

$$\begin{pmatrix} 0.3 + 0.4i & -0.173205i & 0.773746 & 0 \\ 0.866025 & 0.08 + 0.06i & -0.268034 + 0.357378i & 0 \\ 0 & 0.39358 + 0.411681i & 0.092156 - 0.088104i & 0.220535 + 0.117271i \\ 0 & 0.688373 & -0.154094i & -0.196226 + 0.0648403i \end{pmatrix},$$

see Figure 7.4.

**Example 7.3.** Find the CMV matrix whose numerical range is bounded by a Poncelet 5-ellipse and whose pentagram curve is bounded by an ellipse with foci with foci  $f_1 = 0.3 - 0.4i$  and  $f_2 = 0.2i$ .

Using our initial calculations in Example 7.2 and Section 7.2, we know  $t_1$  will be the semiaxis that corresponds to a pentagram ellipse with the desired foci. Then

$$z(0.0451748) = -0.184376 + 0.476565i,$$

$$w(0.0451748) = 0.305762 - 0.503712i.$$

Then

$$\Phi_4(z) = (z - 0.3 + 0.4i)(z - 0.2i)(z + 0.184376 - 0.476565i)(z - 0.305762 + 0.503712i)$$

with  $\overline{\alpha_3} = 0.305762 + 0.503712i$ . Then by the inverse Szegő recursion, we see that

$$\overline{\alpha_2} = -0.184376 - 0.476565i,$$

$$\overline{\alpha_1} = -0.2i,$$

$$\overline{\alpha_0} = 0.3 + 0.4i,$$

and the desired CMV matrix is  $\mathbf{A} =$

$$\begin{pmatrix} 0.3 + 0.4i & -0.173205i & 0.817164 & 0 \\ 0.866025 & 0.08 + 0.06i & -0.283074 + 0.37743i & 0 \\ 0 & -0.173974 - 0.4497i & -0.09531z + 0.036875i & 0.2628 + 0.43299i \\ 0 & 0.81109 & -0.171918i & 0.2964 - 0.05284i \end{pmatrix},$$

see Figure 7.5.

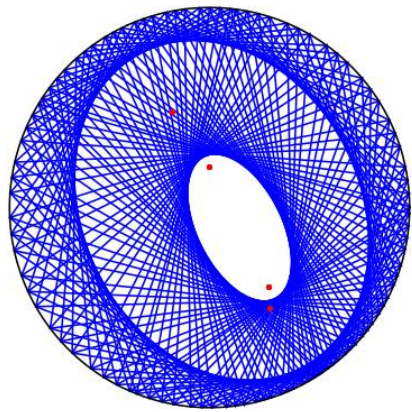


Figure 7.5. The numerical range and pentagram curve of  $A$  in Example 7.3.

## CHAPTER EIGHT

### Future Work

Recall that our goal throughout this dissertation has been to better understand Poncelet polygons and give explicit algorithms for finding CMV matrices whose numerical ranges are elliptical disks with given foci. The previous chapters have thoroughly defined and clarified the terminology and notation regarding Poncelet polygons. However, we currently only have explicit formulations of Poncelet  $n$ -ellipses with given foci for  $n \leq 6$ . Ideally, in the future we will see some patterns for general  $n$ . For example, if  $n$  is even, we have explicit conditions on the OPUC (or equivalently the finite Blaschke product) that defines a CMV matrix whose numerical range is circumscribed by  $n$ -gons whose main diagonals all meet at a specified point. If  $n = 4$ , this condition is necessary and sufficient for the numerical range of the matrix to be an elliptical disk. Similarly, if  $n$  is divisible by three, we can again force an elliptic component of  $C$ . When  $n = 6$ , the combination of this condition and the main diagonals meeting guarantees a numerical range bounded by an ellipse. As  $n$  increases, will we always need a condition on every component,  $C_j, j > 1$ , to guarantee the ellipticity  $C_1$ ? We conjecture not. In general, we suspect that forcing certain elliptic components will force all components to be ellipses. Specifically, we conjecture that if  $C_j$  and  $C_k$  are ellipses and  $j, k$  are relatively prime, then every component of  $C$  will be elliptic. In the case of prime  $n$ , then any  $C_j$  being elliptic forces every component of  $C$  to be elliptic as  $\gcd(j, n) = 1$ . In Chapter Five after Theorem 5.6, we noted that if  $n$  is prime, the existence of any elliptic component makes all the  $C_k$ 's in  $C$  ellipses. For prime  $n$ , decomposing Blaschke products no longer helps us. We must rely on Mirman's iterations. With this conjecture in mind, we have begun experimenting with both the  $n = 7$  and  $n = 12$  cases.

### 8.1 Poncelet Heptagons

As one may expect, our analysis in the heptagon case will be similar to the pentagon case in many ways.

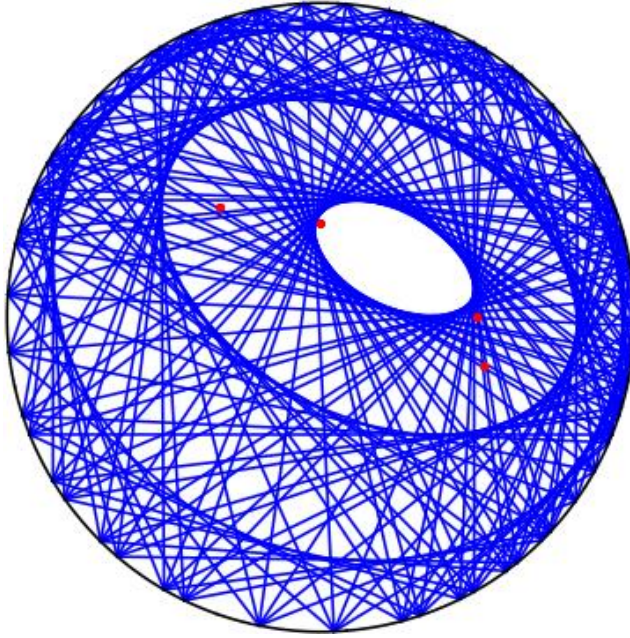


Figure 8.1. A family of Poncelet Heptagons where  $C_1, C_2, C_3$  are almost elliptic.

#### 8.1.1 Mirman's Iterations in the Heptagon Case

For heptagons,  $C$  has three components, none of which are degenerate. Then we have  $\{f_i\}_{i=1}^6$  where  $f_1, f_2$  are the foci of  $C_1$ ,  $f_3, f_4$  are the foci of  $C_2$ , and  $f_5, f_6$  are the foci of  $C_3$ . Then ordering them as in Mirman's inner iterations,

$$\begin{array}{lll} w_1 = f_1 & w_3 = f_5 & w_5 = f_4 \\ w_2 = f_3 & w_4 = f_6 & w_6 = f_2 \end{array}$$

Using the relation 5.12, the heptagon case yeilds the system

$$f_3 f_6 = B_2(f_5; f_1, f_2) \quad f_5 f_4 = B_2(f_6; f_1, f_2)$$

$$f_1 f_5 = B_2(f_3; f_1, f_2) \quad f_6 f_2 = B_2(f_4; f_1, f_2)$$

where

$$B_2(z; f_1, f_2) = \frac{(z - f_1)(z - f_2)}{(1 - \bar{f}_1 z)(1 - \bar{f}_2 z)}. \quad (8.1)$$

Experimentally, this system has sixteen solutions inside  $(\mathbb{C} \setminus \mathbb{D})^4$  and six outside. Of the solutions in  $\mathbb{D}^4$ , three are nontrivial (no  $f_j \neq 0$ ). As with the pentagon case, we have seen some colinearity of the solutions. However, the colinearity we have seen in the heptagon case thus far only involves the colinearity of  $f_1$  and the  $f_4$  values from all three nontrivial solutions and the colinearity of  $f_2$  and the  $f_3$  values from all three nontrivial solutions, but no colinearity results for any of the  $f_5$  or  $f_6$  solution values.

See Figure 8.3.

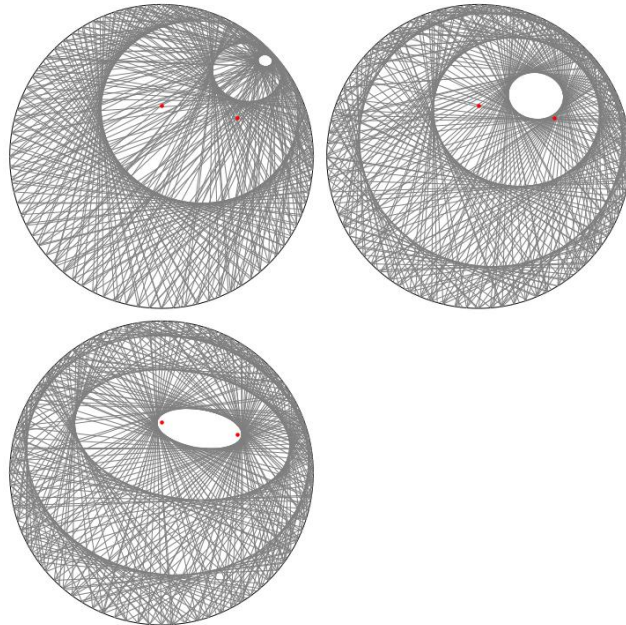


Figure 8.2. The three nontrivial solutions inside  $\mathbb{D}^4$  of Mirman's iterations. In red are the given  $f_1, f_2$  that initiated Mirman's iterations.

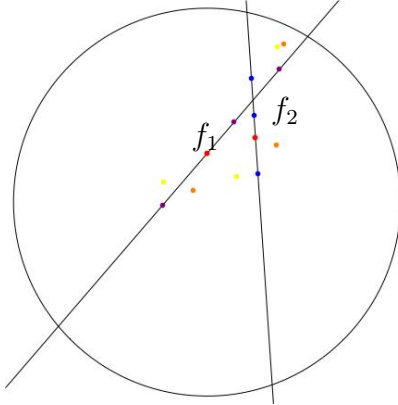


Figure 8.3. The three nonzero solutions to Mirman's iterations in the heptagon case. In red are  $f_1 = 0.25i$  and  $f_2 = 0.25 + 0.33333i$ . The  $f_3$  values appear in blue and  $f_4$  in purple. Note that all the  $f_3$  values are colinear with  $f_2$  and all the  $f_4$  values are colinear with  $f_1$ . The values of  $f_5$  in yellow and  $f_6$  in orange are not colinear.

## 8.2 Poncelet Dodecagons

In contrast to the heptagon case, composition of Blaschke products is again very promising in the  $n = 12$  case. If  $C$  is a 12-Poncelet curve, then  $C$  has six connected components with  $C_6$  possibly degenerate. According to Lemma 5.7, if  $B_{12}(z) = B_6(B_2(z))$ , then main diagonals of the dodecagons defined by  $\mathcal{Z}^\lambda$  all meet at the zero of  $\frac{B_2(z)}{z}$ . Thus  $C_6$  is a degenerate ellipse. Similarly, Lemma 5.8 tells us that if  $B_{12}(z) = B_4(B_3(z))$ ,  $C_4$  is an ellipse. The vertices of each dodecagon are connected as four triangles that circumscribe  $C_4$ . We suspect that if  $B_{12}(z) = B_3(B_4(z))$  where  $B_4(z) = D_2(B_2(z))$  as in Theorem 6.1 then  $C_3$  and  $C_6$  will be elliptic. The polygons circumscribing  $C_3$  would be quadrilaterals, three for each dodecagon. See Figure 8.4. Similarly, from Theorem 6.10, if  $B_{12}(z) = B_2(B_6(z))$  where  $B_6(z) = D_2(D_3(z)) = B_3(B_2(z))$ , then  $C_2, C_4$  and  $C_6$  are ellipses as  $C_2$  is circumscribed by hexagons formed from the vertices of the dodecagons. See Figure 8.5.

Are these two decompositions, forcing  $C_3$  and  $C_4$  to be ellipses, enough to guarantee  $C_1$  is an ellipse? If so, then this would prove a special case of the conjecture given at the beginning of this section. Calculations with these simultaneous decom-

positions will naturally be more computationally involved than in the quadrilateral or hexagon case.

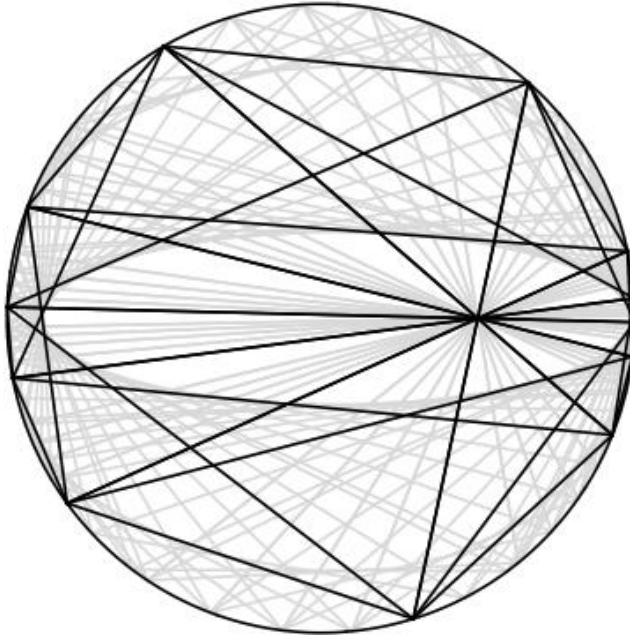


Figure 8.4. Poncelet Dodecagons formed by a composition of degree three and two degree two Blaschke products. The diagonals meet at a single point, and  $C_3$  is an ellipse.

### 8.2.1 Mirman's Iterations in the Dodecagon Case

Again, larger values of  $n$  yield more computational difficulties than the cases discussed in previous chapters. The same is true for Mirman's iterations. We give the explicit equations for Mirman's system below, although we have not yet experimentally observed solutions to this system.

As  $C$  has six connected components, consider  $f_1, f_2$  foci of  $C_1$ ,  $f_3, f_4$  foci of  $C_2$ , and so on with  $f_{11}$  the focus (in the elliptic case, the single point comprising)  $C_6$ . Then in Mirman's terms we have

$$w_1 = f_1 \quad w_4 = f_7 \quad w_7 = f_{10} \quad w_{10} = f_4$$

$$w_2 = f_3 \quad w_5 = f_9 \quad w_8 = f_2 \quad w_{11} = f_2$$

$$w_3 = f_5 \quad w_6 = f_{11} \quad w_9 = f_6$$

that should satisfy

$$\begin{aligned} f_1 f_5 &= B_2(f_3; f_1, f_2) & f_3 f_7 &= B_2(f_5; f_1, f_2) & f_5 f_9 &= B_2(f_7; f_1, f_2) \\ f_7 f_{11} &= B_2(f_9; f_1, f_2) & f_9 f_{10} &= B_2(f_{11}; f_1, f_2) & f_{11} f_8 &= B_2(f_{10}; f_1, f_2) \\ f_{10} f_6 &= B_2(f_8; f_1, f_2) & f_8 f_4 &= B_2(f_6; f_1, f_2) & f_6 f_2 &= B_2(f_4; f_1, f_2). \end{aligned}$$

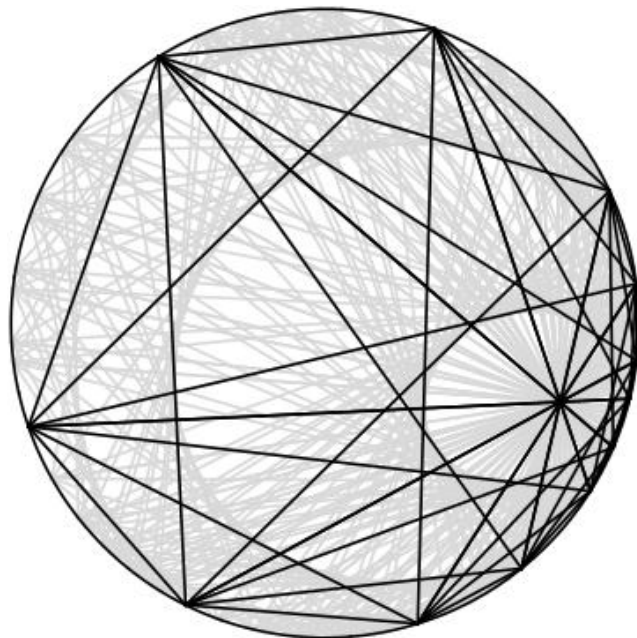


Figure 8.5. Poncelet Dodecagons formed by a composition of degree two and degree six Blaschke products where the degree six Blaschke product decomposes as in Theorem 6.11. The diagonals meet at a single point, and  $C_2, C_4$  are elliptic.

### 8.3 Remaining Question over Poncelet Pentagons

While many questions remain for  $n > 6$ , several questions remain in the pentagon case. As previously noted, the pentagon case is not as computationally clear as the quadrilateral and hexagon cases. For quadrilaterals and hexagons, we have specific factorizations of the characteristic polynomial of the CMV matrix. Within this factorization, geometric interpretations are in a sense encoded, such as the main diagonals meeting at the Verblunsky coefficient of the degree one polynomial. Using Mirman's iterations, we can find the set of foci of  $C$  and then define the OPUC with those zeros. We do not currently see this OPUC factoring in a way that shows the distinctions between the foci of  $C_1$  and  $C_2$  as the factorizations in the degree 4 and 6 cases showed. As OPUC have been so revealing in other cases, one would hope a condition on the characteristic polynomial of a CMV matrix for the boundary of the numerical range to be an ellipse would be illuminating in the pentagon case as well.

Mirman's equations in the pentagon case reveal another puzzling phenomenon. In Section 7.2, we proved the largest solution  $t$  to Mirman's iterations in  $n = 5$  will always correspond to a solution  $(z_3, w_3)$  outside  $\mathbb{D}^2$ . However, currently, there is not a geometric interpretation of  $t_3$  as a semiaxis or of  $(z_3, w_3)$  as foci or in relationship to  $C$ . We have wondered whether this  $t_3$  and pair of points connect somehow to the dual curve, although no results in this direction have yet been found.

## APPENDIX

## APPENDIX

### List of Symbols and Notation

$\mathbf{A}$	a completely nonunitary contraction
$[a, b]$	line segment joining $a, b \in \mathbb{C}$
$\alpha_n$	$n$ th Verblunsky coefficient
$B_n(z), C_n(z), D_n(z)$	degree $n$ Blaschke products
$C$	Poncelet curve of rank $n$
$C_k$	envelope of all the chords $[z, \tau^k(z)]$
$\mathbb{C}^{n \times n}$	set of $n \times n$ matrices with complex entries
$d$	degree of an algebraic curve
$\mathbb{D}$	the unit disk
$\partial\mathbb{D}$	the unit circle
$F(x, y, z)$	homogeneous polynomial that defines a curve in the projective plane
$\Gamma$	real plane algebraic curve
$\Gamma^*$	dual of the real algebraic curve $\Gamma$
$\Gamma(\mathbb{R})$	set of real points of $\Gamma$
$G_A(x, y, z)$	$\det\{x \operatorname{Re} \mathbf{A} + y \operatorname{Im} \mathbf{A} - z \mathbf{I}\}$
$\mathcal{G}$	a CMV matrix
$I_n$	$n \times n$ Identity matrix
$\mathbb{K}$	field (usually $\mathbb{C}$ or $\mathbb{R}$ )
$\mathcal{K}_n$	union of $C_k$ for $1 \leq k \leq \frac{n}{2}$
$\mathcal{K}_n^*$	union of $C_k^*$ for $1 \leq k \leq \frac{n}{2}$
$\lambda$	point on $\mathbb{T}$
$\mu$	probability measure on $\mathbb{C}$
$\mathcal{P}$	polygon
$\mathcal{P}(z)$	a polygon with $z$ as a vertex
$P(z_1, z_2)$	symmetric polynomial used in Mirman's iterations
$\Phi_n(z)$	monic orthogonal polynomial on the unit circle of degree $n$
$\Phi_n^*(z)$	reversed polynomial of $\Phi_n(z)$
$\phi(d)$	Euler's totient function
$\mathbb{P}^2(\mathbb{K})$	projective plane
$\mathbb{P}^2(\mathbb{K})^*$	dual projective plane
$S_n$	set of completely nonunitary contractions of defect index one
$\sigma(A)$	spectrum of a matrix $A$
$\mathcal{S}_{\alpha_{n-1}}$	operation of Szegő recursion with parameter $\alpha_{n-1}$
$\mathcal{T}_{\alpha_{n-1}}$	operation of Szegő recursion on a reverse polynomial
$\Theta_j$	$2 \times 2$ matrix of Verblunsky coefficients
$\mathbb{T}$	$\{z \in \mathbb{C} :  z  = 1\}$
$\tau$	maps one vertex of a cyclic polygon to the next
$U, V$	unitary matrices
$U_\lambda$	unitary rank 1 dilation of a CMV matrix with the parameter $\lambda$
$W(A)$	numerical range of the matrix $A$

$Z_n^\lambda$	paraorthogonal extension of an OPUC
$Z^\lambda$	set of points identified by a Blaschke product
$\zeta$	reciprocal or polar of a point
$\zeta_k(z)$	pole of the line containing $[z, \tau^k(z)]$

## BIBLIOGRAPHY

- [1] George E Andrews, Vladimir Dragović, and Milena Radnović, *Combinatorics of periodic ellipsoidal billiards*, Preprint ArXiv:1908.01026, August 2019.
- [2] Yury Arlinskiĭ, Leonid Golinskiĭ, and Eduard Tsekanovskiĭ, *Contractions with rank one defect operators and truncated cmv matrices*, Journal of Functional Analysis **254** (2008), no. 1, 154–195.
- [3] Mauro C. Beltrametti, Ettore Carletti, Dionisio Gallarati, and Giacomo Monti Bragadin, *Lectures on curves, surfaces and projective varieties*, EMS Textbooks in Mathematics, European Mathematical Society (EMS), Zürich, 2009, A classical view of algebraic geometry, Translated from the 2003 Italian original by Francis Sullivan. MR 2549804
- [4] Marcel Berger, *Geometry I*, Universitext, Springer-Verlag, Berlin, 2009, Translated from the 1977 French original by M. Cole and S. Levy, Fourth printing of the 1987 English translation [MR0882541]. MR 2724360
- [5] Ethan S Brown and Ilya M Spitkovsky, *On Matrices with Elliptical Numerical Ranges*, Linear and Multilinear Algebra **52** (2004), no. 3-4, 177–193.
- [6] Vladimir P Burskii and Alexei S Zhedanov, *On Dirichlet, Poncelet and Abel problems*, Communications on Pure and Applied Analysis **12** (2013), no. 4, 1587–1633.
- [7] Isabelle Chalendar, Pamela Gorkin, and Jonathan R. Partington, *The group of invariants of an inner function with finite spectrum*, Journal of Mathematical Analysis and Applications **389** (2012), no. 2, 1259–1267.
- [8] Mao-Ting Chien and Kuo-Chih Hung, *Elliptic numerical ranges of bordered matrices*, Taiwanese Journal of Mathematics **16** (2012), no. 3, 1007–1016.
- [9] H.S.M. Coxeter, *Projective geometry*, second ed., Springer-Verlag, 1987.
- [10] Ulrich Daapp, Pamela Gorkin, and Raymond Mortini, *Ellipses and Finite Blaschke Products*, The American Mathematical Monthly **109** (2002), no. 9, 785–795.
- [11] Ulrich Daapp, Pamela Gorkin, Andrew Shaffer, Benjamin Sokolowsky, and Karl Voss, *Decomposing finite blaschke products*, Journal of Mathematical Analysis and Applications **426** (2015), no. 2, 1201–1216.

- [12] Ulrich Daepp, Pamela Gorkin, Andrew Shaffer, and Karl Voss, *Möbius transformations and Blaschke products: The geometric connection*, Linear Algebra and its Applications **516** (2017), 186–211.
- [13] ———, *Finding ellipses*, Carus Mathematical Monographs, vol. 34, MAA Press, Providence, RI, 2018, What Blaschke products, Poncelet’s theorem, and the numerical range know about each other. MR 3932079
- [14] Ulrich Daepp, Pamela Gorkin, and Karl Voss, *Poncelet’s theorem, Sendov’s conjecture, and Blaschke products*, Journal of Mathematical Analysis and Applications **365** (2010), no. 1, 93–102.
- [15] G. Darboux, *Principes de géométrie analytique*, Gauthier-Villars, Paris, 1917.
- [16] Andrea Del Centina, *Poncelet’s porism: a long story of renewed discoveries, i*, Archive for History of Exact Sciences **70** (2016), no. 1, 1–122.
- [17] ———, *Poncelet’s porism: a long story of renewed discoveries, II*, Archive for History of Exact Sciences **70** (2016), no. 2, 123–173.
- [18] Vladimir Dragovic and Milena Radnovic, *Poncelet porisms and beyond*, 01 2011.
- [19] Vladimir Dragović and Milena Radnovic, *Bicentennial of the Great Poncelet Theorem (1813–2013): Current advances*, Bulletin of the American Mathematical Society **51** (2014), no. 3, 373–445.
- [20] ———, *Caustics of Poncelet Polygons and Classical Extremal Polynomials*, Regular and Chaotic Dynamics **24** (2019), no. 1, 1–35.
- [21] Leopold Flatto, *Poncelet’s theorem*, American Mathematical Society, Providence, RI, 2009, Chapter 15 by S. Tabachnikov. MR 2465164
- [22] Masayo Fujimura, *Inscribed Ellipses and Blaschke Products*, Computational Methods and Function Theory **13** (2013), no. 4, 557–573.
- [23] ———, *Blaschke Products and Circumscribed Conics*, Computational Methods and Function Theory **17** (2017), no. 4, 635–652.
- [24] ———, *Interior and exterior curves of finite Blaschke products*, Journal of Mathematical Analysis and Applications **467** (2018), no. 1, 711–722.
- [25] Shuhong Gao, *Absolute irreducibility of polynomials via newton polytopes*, Journal of Algebra **237** (2001), no. 2, 501 – 520.
- [26] Hwa-Long Gau, *Elliptic Numerical Ranges of  $4 \times 4$  Matrices*, Taiwanese Journal of Mathematics **1** (2006), 117–128.
- [27] Hwa-Long Gau and Pei Yuan Wu, *Dilation to inflations of  $S(\phi)$* , Linear and Multilinear Algebra **45** (1998), no. 2-3, 109–123.

- [28] ———, *Numerical range of  $S(\phi)$* , Linear and Multilinear Algebra **45** (1998), no. 1, 49–73.
- [29] ———, *Condition for the numerical range to contain an elliptic disc*, Linear Algebra and its Applications **364** (2003), 213–222.
- [30] ———, *Numerical range and Poncelet property*, Taiwanese Journal of Mathematics **7** (2003), no. 2, 173–193.
- [31] Hwa-Long Gau and Pei Yuan Wu, *Numerical range circumscribed by two polygons*, Linear Algebra and its Applications **382** (2004), 155–170.
- [32] J. Geronimus, *On the trigonometric moment problem*, Annals of Mathematics **47** (1946), no. 4, 742–761.
- [33] Ja. L. Geronimus, *Polynomials orthogonal on a circle and interval*, Translated from the Russian by D. E. Brown; edited by Ian N. Sneddon. International Series of Monographs on Pure and Applied Mathematics, Vol. 18, Pergamon Press, New York-Oxford-London-Paris, 1960. MR 0133642
- [34] David M. Goldschmidt, *Algebraic functions and projective curves*, Graduate Texts in Mathematics, vol. 215, Springer-Verlag, New York, 2003. MR 1934359
- [35] Leonid Golinskii and Mikhail Kudryavtsev, *An inverse spectral theory for finite cmv matrices*, 2007.
- [36] Pamela Gorkin, *Four Theorems with Their Foci on Ellipses*, American Mathematical Monthly **126** (2019), no. 2, 99–111.
- [37] Pamela Gorkin and Nathan Wagner, *Ellipses and compositions of finite Blaschke products*, Journal of Mathematical Analysis and Applications **445** (2017), no. 2, 1354–1366.
- [38] P Griffiths and J Harris, *On Cayley’s explicit solution to Poncelet’s porism*, L’Enseignement Mathématique **24** (1978), 31–40.
- [39] Uffe Haagerup and Pierre de la Harpe, *The numerical radius of a nilpotent operator on a Hilbert space*, Proc. Amer. Math. Soc. **115** (1992), no. 2, 371–379. MR 1072339
- [40] P. R. Halmos, *A Hilbert space problem book*, 2nd. ed., Springer-Verlag, New York, 1982.
- [41] Roger A. Horn and Charles R. Johnson, *Matrix analysis*, second ed., Cambridge University Press, Cambridge, 2013. MR 2978290
- [42] Markus Hunziker, Andrei Martínez-Finkelshtein, Taylor Poe, and Brian Simanek, *On foci of ellipses inscribed in cyclic polygons*, Preprint, 2021.

- [43] ———, *Poncelet-Darboux, Kippenhahn, and Szegő: interactions between projective geometry, matrices and orthogonal polynomials*, Preprint, 2021.
- [44] Dennis S. Keeler, Leiba Rodman, and Ilya M. Spitkovsky, *The numerical range of  $3 \times 3$  matrices*, Linear Algebra and Its Applications **252** (1997), no. 1-3, 115–139 (English (US)), Copyright: Copyright 2018 Elsevier B.V., All rights reserved.
- [45] Keith Kendig, *A guide to plane algebraic curves*, The Dolciani Mathematical Expositions, vol. 46, Mathematical Association of America, Washington, DC, 2011, MAA Guides, 7. MR 2815937
- [46] Rudolf Kippenhahn, *Über den Wertevorrat einer Matrix*, Math. Nachr. **6** (1951), 193–228. MR 59242
- [47] ———, *On the numerical range of a matrix*, Linear Multilinear Algebra **56** (2008), no. 1-2, 185–225, Translated from the German by Paul F. Zachlin and Michiel E. Hochstenbach [MR0059242]. MR 2378310
- [48] E. A. Kudryavtseva, *Liouville integrable generalized billiard flows and theorems of Poncelet type*, Fundam. Prikl. Mat. **20** (2015), no. 3, 113–152. MR 3519751
- [49] Joel C Langer and David A Singer, *Foci and Foliations of Real Algebraic Curves*, Milan Journal of Mathematics **75** (2007), no. 1, 225–271.
- [50] Yoram Last and Barry Simon, *Fine structure of the zeros of orthogonal polynomials. IV. A priori bounds and clock behavior*, Comm. Pure Appl. Math. **61** (2008), no. 4, 486–538. MR 2383931
- [51] Chi-Kwong Li, *A simple proof of the elliptical range theorem*, Proc. Amer. Math. Soc. **124** (1996), no. 7, 1985–1986. MR 1322932
- [52] M. S. Livshitz, *On a certain class of linear operators in Hilbert space*, Rec. Math. [Mat. Sbornik] N.S. **19(61)** (1946), 239–262. MR 0020719
- [53] M. Marden, *Geometry of polynomials*, 2nd. ed., Math. Surveys, vol. 3, Amer. Math. Soc., Providence, R. I., 1966.
- [54] Andrei Martínez-Finkelshtein, Brian Simanek, and Barry Simon, *Poncelet’s theorem, paraorthogonal polynomials and the numerical range of compressed multiplication operators*, Adv. Math. **349** (2019), 992–1035. MR 3945586
- [55] Boris Mirman, *UB-matrices and conditions for Poncelet polygon to be closed*, Linear Algebra and its Applications **360** (2003), 123–150.
- [56] ———, *Explicit solutions to Poncelet’s porism*, Linear Algebra and its Applications **436** (2012), no. 9, 3531–3552.
- [57] Boris Mirman and Pradeep Shukla, *A characterization of complex plane Poncelet curves*, Linear Algebra and its Applications **408** (2005), 86–119.

- [58] Maria Monks, *Duality of plane curves*, 2011.
- [59] Laurent Moret-Bailly, *Private communication*, 2021.
- [60] Valentin Ovsienko, Richard Schwartz, and Serge Tabachnikov, *The Pentagram Map: A Discrete Integrable System*, Communications in Mathematical Physics **299** (2010), no. 2, 409–446.
- [61] Daniel Pecker, *Poncelet’s theorem and billiard knots*, Geom. Dedicata **161** (2012), 323–333. MR 2994045
- [62] Jean-Victor Poncelet, *Traité sur les propriétés projectives des figures*, ProQuest LLC, Ann Arbor, MI, 1822.
- [63] Jürgen Richter-Gebert, *Perspectives on projective geometry*, Springer, Heidelberg, 2011, A guided tour through real and complex geometry. MR 2791970
- [64] George Salmon, *A treatise on conic sections : containing an account of some of the most important modern algebraic and geometric methods / by george salmon*, 3rd ed. rev. and enl. ed., Longmans, Brown, Green and Longmans London, 1855 (English).
- [65] ———, *Xxxi. on the problem of the in-and-circumscribed triangle*, The London, Edinburgh, and Dublin Philosophical Magazine and Journal of Science **13** (1857), no. 85, 190–191.
- [66] Richard Evan Schwartz, *The pentagram map*, Experimental Mathematics **1** (1992), 71–81.
- [67] ———, *The pentagram integrals for Poncelet families*, Journal of Geometry and Physics **87** (2015), 432–449.
- [68] Igor R. Shafarevich, *Basic algebraic geometry. 1*, Russian ed., Springer, Heidelberg, 2013, Varieties in projective space. MR 3100243
- [69] Jörg Siebeck, *Ueber eine neue analytische Behandlungweise der Brennpunkte*, J. Reine Angew. Math. **64** (1864), 175–182.
- [70] B. Simon, *Orthogonal polynomials on the unit circle I and II*, AMS Colloquium Publications, vol. 54, American Mathematical Society, Providence, RI, 2005.
- [71] Barry Simon, *Opuc on one foot*, Bulletin of the American Mathematical Society **42** (2005).
- [72] Barry Simon and Vilmos Totik, *Limits of zeros of orthogonal polynomials on the circle*, Mathematische Nachrichten **278** (2005), no. 12-13, 1615–1620.
- [73] Mihai Stoiciu, *The statistical distribution of the zeros of random paraorthogonal polynomials on the unit circle*, J. Approx. Theory **139** (2006), no. 1-2, 29–64. MR 2220032

- [74] Alex Svirin, *Envelope of a family of curves*.
- [75] Béla Sz.-Nagy, Ciprian Foias, Hari Bercovici, and László Kérchy, *Harmonic analysis of operators on Hilbert space*, enlarged ed., Universitext, Springer, New York, 2010. MR 2760647
- [76] G. Szegő, *Orthogonal polynomials*, fourth ed., Amer. Math. Soc. Colloq. Publ., vol. 23, Amer. Math. Soc., Providence, RI, 1975.
- [77] Serge Tabachnikov, *Kasner meets Poncelet*, Math. Intelligencer **41** (2019), no. 4, 56–59. MR 4030385
- [78] H. S. White, *Poncelet polygons*, Science **43** (1916), no. 1101, 149–158.
- [79] Pei Yuan Wu, *Polygons and numerical ranges*, American Mathematical Monthly **107** (2000), no. 6, 528–540.
- [80] Maxim L. Yattselev, *Lecture notes on orthogonal polynomials*.